

Old Dominion University

## ODU Digital Commons

---

Electrical & Computer Engineering Theses & Dissertations

Electrical & Computer Engineering

---

Summer 2015

# A Vector Channel Based Approach to MIMO Radar Waveform Design for Extended Targets

Amanda Joan Angell Daniel  
*Old Dominion University*

Follow this and additional works at: [https://digitalcommons.odu.edu/ece\\_etds](https://digitalcommons.odu.edu/ece_etds)



Part of the [Electrical and Computer Engineering Commons](#)

---

### Recommended Citation

Daniel, Amanda J.. "A Vector Channel Based Approach to MIMO Radar Waveform Design for Extended Targets" (2015). Doctor of Philosophy (PhD), Dissertation, Electrical & Computer Engineering, Old Dominion University, DOI: 10.25777/68y4-6p29  
[https://digitalcommons.odu.edu/ece\\_etds/62](https://digitalcommons.odu.edu/ece_etds/62)

This Dissertation is brought to you for free and open access by the Electrical & Computer Engineering at ODU Digital Commons. It has been accepted for inclusion in Electrical & Computer Engineering Theses & Dissertations by an authorized administrator of ODU Digital Commons. For more information, please contact [digitalcommons@odu.edu](mailto:digitalcommons@odu.edu).

**A VECTOR CHANNEL BASED APPROACH TO MIMO  
RADAR WAVEFORM DESIGN FOR EXTENDED  
TARGETS**

by

Amanda Joan Angell Daniel  
B.S. May 2007, Northeastern University  
M.S. May 2009, Stanford University

A Dissertation Submitted to the Faculty of  
Old Dominion University in Partial Fulfillment of the  
Requirements for the Degree of

DOCTOR OF PHILOSOPHY

ELECTRICAL AND COMPUTER ENGINEERING

OLD DOMINION UNIVERSITY  
August 2015

Approved by:

  
Dimitrie C. Popescu (Director)

  
Dean Krusienski (Member)

  
Roland Mielke (Member)

  
W. Steven Gray (Member)

# ABSTRACT

## A VECTOR CHANNEL BASED APPROACH TO MIMO RADAR WAVEFORM DESIGN FOR EXTENDED TARGETS

Amanda Joan Angell Daniel  
Old Dominion University, 2015  
Director: Dr. Dimitrie C. Popescu

Radar systems have been used for many years for estimating, detecting, classifying, and imaging objects of interest (targets). Stealthier targets and more cluttered environments have created a need for more sophisticated radar systems to gain more precise information about the radar environment. Because modern radar systems are largely defined in software, adaptive radar systems have emerged that tailor system parameters such as the transmitted waveform and receiver filter to the target and environment in order to address this need.

The basic structure of a radar system exhibits many similarities to the structure of a communication system. Recognizing the parallel composition of radar systems and information transmission systems, initial works have begun to explore the application of information theory to radar system design, but a great deal of work still remains to make a full and clear connection between the problems addressed by radar systems and communication systems. Forming a comprehensive definition of this connection between radar systems and information transmission systems and associated problem descriptions could facilitate the cross-discipline transfer of ideas and accelerate the development and improvement of new system design solutions in both fields. In particular, adaptive radar system design is a relatively new field which stands to benefit

from the maturity of information theory developed for information transmission if a parallel can be drawn to clearly relate similar radar and communication problems.

No known previous work has yet drawn a clear parallel between the general multiple-input multiple-output (MIMO) radar system model considering both the detection and estimation of multiple extended targets and a similar multiuser vector channel information transmission system model. The goal of this dissertation is to develop a novel vector channel framework to describe a MIMO radar system and to study information theoretic adaptive radar waveform design for detection and estimation of multiple radar targets within this framework.

Specifically, this dissertation first provides a new compact vector channel model for representing a MIMO radar system which illustrates the parallel composition of radar systems and information transmission systems. Second, using the proposed framework this dissertation contributes a compressed sensing based information theoretic approach to waveform design for the detection of multiple extended targets in noiseless and noisy scenarios. Third, this dissertation defines the multiple extended target estimation problem within the framework and proposes a greedy signal to interference-plus-noise ratio (SINR) maximizing procedure based on a similar approach developed for a collaborative multibase wireless communication system to optimally design waveforms in this scenario.

For my mother, Shelly Angell from whom I am eager to continue learning for many  
years to come.

## ACKNOWLEDGMENTS

First and foremost I would like to extend my most sincere thanks to my advisor Dimitrie Popescu. I am proud to have worked under his guidance and could not have completed this work without his encouragement, keen insight, level-headed perspective, and confidence in my abilities which have all been key factors in helping me to grow academically and professionally. He has provided direction and perspective in my work, while also allowing me to also pursue research directions and open questions that I found interesting. I cannot express in words my appreciation for the amount of time and effort he has devoted to our many meetings, in which he always asked the right questions to clarify new directions to pursue, and for his many hours of editorial input on each written endeavor. Additionally, his impeccable memory and uncanny ability to always recall the most pertinent related work, bringing them up at a moment's notice, always helped address any difficulty I encountered in my work. His confidence in my abilities has driven me to do better work while his respect of my family and life beyond research has allowed me to be a better person.

I thank all my committee members: Dean Krusienski, Roland Mielke and W. Steven Gray. I appreciate the time and insight they have invested in my research and education. I would be remiss without a special thank you to Steven Gray for his helpful comments and suggestions, which have undoubtedly improved this work.

I thank Linda Marshall and Romina Samson who have been incredibly important in their support with all my administrative needs and who have assisted me in understanding and working through Old Dominion University's academic procedures.

I would also like to extend a heartfelt thanks to my supportive family. Most

importantly, my thanks go to my husband Mark who has been my rock through this entire endeavor. He has provided love and moral support and has been an attentive father to our two children while meeting the demands of his own career as a naval officer. My accomplishments are as much his as they are mine. I would also like to thank my son Joseph and my daughter Julia for their cheery smiles, warm hugs and exuberance of life, and for being such good siblings to one another. They give me great joy and purpose and make it fun to be a mother while pursuing a PhD. I would like to thank my mother Shelly, father Daryl and my grandparents Shiela and Robert Beyer for a continuing lifetime of love, friendship, support and encouragement throughout my academic and personal pursuits.

## TABLE OF CONTENTS

	Page
LIST OF TABLES . . . . .	xi
LIST OF FIGURES . . . . .	xiii
 Chapter	
I INTRODUCTION . . . . .	1
I.1 RADAR SYSTEM SETUP . . . . .	1
I.2 RESEARCH MOTIVATION . . . . .	4
I.2.1 ADAPTIVE/COGNITIVE RADAR SYSTEMS . . . . .	5
I.2.2 INFORMATION THEORY AND RADAR SYSTEM DESIGN . . . . .	7
I.2.3 PROBLEM STATEMENT . . . . .	10
I.3 DISSERTATION CONTRIBUTIONS . . . . .	10
I.4 DISSERTATION ORGANIZATION . . . . .	11
II MODELING THE MIMO RADAR SYSTEM AS A VECTOR CHANNEL . . . . .	14
II.1 SYSTEM SETUP . . . . .	15
II.2 TARGET MODELING . . . . .	19
II.2.1 REFLECTION CENTERS AND AZIMUTH AMBIGUITY . . . . .	20
II.2.2 REFLECTION COEFFICIENTS . . . . .	21
II.3 THE FREQUENCY DOMAIN VECTOR CHANNEL MODEL . . . . .	22
II.4 THE TIME DOMAIN VECTOR CHANNEL MODEL . . . . .	26
II.5 RELATING THE TIME AND FREQUENCY DOMAIN MODELS . . . . .	30
II.6 CHAPTER SUMMARY . . . . .	31
III COMPRESSED SENSING DESIGN OF RADAR WAVEFORMS AND RECEIVER FILTERS FOR TARGET DETECTION . . . . .	32

Chapter	Page
III.1 COMPRESSED SENSING FOR MIMO RADAR . . . . .	35
III.1.1 OPTIMAL WAVEFORM DESIGN PROCEDURE . . . . .	40
III.1.2 OPTIMAL RECEIVER FILTER DESIGN PROCEDURE . . . . .	41
III.1.3 JOINT WAVEFORM-RECEIVER FILTER DESIGN PROCEDURE . . . . .	41
III.2 TARGET DETECTION . . . . .	42
III.3 SIMULATIONS AND NUMERICAL RESULTS . . . . .	45
III.3.1 RECONSTRUCTION RESULTS . . . . .	48
III.3.2 DETECTION RESULTS . . . . .	49
III.4 CHAPTER SUMMARY . . . . .	50
IV COMPRESSED SENSING DESIGN OF RADAR WAVEFORMS AND RECEIVER FILTERS FOR TARGET DETECTION IN NOISY ENVI- RONMENT . . . . .	52
IV.1 SCENE RECONSTRUCTION FROM NOISY MEASUREMENTS . . . . .	52
IV.2 SIMULATIONS AND NUMERICAL RESULTS . . . . .	53
IV.2.1 RECONSTRUCTION RESULTS . . . . .	55
IV.2.2 DETECTION RESULTS . . . . .	57
IV.3 CHAPTER SUMMARY . . . . .	65
V GREEDY SINR MAXIMIZATION BASED DESIGN OF RADAR WAVEFORMS FOR TARGET ESTIMATION . . . . .	66
V.1 WAVEFORM DESIGN FOR MULTIPLE TARGET ESTIMATION . . . . .	67
V.2 GREEDY SINR MAXIMIZATION FOR MULTIPLE TARGET ES- TIMATION . . . . .	71
V.3 SIMULATIONS AND NUMERICAL RESULTS . . . . .	74
V.3.1 Weak Interference . . . . .	75
V.3.2 Moderate Interference . . . . .	79
V.3.3 Strong Interference . . . . .	82

Chapter	Page
V.4 CHAPTER SUMMARY . . . . .	86
VI CONCLUSIONS AND FUTURE RESEARCH . . . . .	88
VI.1 CONCLUSIONS . . . . .	88
VI.2 FUTURE RESEARCH . . . . .	90
BIBLIOGRAPHY . . . . .	91
APPENDICES . . . . .	100
A PROOF THAT $\mathbf{R}_n$ IS DIAGONAL . . . . .	101
B COMPRESSED SENSING BACKGROUND . . . . .	104
VITA . . . . .	108

## LIST OF TABLES

Table	Page
1 Organization of the Dissertation . . . . .	12
2 Observed error for point targets . . . . .	49
3 Observed error for known extended targets . . . . .	49
4 Observed error for fluctuating extended targets . . . . .	49
5 Observed detection rates for point targets in the noiseless scenario . . . . .	50
6 Observed false alarm rates for point targets in the noiseless scenario . . . . .	50
7 Observed detection rates for extended targets in the noiseless scenario . . . . .	50
8 Observed false alarm rates for the noiseless scenario . . . . .	51
9 Observed reconstruction error for point targets . . . . .	56
10 Observed reconstruction error for known extended targets . . . . .	56
11 Observed reconstruction error for fluctuating extended targets . . . . .	56
12 Observed reconstruction error for point targets in cluttered environment . . . . .	57
13 Observed reconstruction error for known extended targets in cluttered environment . . . . .	57
14 Observed reconstruction error for fluctuating extended targets in clut- tered environment . . . . .	57

## LIST OF FIGURES

Figure	Page
1 Conceptual system diagram . . . . .	2
2 Radar System versus Communication System . . . . .	7
3 System setup . . . . .	16
4 Azimuth ambiguity as seen in the bistatic MIMO radar system with beamforming . . . . .	21
5 Compressed sensing based radar waveform design algorithm . . . . .	41
6 Compressed sensing based radar receiver filter design algorithm . . . . .	42
7 Compressed sensing based joint waveform and receiver filter design algorithm . . . . .	43
8 Reflection coefficients for the simulated example . . . . .	46
9 Target impulse responses where $x$ is the distance along the target in meters and $c = 3 \times 10^8$ m/s (assuming free space wave propagation) . . . . .	46
10 Compressed sensing based joint waveform and receiver filter design algorithm for noisy scenario . . . . .	54
11 Detection and false alarm rates for point targets in noisy environment . . . . .	59
12 Detection and false alarm rates for known extended targets in noisy environment . . . . .	60
13 Detection and false alarm rates for fluctuating extended targets in noisy environment . . . . .	61
14 Detection and false alarm rates for point targets in noisy environment with clutter . . . . .	62
15 Detection and false alarm rates for known extended targets in noisy environment with clutter . . . . .	63

Figure	Page
16 Detection and false alarm rates for fluctuating extended targets in noisy environment with clutter . . . . .	64
17 Greedy SINR-maximization based joint waveform and receiver filter design algorithm . . . . .	73
18 Waveforms designed for two weakly-interfering targets (a) High SNR (b) Low SNR . . . . .	76
19 Sum Capacity for weakly-interfering targets (a) High SNR (b) Low SNR . . . . .	78
20 Waveforms designed for two moderately-interfering targets (a) High SNR (b) Low SNR . . . . .	80
21 Sum Capacity for moderately-interfering targets (a) High SNR (b) Low SNR . . . . .	81
22 Waveforms designed for two strongly-interfering targets (a) High SNR (b) Low SNR . . . . .	84
23 Sum Capacity for strongly-interfering targets (a) High SNR (b) Low SNR . . . . .	85
24 Conceptual diagram of compressed sensing problem . . . . .	105

# CHAPTER I

## INTRODUCTION

Radar has been used for many decades to estimate, detect and track objects of interest (targets) within a given environment and has been of interest to both military and civilian communities, with applications including air traffic control, environmental sensing, and surveillance (ex. [1-3]).

Despite the longstanding history of radar, there remains a good deal of room for improving system performance in the presence of difficult targets and environments, and radar system design remains an active area of research. In particular, it is still challenging to obtain information about targets that appear small to the radar system and to diminish noise seen at the radar receiver, clutter due to errant reflections from objects not of interest, or interference due to other nearby radio frequency (RF) transmitters. Recently, the development of adaptive radar systems has allowed radar system characteristics to change with the target or environment in an effort to better address these difficulties [4].

This chapter provides a brief description of the basic operation of a radar system as well as some background regarding adaptive radar system technology and its implementation and concludes by stating the research goals of this dissertation.

### I.1 RADAR SYSTEM SETUP

The basic operational concept employed by a radar system is as follows: a radar transmitter sends an electromagnetic pulse, a target reflects that signal, and finally

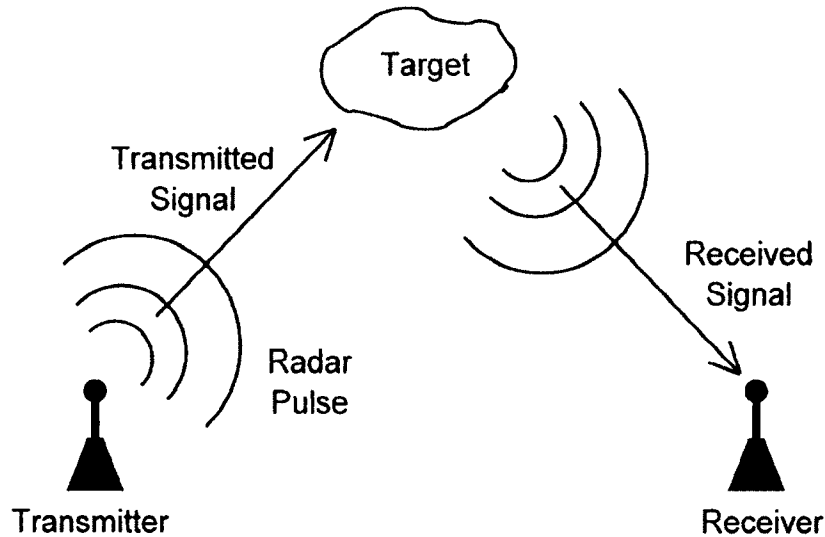


Fig. 1: Conceptual system diagram

a radar receiver processes the reflected signal in order to gain information about the target as shown in Fig. 1. Information gained regarding the target could include its range as determined by the delay of the transmitted pulse, its azimuth angle with respect to the transmitter or receiver as determined by the angle of incidence of the reflected signal seen at the receiver, characteristics regarding its size and form as determined by the amplitude and shape of the received signal, or its velocity as determined by the Doppler frequency shift of the received signal.

Depending on what information about the target interests the end user, there are several distinct problems that a radar system might address:

- *Estimation*: In the estimation scenario, the system looks to gain as much information as possible regarding a target that is known to be present but whose description is unknown [5, 6].
- *Detection*: In the detection scenario, the system aims to determine the presence

or absence of a target with a known description [5,6].

- *Classification*: In the classification scenario, the system looks to assign a target that is known to be present in a scene to one of several known target categories [5].
- *Tracking*: The radar tracking scenario considers the time-varying characteristics of targets by determining and maintaining an estimate of the current state and projected future state of each detected target from pulse to pulse [7].
- *Imaging*: In the imaging scenario, the system aims to reconstruct as many details as possible about the entire radar scene to form an image of an area [8].

Many complex radar systems have been considered, addressing each of these problems for various platforms and scene topographies, and it is beyond the scope of this work to address all the details of every type of radar system in use or development. However, for the reader's convenience a few radar system definitions that will prove most relevant to this work are provided as follows.

- *Point Target*: A point target is defined as a single point scatterer that acts upon the transmitted pulse.
- *Extended Target*: An extended target is a collection of scatterers all reflecting the same transmitted pulse and belonging to a single larger target.
- *Monostatic Radar System*: Radar system in which the transmitter and receiver are colocated.

- *Bistatic Radar System*: Radar system in which the transmitter and receiver are not colocated but rather are separated by some distance.
- *MIMO Radar System*: Many modern radar systems use not just one antenna but rather an array of antennas at the transmitter, receiver, or both to form a multiple-input multiple-output (MIMO) radar system. Using an array of antennas at the transmitter provides the ability to focus the beam containing the transmitted waveform [9]. Similarly, using an array of antennas at the radar receiver allows for focused processing of the returned signal from a particular direction.

In the interest of maintaining the generality of the system description, it is assumed in this work that a bistatic MIMO radar system is used for the detection and estimation of extended targets.

## **I.2 RESEARCH MOTIVATION**

With the development of stealthier radar targets as well as the emergence of more highly cluttered environments where a great deal of electromagnetic interference may be present due to other nearby targets and transmitters, there is a need for more sophisticated radar systems that can provide more precise information about targets of interest while mitigating the effects of surrounding clutter. The ideal radar system should find the best way to operate in the presence of many other interfering systems and targets that may diminish the visibility of objects of interest.

### I.2.1 ADAPTIVE/COGNITIVE RADAR SYSTEMS

Historically, radar system parameters were statically defined since transmission and reception schemes were implemented in hardware and any change would likewise require modifications to the hardware of the radar system. Since radar systems are now largely software-based [10], transmission and reception schemes can be tailored to the target or environment. Any radar system that designs system parameters in this way is referred to as an adaptive radar system. There are three levels within which to classify an adaptive radar system: traditional active radar, fore-active radar, and cognitive radar, each progressively more integrated in the way it functions [11].

Traditional adaptive radar techniques have been explored for improving system performance by changing the transmitted waveform or the receiver characteristics using known information about the target or the sensing environment. The groundwork for adaptive radar system technology was laid in [6], in which the optimal transmitted waveform was designed for the estimation of a single extended target, and the optimal transmitted waveform and receiver filter were designed for the detection of a single extended target using an information theoretic approach.

Taking this concept a step further led to the definition of a fore-active radar system, which uses observed data (from the radar return or any other pertinent sensory data) as the input to a scene analyzer and bayesian target tracker to dynamically modify the way that the radar transmitter illuminates the scene or the way that the radar receiver processes the received signal [12–14].

Finally, the concept of a fully cognitive radar system was first introduced in [15]

and employed a closed feedback loop in which the system progressively learns its behavior methods using “memory, attention and enhanced intelligence” throughout its operation [11, 13]. Over the brief time since its inception, a great deal of attention and interest have been devoted to the development, application and improvement of cognitive radar techniques for detection [16–18] estimation [11] and classification [19] of radar targets. In [16] a networked radar system architecture was proposed for detecting the position and velocity of extended targets while simultaneously estimating the surrounding complex urban environment. In [17] an “estimation before detection” process was introduced, which fuses the detection and estimation problems for detection of a single extended target, with an estimator providing iterative updates to the “known” target impulse estimate while the system also adaptively updated the transmitted waveform. In [18] the transmitted beamsteering vector was adaptively designed to detect and track multiple point targets, while [11] described a cognitive radar system patterned after the visual brain to perform estimation and tracking of targets. Additionally, [19] proposed a method to iteratively design the transmitted waveform for the optimal classification of a single extended target.

The traditional adaptive radar, fore-active radar, and cognitive radar system descriptions as discussed have considered the high-level operational concepts of each system; however, in order to understand the methods supporting these concepts more precisely, some background on the application of information theory in the radar context is presented in the following section.

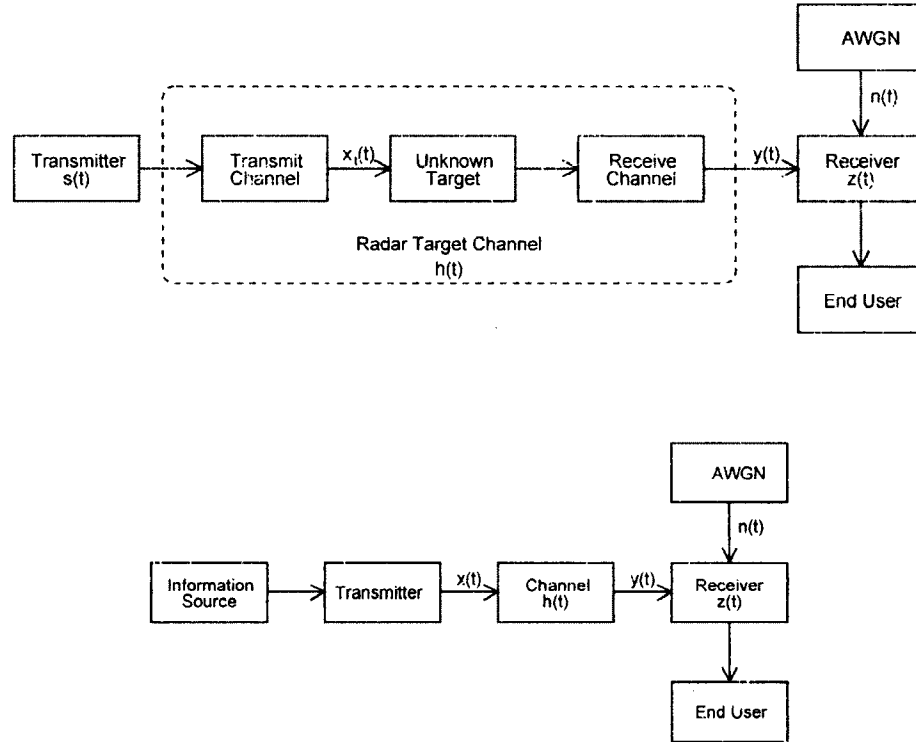


Fig. 2: Radar System versus Communication System

## 1.2.2 INFORMATION THEORY AND RADAR SYSTEM DESIGN

The idea of the radar target channel was introduced in [20, Ch. 2] in order to enable an information-theoretic approach to the design of radar waveforms. As outlined in [20, Ch. 2] the target channel can be represented schematically as shown in Figure 2. Note that although the radar channel appears to be similar to the channel in a traditional communication system also sketched in Figure 2, there is a subtle difference between them: the radar system aims to extract information from the channel, while the communication system aims to transmit information over the channel. Specifically, the following holds true.

- In the radar system the information sought by the end user of information is

related to the target and is embedded in the physical channel that links the transmitter and receiver. In this case the goal is to design the transmitted waveform to extract information about the target and/or to reduce the uncertainty about the target parameters, and in this case the transmitter has no knowledge about the information pursued by the end user of information.

- By contrast, in the traditional communication system the goal is to design the transmitted waveform to efficiently and reliably convey the information from the information source to the end user of information, and in this case the transmitter may take advantage of its knowledge about the information to be transmitted to use specific encoding strategies (such as the “*dirty paper coding*” techniques [21] for example).

Nevertheless, similar problems arise in the information-theoretic optimization of the transmitted waveforms for the two channels.

Information theory was developed for designing information transmission systems and has been used extensively to solve problems in the communications field. Linking the radar and communication system descriptions and problem descriptions can facilitate the cross-discipline transfer of ideas and accelerate the development and improvement of new system design solutions in both fields. In particular, since adaptive and cognitive radar system design is a relatively new field, there is much to be gained from the maturity of information theory if a parallel can be drawn to clearly relate similar radar and information transmission problems. Initial works have begun to explore the application of information theory to radar system design, but a great deal of work still remains to make a full and clear connection.

The first application of information theory to improve the performance of radar systems was for the design of radar receivers [22–24] and has been extended in recent years to adaptively design the transmitted radar waveforms in response to changes in targets, clutter and noise present in the environment as a means for improving radar system performance [4].

Among the first works to discuss information theoretic radar waveform design was [6] which studied optimal waveforms for detection and estimation of a single extended target from the information theoretic perspective. As discussed in [6], in the detection case a threshold is used to determine target presence or absence, and the optimal detection waveform maximizes the Signal- to-Noise Ratio (SNR) while in the estimation case the radar system seeks information about targets known to be present in the environment with the optimal estimation waveform maximizing the mutual information between the target impulse response and the reflected signal seen at the receiver. In [25] this study was extended for the design of optimal estimation waveforms in some specific multiple-target multiple-waveform scenarios. More precisely, [25] considers a MIMO radar system and proposed a waveform design algorithm for multiple-target multiple-waveform estimation based on maximizing a weighted sum of mutual information measures corresponding to each targets and transmitted radar waveform. Also worth noting is the related work regarding waveform design for target estimation using a MIMO radar system in [26], which discussed the equivalence between the maximum mutual information and minimum mean square estimation (MMSE) error and [27] which presented a closed-form expression for the transmitted waveform and receiver filter that minimizes the mean

square estimation error when estimating a single extended target in the presence of signal-dependent clutter. Additionally, [28] addressed the problem of designing waveforms for the detection of a single extended target using a multiple-receiver system in the presence of signal-dependent clutter using a divergence criterion for optimality.

No known previous work has yet drawn a clear parallel between the general MIMO radar system model considering both the detection and estimation of multiple extended targets and a similar multiuser vector channel communication system model.

### **I.2.3 PROBLEM STATEMENT**

The goal of this dissertation is to build a framework for describing a MIMO radar system with multiple targets of interest that clearly exposes the parallel between radar systems and information transmission systems and then to use this model to develop solutions to the radar detection and radar estimation problems based upon corresponding information-theoretic solutions used in communication systems. For each problem, attention will be focused on the optimal waveform and receiver filter design portion of the overall adaptive/cognitive radar system. Tracking and closed-loop behavioral learning aspects are outside the scope of this work.

### **I.3 DISSERTATION CONTRIBUTIONS**

This dissertation proposes a novel approach to model a MIMO radar system for the detection and estimation of multiple extended targets. The proposed model creates an overarching framework that draws a parallel between the MIMO radar system and information transmission systems, allowing the application of information theoretic techniques for radar waveform design. The contributions of this dissertation are as

follows.

- A vector channel model is presented illustrating the parallel composition of the general MIMO radar system and the multiuser vector communication channel.
- Using this framework, the multiple target detection problem is defined, and procedures are presented for designing optimal waveforms and receiver filters by applying a compressed sensing based procedure in both noiseless and noisy scenarios.
- The multiple target estimation problem is examined, and a procedure is presented for designing optimal transmitted waveforms which leverages a similar solution used in the context of waveform design for a collaborative multi-base wireless communication system.

#### I.4 DISSERTATION ORGANIZATION

The organization of this dissertation is shown in Table 1. Chapter II presents the considered MIMO radar system setup and the proposed vector channel framework for representing the system in both the time and frequency domain. Aspects of target modeling are discussed, and some parallels regarding the composition of the considered radar system and similar information transmission systems within the proposed framework are indicated.

Chapter III considers a MIMO radar system used for detection of multiple extended targets in which the scene is spatially partitioned using beamforming. Under the assumption that few targets of interest are present, a compressed sensing based

Table 1: Organization of the Dissertation

<b>Chapter I</b> Introduction			
<b>Chapter II</b> Modeling the MIMO Radar System as a Vector Channel	<b>Chapter III</b> Compressed Sensing Design of Radar Waveforms and Receiver Filters for Detection	<b>Chapter IV</b> Compressed Sensing Design of Radar Waveforms and Receiver Filters for Detection in Noisy Environment	<b>Chapter V</b> Greedy SINR Maximization Based Design of Radar Waveforms For Multiple Target Estimation
<b>Chapter VI</b> Conclusions and Future Research			

procedure is presented for designing waveforms and linear receiver filters for scene reconstruction and target detection.

Chapter IV extends the work of chapter III to consider the case in which additive white noise corrupts the reflected signal at the receiver. In this scenario, the receiver filter designed for the noiseless case is no longer optimal. A procedure is presented for designing the receiver filter specifically to reduce the effect of noise in the reconstructed scene.

Chapter V studies the multiple extended target estimation problem in the framework of the vector channel model. Specifically, a MIMO radar system is considered that uses beamforming to look in the known location of each of multiple targets and estimate its unknown impulse response. To this end, a greedy SINR maximizing procedure for joint waveform design is presented based on a similar solution used in an

information transmission system scenario.

Chapter VI presents closing remarks and indicates open directions for future research.

## CHAPTER II

# MODELING THE MIMO RADAR SYSTEM AS A VECTOR CHANNEL

When the radar target is considered as a linear system acting on the transmitted waveform to produce the received reflected signal as in [6], the parallel between communication systems and radar systems can readily be recognized (see Fig. 2). The two systems are even similar enough that recent radar system design efforts have included the use of communication system based encoding schemes such as Orthogonal Frequency Division Multiplexing (OFDM) to modulate transmitted signals [29–31], and dual purpose hybrid radar/communication systems have been proposed [32, 33].

One major distinction between radar systems and communication systems is that the information the end user seeks in the communication problem is known a-priori at the transmitter, whereas in the radar problem, the information the end user seeks is not known at the transmitter. Rather, it is embedded in the channel itself [6]. Thus, in a communication system the information regarding the transmitted information may be used at the transmitter to determine the best encoding strategy for the message while in a radar system there is no such knowledge of the information that is sought. That is, information regarding the target is unknown to the transmitter. Some implications of this difference are as follows.

- In a communication system, the goal is to optimally reconstruct the signal sent from the transmitter. Therefore, transmission strategies reducing the extent to which the channel affects the signal are sought. By contrast, in a radar

system the goal is to gain knowledge of the target so that transmission strategies emphasizing the effect of the radar target channel on the transmitted signal are sought.

- Another interesting aspect of this difference is illustrated when multiple transmitting users are sharing bandwidth to send simultaneous messages versus when multiple waveforms are used to view multiple radar targets. In the communication system case, the way that one user's message is encoded may not necessarily dictate the encoding scheme of other users' signals. However, if multiple radar waveforms are transmitted for multiple targets, the waveform designed for one target will be reflected from other targets as well so that separating information from each target cannot be done in a straightforward manner using only the modulation scheme of the transmitted waveform.

Despite these complications, it is possible to formulate very similar models and solutions for many problems addressed by radar systems and information transmission systems. This chapter formulates such a model of a general MIMO radar system that reveals the similarities with a multiuser vector communication channel.

## II.1 SYSTEM SETUP

The system under consideration is a general MIMO radar system in which multiple antennas are used for the transmission and processing of multiple waveforms and in which multiple targets may be present within the radar scene. Using transmit and receive beamforming, the radar scene is partitioned into a set of disjoint regions, or cells, such that a given cell may contain one or more targets as outlined in Figure 3.

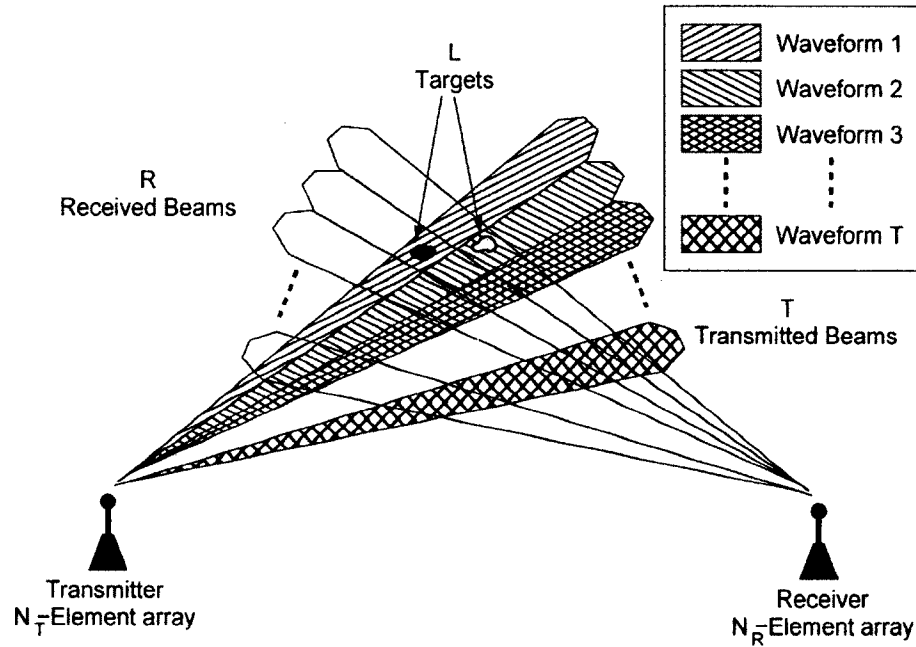


Fig. 3: System setup

Using this setup some analogies between specific characteristics of communication systems and radar systems can be drawn by considering particular components of the general model.

- The targets present in the radar system may be directly related both to the number of transmitting users in a communication system and to the number of channels over which messages are transmitted in a communication system.
- The transmitted radar pulses may be related to the waveforms used to encode digital information in a communication system.
- Increasing the number of transmit or receive directions in the described radar system is analogous to increasing the number of channels in a communication system. This increase is not necessarily linear but is instead dependent on the number of cells with nonzero reflection coefficients. For example, consider

the following: if the beams were perfectly directed so that all energy for each transmit/receive beam pair was contained within a single cell of the spatially discretized scene, the number of channels would be equal to the number of transmit beams times the number of receive beams. However, since the beams will not be perfectly directed to only a single cell, each beam will be reflected at many points within the space (though the strength of that reflection will vary with the magnitude of each reflection coefficient).

Proceeding with the mathematical description of the system, let  $L$  be the number of targets of interest to be detected, with the impulse response of a given target  $\ell$  denoted by  $h_\ell(t)$  and assumed normalized to have unit energy. Furthermore, let  $\alpha_T^{(\ell)}$  and  $\alpha_R^{(\ell)}$  be the pathloss coefficients corresponding to the free-space propagation between the radar transmitter and target  $\ell$  and between the target and the radar receiver, respectively. Similar to [25], the radar transmitter sends multiple waveforms  $s_d(t)$  normalized to unit energy with energy levels  $p_d$ ,  $d = 1, \dots, T$ , with each waveform focused in a specific direction by transmit beamforming vector  $\mathbf{u}_d \in \mathbb{C}^{N_T \times 1}$ , where  $N_T$  is the number of transmit antennas in the transmitter array. Thus, the transmitted MIMO radar signal is a sum of all the beamformed waveforms:

$$\mathbf{s}(t) = \sum_{d=1}^T \mathbf{u}_d s_d(t) \sqrt{p_d}. \quad (\text{II.1.1})$$

Assuming that target  $\ell$  is at azimuth angle  $\tau_\ell$  relative to the transmit antenna array and that the transmit array manifold vector in the direction of the target is represented by  $\mathbf{a}_T(\tau_\ell) \in \mathbb{C}^{N_T \times 1}$ , the signal reflected by the target  $\ell$  can be written as

$$y_\ell(t) = h_\ell(t) \star [\mathbf{a}_T^H(\tau_\ell) \mathbf{s}(t) \alpha_T^{(\ell)}], \quad \ell = 1, \dots, L, \quad (\text{II.1.2})$$

where  $\star$  represents the convolution operation, and  $(\cdot)^H$  denotes the complex conjugate transpose operation.

At the MIMO receiver, the signal reflected by target  $\ell$  (II.1.2) is received from azimuth direction  $\rho_\ell$  through the receive antenna array with manifold vector  $\mathbf{a}_R(\rho_\ell) \in \mathbb{C}^{N_R \times 1}$  in the direction of the target, and the corresponding received signal  $\mathbf{z}_\ell(t) = \alpha_R^{(\ell)} \mathbf{a}_R(\rho_\ell) y_\ell(t)$  is written as:

$$\mathbf{z}_\ell(t) = [\alpha_R^{(\ell)} \mathbf{a}_R(\rho_\ell) \mathbf{a}_T^H(\tau_\ell) \alpha_T^{(\ell)}] \sum_{d=1}^T \mathbf{u}_d [h_\ell(t) \star s_d(t)] \sqrt{p_d}. \quad (\text{II.1.3})$$

Combining signals reflected from all targets and assuming that a vector noise process  $\mathbf{w}(t)$  corrupts signals at the receive antenna array, the total received signal expression becomes:

$$\mathbf{z}(t) = \sum_{\ell=1}^L \mathbf{z}_\ell(t) + \mathbf{w}(t). \quad (\text{II.1.4})$$

The noise processes in  $\mathbf{w}(t)$  correspond to bandpass filtered versions of the noise processes that corrupt signals at all receive antennas, which are assumed to be white and Gaussian with power spectral density (PSD)  $Q_\epsilon(f) = \sigma^2$  for all frequencies  $f$  and all receive antennas  $\epsilon = 1, \dots, N_R$ .

The received signal vector  $\mathbf{z}(t)$  is processed by the  $N_R$ -antenna array of the MIMO radar receiver through beamforming vectors  $\mathbf{v}_r \in \mathbb{C}^{N_R \times 1}$  to yield scalar signals  $z_r(t) = \mathbf{v}_r^H \mathbf{z}(t)$  for each of the  $r = 1, \dots, R$  receive directions, where

$$z_r(t) = \sum_{\ell=1}^L \sum_{d=1}^T \lambda_{rd}^{(\ell)} [h_\ell(t) \star s_d(t)] \sqrt{p_d} + \mathbf{v}_r^H \mathbf{w}(t) \quad (\text{II.1.5})$$

and  $\lambda_{rd}^{(\ell)} = \alpha_R^{(\ell)} \mathbf{v}_r^H \mathbf{a}_R(\rho_\ell) \mathbf{a}_T^H(\tau_\ell) \mathbf{u}_d \alpha_T^{(\ell)}$ . The scalar  $\lambda_{rd}^{(\ell)}$  combines the pathloss coefficients along with the transmit and receive beamforming and array manifold vectors, and, due to the uncertain position of the target implied by angles  $\rho_\ell$  and  $\tau_\ell$ , is a random coefficient corresponding to target  $\ell$ , transmit waveform/direction  $d$  and receive

direction  $r$ .

Taking the Fourier transform of (II.1.5) results in the frequency domain representation

$$Z_r(f) = \sum_{\ell=1}^L \sum_{d=1}^T \lambda_{rd}^{(\ell)} H_\ell(f) S_d(f) \sqrt{p_d} + \mathbf{v}_r^H \mathbf{W}(f), \quad (\text{II.1.6})$$

where  $\mathbf{W}(f)$  is a vector of random functions in the frequency domain with statistics implied by the PSD of the noise processes that make up  $\mathbf{w}(t)$ . Since the noise processes in vector  $\mathbf{w}(t)$  affecting signals at the receive antennas are bandpass and have finite energy, their sample functions can be assumed Fourier transformable [6].

## II.2 TARGET MODELING

In the discussion and simulations in subsequent chapters, specific range-extended targets are considered to be a sum of point targets, or “reflection centers”, spread out in range that make up a single extended target, and each of the extended targets is assumed to reside in a single transmit/receive beam pair cell. This assumption is not excessively restrictive, as even beams with small radial width will cover a large area relative to the target size when the target is distant from the transmitter and receiver. Mathematically, the extended target model can be expressed as follows:

$$h_\ell(t) = \sum_{r_c=1}^{R_c} \eta_{r_c}^{(\ell)} \delta(t - \tau_{r_c}^{(\ell)}) \quad (\text{II.2.1})$$

where  $r_c$  is the index of each reflection center, and  $\eta_{r_c}^{(\ell)}$  is the magnitude of the response from each reflection center received with a corresponding delay  $\tau_{r_c}^{(\ell)}$  determined by its range.

### II.2.1 REFLECTION CENTERS AND AZIMUTH AMBIGUITY

When using this target model in the considered bistatic radar system along with the assumption that the array manifold is essentially constant over the radial extent of the target, there is some inherent ambiguity as to the exact radial configuration of reflection centers that compose the range-extended target. This ambiguity is not a shortcoming of the proposed model. Rather, it is an artifact of the considered bistatic system which, though not necessarily explicitly discussed, will be present in similar models of the same system (e.g. [26]). Consider the following: when looking at the bistatic radar scenario in Figure 3, target extension in range implies extension in the total range observed from the transmitter to reflection center and then to the receiver. Thus, a reflection center with a range of  $d_{rc}^{(\ell)}$  must lie on an ellipse with foci defined at the transmitter and receiver. Using linear beamforming as defined in the system model, each reflection center can be further localized to belong within a transmit/receive beam pair cell as shown in Figure 4. Thus, knowledge of the range distribution of reflection centers corresponding to a given target may not uniquely represent only that target. However, when coupled with additional information, range distribution knowledge is still useful. For example, in the detection case, the system may decide a target is present when characterized by a collection of reflection centers of known range distribution, and it may be unlikely that any target other than the target sought would fit this description. In the event that another target had the same range distribution of reflection centers the result would be a false positive. In the estimation case, knowing the range distribution of reflection centers may still provide a good deal of information about the unknown target of interest since there

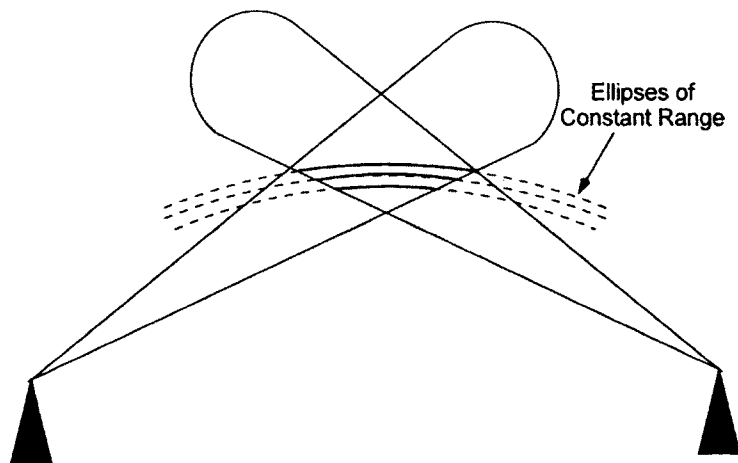


Fig. 4: Azimuth ambiguity as seen in the bistatic MIMO radar system with beamforming

may not exist many targets that have the specified range distribution of reflection centers. Though these are interesting points to note, further consideration of this issue is beyond the scope of this work.

Future work in developing techniques to mitigate effects of azimuth ambiguity could include analysis of small variations in the array manifold over small changes in the azimuth extent of the target, incremental beam scanning to further specify the location of each reflection center, or inclusion of known target-specific geometries (e.g., all targets are assumed to have a linear configuration of reflection centers).

## II.2.2 REFLECTION COEFFICIENTS

There are a few interesting points to note regarding the reflection coefficients associated with each target.

- Although targets are assumed stationary in the current model, Doppler shift

could be considered by adding a parameter to this reflection coefficient description, resulting in an additional dimension to be considered during what is later described as the scene reconstruction phase of the problem.

- If the spatial diversity condition as described in [34] is satisfied, each of these reflection coefficients will be uncorrelated with one another. However, meeting this condition is not required in this study.
- Equation (II.1.5) implies an extended target model similar to the one used in [28] where targets are represented by random complex reflection factors multiplying the known (deterministic) part of the target impulse response.

### II.3 THE FREQUENCY DOMAIN VECTOR CHANNEL MODEL

Choosing  $K$  frequencies,  $\{f_1, \dots, f_k, \dots, f_K\}$  of interest over which to discretize the frequency domain signal and assuming that the frequency intervals are chosen to be small enough so that  $H_t(f)$ ,  $S_d(f)$  and  $\mathcal{W}(f)$  can be considered to remain constant over a given frequency interval as in [6], the received signal vector and transmitted signal vector can be defined as:

$$\mathbf{z}_r = \begin{bmatrix} Z_r(f_1) \\ \vdots \\ Z_r(f_k) \\ \vdots \\ Z_r(f_K) \end{bmatrix}, \mathbf{s}_d = \begin{bmatrix} S_d(f_1) \\ \vdots \\ S_d(f_k) \\ \vdots \\ S_d(f_K) \end{bmatrix}, \quad (\text{II.3.1})$$

along with the  $K \times K$  diagonal target frequency response matrix for the  $\ell$ -th target

$$\mathbf{H}_\ell = \begin{bmatrix} H_\ell(f_1) & \dots & \dots & \dots & 0 \\ \vdots & \ddots & \vdots & \vdots & \vdots \\ 0 & \dots & H_\ell(f_k) & \dots & 0 \\ \vdots & \vdots & \vdots & \ddots & \vdots \\ 0 & \dots & \dots & \dots & H_\ell(f_K) \end{bmatrix}, \quad (\text{II.3.2})$$

and the  $K \times N_R$  matrix of noise at each antenna element over all frequencies:

$$\mathbf{W} = \begin{bmatrix} \mathcal{W}_1(f_1) & \dots & \mathcal{W}_n(f_1) & \dots & \mathcal{W}_{N_R}(f_1) \\ \vdots & \ddots & \vdots & \vdots & \vdots \\ \mathcal{W}_1(f_k) & \dots & \mathcal{W}_n(f_k) & \dots & \mathcal{W}_{N_R}(f_k) \\ \vdots & \vdots & \vdots & \ddots & \vdots \\ \mathcal{W}_1(f_K) & \dots & \mathcal{W}_n(f_K) & \dots & \mathcal{W}_{N_R}(f_K) \end{bmatrix}. \quad (\text{II.3.3})$$

With this notation the received signal can be written using a compact vector channel form as:

$$\mathbf{z}_r = \sum_{\ell=1}^L \sum_{d=1}^T \lambda_{rd}^{(\ell)} \mathbf{H}_\ell \mathbf{s}_d \sqrt{p_d} + \mathbf{W} \mathbf{v}_p^*, \quad r = 1, \dots, R, \quad (\text{II.3.4})$$

where  $*$  denotes the complex conjugate operation. Combining the receiver beamforming vector and noise correlation matrix to a single vector  $\mathbf{n}_p$  gives

$$\mathbf{z}_r = \sum_{\ell=1}^L \sum_{d=1}^T \lambda_{rd}^{(\ell)} \mathbf{H}_\ell \mathbf{s}_d \sqrt{p_d} + \mathbf{n}_r, \quad r = 1, \dots, R, \quad (\text{II.3.5})$$

Furthermore, the following are assumed:

1. The transmit and receive beamforming vectors have unit norm.
2. Components of  $\mathbf{w}(t)$  are uncorrelated between receive antenna elements.

3. Components of  $\mathcal{W}(f)$  are uncorrelated over distinct frequencies at the same antenna element.

Assumptions 2 and 3 imply that the noise correlation matrix  $\mathbf{R}_{\mathbf{n}_r} = E\{\mathbf{n}_r \mathbf{n}_r^H\}$  is diagonal. That is,  $\mathbf{R}_{\mathbf{n}_r} = \text{diag}\{\sum_{\epsilon=1}^{N_R} |v_{r\epsilon}|^2 Q_\epsilon(f_1), \dots, \sum_{\epsilon=1}^{N_R} |v_{r\epsilon}|^2 Q_\epsilon(f_K)\}$ , where  $Q_\epsilon(f_k)$  is the PSD of the noise at antenna  $\epsilon$  evaluated at frequency  $f_k$ . This is shown to be true in Appendix A.

Define the  $T \times T$  diagonal matrix of transmit waveform energies

$$\mathbf{P} = \text{diag}\{p_1 \dots p_T\}, \quad (\text{II.3.6})$$

constructing the  $T \times R$  matrices of reflection coefficients for all targets  $\ell = 1, \dots, L$ , at each position  $d$  and  $r$  within the grid of transmitted and received beams,

$$\Lambda_\ell = \begin{bmatrix} | & & | \\ \lambda_1^{(\ell)} & \dots & \lambda_R^{(\ell)} \\ | & & | \end{bmatrix}, \text{ with } \lambda_r^{(\ell)} = \begin{bmatrix} \lambda_{r1}^{(\ell)} \\ \vdots \\ \lambda_{rT}^{(\ell)} \end{bmatrix}.$$

Define the  $K \times T$  matrix of transmitted waveform vectors

$$\mathbf{S} = \begin{bmatrix} | & & | \\ \mathbf{s}_1 & \dots & \mathbf{s}_T \\ | & & | \end{bmatrix}, \quad (\text{II.3.7})$$

and group the received signal and noise vectors  $\mathbf{z}_p$  and  $\mathbf{n}_r$  over all received directions  $r = 1, \dots, R$  into  $K \times R$  matrices

$$\mathbf{Z} = \begin{bmatrix} | & & | \\ \mathbf{z}_1 & \dots & \mathbf{z}_R \\ | & & | \end{bmatrix} \text{ and } \mathbf{N} = \begin{bmatrix} | & & | \\ \mathbf{n}_1 & \dots & \mathbf{n}_R \\ | & & | \end{bmatrix}. \quad (\text{II.3.8})$$

A compact model for the considered multi-waveform multi-target radar scenario is obtained and described by the matrix equation:

$$\mathbf{Z} = \sum_{\ell=1}^L \mathbf{H}_\ell \mathbf{S} \mathbf{P}^{1/2} \boldsymbol{\Lambda}_\ell + \mathbf{N}. \quad (\text{II.3.9})$$

This notation can be written more compactly by defining the target impulse response matrix,  $\mathbf{H}$ :

$$\mathbf{H} = [\mathbf{H}_1 | \cdots | \mathbf{H}_\ell | \cdots | \mathbf{H}_L], \quad (\text{II.3.10})$$

and the  $KL \times TL$  transmitted waveform matrix  $\bar{\mathbf{S}} = \mathbf{I}_L \otimes \mathbf{S}$ , where  $\otimes$  is the Kronecker product as defined in [35] so that:

$$\bar{\mathbf{S}} = \begin{bmatrix} \mathbf{S} & \cdots & 0 & \cdots & 0 \\ \vdots & \ddots & \vdots & \vdots & \vdots \\ 0 & \cdots & \mathbf{S} & \cdots & 0 \\ \vdots & \vdots & \vdots & \ddots & \vdots \\ 0 & \cdots & 0 & \cdots & \mathbf{S} \end{bmatrix}, \quad (\text{II.3.11})$$

as well as the  $TL \times R$  block matrix  $\boldsymbol{\Lambda}$  combining all reflection coefficients:

$$\boldsymbol{\Lambda} = \begin{bmatrix} \boldsymbol{\Lambda}_1 \\ \vdots \\ \boldsymbol{\Lambda}_\ell \\ \vdots \\ \boldsymbol{\Lambda}_L \end{bmatrix}. \quad (\text{II.3.12})$$

With these notations and assuming for mathematical simplicity that all transmit waveform energies are equal to  $p$  (that is  $\mathbf{P} = p\mathbf{I}_T$ ), equation (II.3.9) is equivalent to

$$\mathbf{Z} = \sqrt{p} \mathbf{H} \bar{\mathbf{S}} \boldsymbol{\Lambda} + \mathbf{N}. \quad (\text{II.3.13})$$

From the models presented in (II.3.9) and (II.3.13), some similarity to a MIMO multiple access vector communication channel scenario can be observed. Additionally, several notable specific scenarios are encompassed within this framework.

1. The case in which a single waveform is transmitted over a single transmit/receive beam pair to illuminate a single target ( $T = R = L = 1$ ) reduces to a model directly comparable to the single-user vector communication channel as in [36].
2. A single waveform/multiple target scenario corresponds to the case of  $T = 1$  and  $L > 1$ , in which case the transmitted waveform matrix becomes a single vector. Assuming that the transmit and receive beamforming vectors are designed such that the corresponding scalar coefficients  $\lambda_p^{(\ell)} \simeq 0$ , for  $\ell \neq p$ , this scenario corresponds to a broadcast communication channel scenario.
3. When the number of radar pulses and targets are the same,  $T = L$ , and assuming again that the transmit and receive beamforming vectors are designed such that the scalar coefficients  $\lambda_{p,d}^{(\ell)} \simeq 0$ , for all  $d = 1, \dots, T$  and  $\ell \neq p$ , equation (II.3.5) can be rewritten as

$$\mathbf{z}_r = \sum_{\ell=1}^L \lambda_{r,d}^{(\ell)} \mathbf{H}_\ell \mathbf{s}_\ell + \mathbf{n}_r, \quad r = 1, \dots, L, \quad (\text{II.3.14})$$

and corresponds to an interference channel scenario.

## II.4 THE TIME DOMAIN VECTOR CHANNEL MODEL

To formulate the time domain vector channel, recall the equation of the received signal from direction  $r$  given by (II.1.5). Additionally, using the target model of II.2.1 the target impulse response can be rewritten as a finite impulse response (FIR) filter

with uniform sampling as

$$h_\ell(t) = \sum_{v=1}^{\Upsilon} g_\ell(vT)\delta(t - vT) \quad (\text{II.4.1})$$

where  $T$  is the sampling period, and  $g_\ell$  is the magnitude of the response from each reflection center seen along the extended target which is equal to  $\eta_{r_c}^{(\ell)}$  when a reflection center is present and zero when no reflection center is present at the location corresponding to a delay of  $vT$  along the target.

The expression for the convolution of  $h_\ell(t)$  with  $s_d(t)$  can be expanded to rewrite (II.1.5) as:

$$\begin{aligned} z_r(t) &= \sum_{\ell=1}^L \sum_{d=1}^T \lambda_{rd}^{(\ell)} \left[ \int_{-\infty}^{\infty} \sum_{v=1}^{\Upsilon} g_\ell(vT)\delta(\tau - vT)s_d(t - \tau)d\tau \right] \sqrt{p_d} + n_r(t), r = 1, \dots, R \\ &= \sum_{\ell=1}^L \sum_{d=1}^T \lambda_{rd}^{(\ell)} \sum_{v=1}^{\Upsilon} g_\ell(vT)s_d(t - vT)\sqrt{p_d} + n_r(t), r = 1, \dots, R. \end{aligned} \quad (\text{II.4.2})$$

Sampling the output at  $t = 0, \dots, kT, \dots, KT$  gives the discrete time domain representation of the received signal

$$z_r(k) = \sum_{\ell=1}^L \sum_{d=1}^T \sum_{v=1}^{\Upsilon} \lambda_{rd}^{(\ell)} g_\ell(v)s_d(k - v)\sqrt{p_d} + n_r(k), r = 1, \dots, R. \quad (\text{II.4.3})$$

In vector-matrix notation, the received signal can be represented as

$$\mathfrak{z}_r = \sum_{\ell=1}^L \sum_{d=1}^T \lambda_{rd}^{(\ell)} \sqrt{p_d} \mathcal{S}_d \mathbf{g}_\ell + \mathbf{n}_r, r = 1, \dots, R, \quad (\text{II.4.4})$$

when the  $K \times 1$  discrete time domain received signal vector is defined as

$$\mathfrak{z}_r = \begin{bmatrix} z_r(k) \\ \vdots \\ z_r(k + K - 1) \end{bmatrix}, \quad (\text{II.4.5})$$

the  $K \times \Upsilon$  circulant convolution matrix for the transmitted waveform in direction  $d$  is defined as

$$\mathbf{S}_d = \begin{bmatrix} s_d(k) & \dots & s_d(k - \Upsilon) \\ \vdots & \ddots & \vdots \\ s_d(k + K - 1) & \dots & s_d(k + K - 1 - \Upsilon) \end{bmatrix}, \quad (\text{II.4.6})$$

and the  $\Upsilon \times 1$  target impulse response vector is defined as

$$\mathbf{g}_\ell = \begin{bmatrix} g_\ell(0) \\ \vdots \\ g_\ell(\Upsilon) \end{bmatrix}, \quad (\text{II.4.7})$$

as well as the noise vector observed in receive direction  $r$

$$\mathbf{n}_r = \begin{bmatrix} n_r(k) \\ \vdots \\ n_r(k + K - 1) \end{bmatrix}. \quad (\text{II.4.8})$$

With these notations, the radar target channel model appears similar to that of OFDM multicarrier modulation in communications [37, Ch. 12.4] where instead of representing the channel with a circulant matrix, the transmitted waveforms are represented with a circulant matrix. This is intuitive given the intrinsic difference of radar and communication systems in that the location of the known quantities (the channel in the case of communication system, and the transmitted waveform in the case of the radar system) are contained in the circulant matrix.

For a more compact representation,  $\mathbf{S}_d$  and  $\lambda_{r_d}^{(\ell)}$  as defined in (II.4.4) can each be

combined over  $T$  transmit directions as follows

$$\bar{\mathbf{S}} = \left[ \sqrt{p_1} \mathbf{S}_1 | \dots | \sqrt{p_T} \mathbf{S}_T \right], \Lambda_r^{(\ell)} = \begin{bmatrix} \lambda_{r1}^{(\ell)} \mathbf{I}_R & \dots & 0 \\ \vdots & \ddots & \vdots \\ 0 & \dots & \lambda_{rT}^{(\ell)} \mathbf{I}_R \end{bmatrix}, \quad (\text{II.4.9})$$

while also forming the combined vector  $\bar{\mathbf{g}}_\ell$  in which  $\mathbf{g}_\ell$  is repeated  $T$  times:

$$\bar{\mathbf{g}}_\ell = \begin{bmatrix} \mathbf{g}_\ell \\ \vdots \\ \mathbf{g}_\ell \end{bmatrix} \quad (\text{II.4.10})$$

so that the received signal vector can be written as

$$\mathbf{z}_r = \sum_{\ell=1}^L \bar{\mathbf{S}}_d \Lambda_r^{(\ell)} \bar{\mathbf{g}}_\ell + \mathbf{n}_r, \quad r = 1, \dots, R. \quad (\text{II.4.11})$$

Finally, combining the received signal vectors from all directions into a single vector gives the following more compact representation:

$$\mathbf{z} = \bar{\bar{\mathbf{S}}} \Lambda \mathbf{g} + \mathbf{n} \quad (\text{II.4.12})$$

where

$$\mathbf{z} = \begin{bmatrix} \mathbf{z}_1 \\ \vdots \\ \mathbf{z}_R \end{bmatrix}, \quad \mathbf{g} = \begin{bmatrix} \mathbf{g}_1 \\ \vdots \\ \mathbf{g}_L \end{bmatrix}, \quad \mathbf{n} = \begin{bmatrix} \mathbf{n}_1 \\ \vdots \\ \mathbf{n}_R \end{bmatrix} \quad (\text{II.4.13})$$

and

$$\bar{\bar{\mathbf{S}}} = \mathbf{I}_R \otimes \bar{\mathbf{S}}, \quad \Lambda_r = \left[ \Lambda_r^{(1)} | \dots | \Lambda_r^{(L)} \right]. \quad (\text{II.4.14})$$

This is similar to the bistatic MIMO radar system model in [26] but extended to consider the case in which beamforming is used and multiple extended targets of interest are present.

## II.5 RELATING THE TIME AND FREQUENCY DOMAIN MODELS

Assuming the target response is observed for the same duration as the transmitted pulse duration so that  $K = T$  allows application of the  $K$ -Point DFT matrix  $\mathcal{F}$  to the reflected signal to obtain the frequency domain representation:

$$\underbrace{\mathcal{F}y_r}_{\mathbf{y}_r} = \sum_{\ell=1}^L \sum_{d=1}^T \lambda_{rd}^{(\ell)} \sqrt{p_d} \underbrace{\mathcal{F}\mathbf{S}_d\mathcal{F}^H}_{\underline{\mathbf{S}}_d} \underbrace{\mathcal{F}\mathbf{g}_\ell}_{\mathbf{h}_\ell}, r = 1, \dots, R \quad (\text{II.5.1})$$

where  $\underline{\mathbf{S}}_d = \mathcal{F}\mathbf{S}_d\mathcal{F}^H$  is a diagonal matrix containing the frequency domain representation of the transmitted waveform defined for frequency bins of width  $f_s$  centered at frequencies  $f_k = f_s k, k = 0, \dots, (K - 1)$  along the diagonal since  $\mathbf{S}_d$  is circulant, and  $\mathbf{h}_\ell$  is the discretized target frequency response. Including the noise term, where the frequency domain representation of the noise vector  $\mathbf{n}_r$  is determined by statistics implied by the stochastic process  $n_r(t)$  at each frequency  $f_k, k = 0, \dots, K$  gives an equivalent model to the frequency domain vector channel model of equation (II.3.5).

That is,

$$\begin{aligned} \mathbf{z}_r &= \sum_{\ell=1}^L \sum_{d=1}^T \lambda_{rd}^{(\ell)} \sqrt{p_d} \underline{\mathbf{S}}_d \mathbf{h}_\ell + \mathbf{n}_r \\ &= \sum_{\ell=1}^L \sum_{d=1}^T \lambda_{rd}^{(\ell)} \sqrt{p_d} \mathbf{H}_\ell \mathbf{s}_d + \mathbf{n}_r, r = 1, \dots, R. \end{aligned} \quad (\text{II.5.2})$$

Also worth noting at this point is that neither the time domain nor frequency domain representation has specified whether the detection or estimation scenario is considered, as the model is applicable to both problems. Recognizing this, the next step is to individually approach the detection and estimation problems from this new framework which is the subject of following chapters, both for specific instances contained within the general setup (i.e. single-target, single-waveform, or single receiver filter

design problems), as well as the more general multiple target, multiple waveform and multiple receiver filter design problems.

## II.6 CHAPTER SUMMARY

This chapter presented the system setup as well as a vector-channel model describing that system which will allow for easier application of linear algebra techniques than traditional scalar representations. Both time domain and frequency domain versions of this system model were included. Parallels between the considered radar system and similar information transmission systems were indicated, and specific components of the radar system were related to various components of communication systems.

The proposed framework is novel because of the compact notation presented which closely resembles a multiuser communication channel while describing a general multi-target MIMO radar system which can easily be particularized for different scenarios. It has not yet inherently specified whether detection or estimation is the goal so that either problem can be addressed using this model. As such, this description facilitates comparison of the two systems and provides a basis for realizing similarities in the resulting optimal waveform design methods.

# CHAPTER III

## COMPRESSED SENSING DESIGN OF RADAR WAVEFORMS AND RECEIVER FILTERS FOR TARGET DETECTION

In the case of radar target detection, the end user seeks knowledge of whether or not a target with a known description is present in the radar scene. In many practical scenarios, the radar detection problem can be posed as a sparse reconstruction problem since relatively few targets of interest are present within a larger scene. This perspective allows the use of compressed sensing techniques [38,39] to reconstruct the radar scene.

Though compressed sensing is not a traditional information theoretic concept, compressed sensing aims to convey information efficiently to the end user and as such the compressed sensing measurement system can itself be considered as an information transmission system [40]. Additionally, compressed sensing has been applied for channel estimation in information transmission systems in recent literature [41–43].

Compressed sensing has also been of interest for use with radar systems, as the radar scene is generally sparse in some domain when few targets of interest are present. Several motivating factors for using compressed sensing in the radar context have been stated in recent literature. These include reducing the analog-to-digital conversion bandwidth, allowing receiver processing without the use of a matched filter, and the opportunity to achieve higher resolution between targets [44].

In both of these scenarios, compressed sensing is used to extract sparse data of

interest from either the radar target channel or the information transmission channel. As such, compressed sensing can be considered a technique that is applicable to both radar systems and communication systems, suggesting again that similar techniques may be used in the context of both systems. Within the proposed framework it will be shown that compressed sensing provides a way to design waveforms and linear receiver filters for detection of multiple extended targets with known frequency responses, essentially allowing simultaneous detection and classification of these targets. An overview of the main concepts of compressed sensing is given in Appendix B.

Compressed sensing has been applied to study detection of multiple point targets in the classical radar setup [45, 46] by exploiting sparsity in the range-Doppler or range/cross-range plane, with [47–50] extending this concept for MIMO radar. Additionally, [44] presented a simultaneous waveform and receiver filter design algorithm for compressed sensing based detection of point targets in a MIMO radar system. In the case of extended targets, the range-Doppler representation of the target scene commonly used for detecting point targets is no longer sparse even when only a few targets are present, and direct application of existing compressed sensing techniques is not straightforward. To the best of the author’s knowledge, no other work has considered the optimization of multiple transmitted waveforms and of corresponding receiver filters for the reconstruction of a spatially sparse scene containing multiple *extended* targets in the context of compressed sensing, which is addressed in this work. This motivates the work presented in this chapter, which studies application of compressed sensing techniques to waveform design in MIMO radar systems for detection of multiple extended targets.

Specifically, transmit-receive beamforming is used in conjunction with a compact representation of radar waveforms in terms of a set of discrete frequencies to partition a radar scene with multiple extended targets and to cast the extended target detection problem similar to the one presented in [51] in terms of an equivalent sparse scene reconstruction problem. This allows application of compressed sensing theory to perform joint optimization of radar waveforms and receiver filters and subsequent scene reconstruction using known techniques.

Compressed sensing was used in [44] for the detection of multiple, sparsely distributed point targets within the range-Doppler plane. Unfortunately, the extension of their work for the detection of multiple point targets is not straightforward since the representation of extended targets would not necessarily result in a sparse distribution of targets in the range-Doppler plane in their presented framework. For example, consider the target modeled by II.2.1 where the extended target is modeled as a collection of scatterers, each with known reflection factor  $\eta_{r_c}^{(\ell)}$ . Placing this description in the model presented in [44], one can see that the resulting distribution of target points within the range-Doppler grid will not necessarily be sparse since extended targets appear as clusters of point targets. However, if the scene is spatially partitioned using beamforming as indicated in the proposed system model, the reflection coefficients  $\lambda_{r_d}^{(\ell)}$  will be small in locations where targets are not present, and large in locations where targets are present. That is,  $\lambda_{r_d}^{(\ell)}$  will be large when the beamforming vector aligns with the direction of the target so that the combined value of the beamforming vector and array manifold in the direction of the target will be large. This will result in a spatially sparse grid of reflection coefficients as long as the

number of transmit/receive beam cells is much greater than the number of targets present in the scene. This sparsity in the presented framework can be exploited so that techniques similar to those used in [44] can be used for waveform and receiver filter design and subsequently reconstruct the scene and detect targets of interest.

### III.1 COMPRESSED SENSING FOR MIMO RADAR

Within the proposed framework of (II.3.13) the presence of a specific target  $m$  may be detected by looking at its corresponding reflection coefficients  $\lambda_{rd}^{(m)}$  in the reflection coefficient matrix  $\mathbf{\Lambda}$ . This implies that the problem of detecting a target with known response can be solved by reconstructing the matrix of reflection coefficients, and applying a threshold to determine whether each target is present at each location in the partitioned scene based on the corresponding reflection coefficients. In this case, the optimal transmitted waveforms and associated receiver processing method would be designed to optimally reconstruct the reflection coefficient matrix.

Designing waveforms and receiver filters for optimal reconstruction of the reflection coefficient matrix is not a straightforward problem to solve using traditional methods within the proposed framework. Using traditional methods, the optimal receiver filter should be matched to the reflected signal while maximizing the SNR observed at the receiver when considering an extended target as in [6], which would require knowledge of the statistics of the reflection coefficients. The statistics of the reflection coefficients are not known since the reflection coefficients are functions of the unknown (stochastic) orientation of each target with respect to the transmitter and receiver. These statistics would be difficult to define even assuming that a target

is assumed to be present within a given cell. However, as each target's presence or absence is unknown, there is further uncertainty in the value of the reflection coefficient since it will only be nonzero when the corresponding target is present somewhere in the scene. Instead, avoiding consideration of the specific statistics of the reflection coefficients and using the knowledge that the reflection coefficient matrix should be sparse, suitable waveforms and receiver filters can be defined such that the reconstruction can be performed nearly optimally as long as the grid of reflection coefficients  $\mathbf{\Lambda}$  is sufficiently sparse, and there is low coherence between the linear receiver filter used for processing the received signal  $\mathbf{C}$  and the combined target frequency response matrix and transmitted waveform matrix  $\mathbf{H}\bar{\mathbf{S}}$ . The condition on the sparsity of the scene can be met as long as the number of targets is small relative to the number of transmit-receive beam pairs ( $L \ll TR$ ), while  $\mathbf{C}$  and  $\mathbf{H}\bar{\mathbf{S}}$  can be specifically designed to meet the requirement of low coherence. This can be accomplished using techniques similar to those in [44] for waveform and receiver filter design and subsequent scene reconstruction and target detection.

Specifically, translating the basic compressed sensing process into the context of the considered radar system results in the following steps for optimizing radar waveforms for detection of multiple extended targets as follows:

**Step 1: Design transmitted waveform matrix  $\mathbf{S}$**  such that the  $K \times TL$  matrix  $\mathbf{H}\bar{\mathbf{S}}$  in (II.3.13) can be used as an overcomplete dictionary. This converts the columns of the cluttered  $\mathbf{\Lambda}$  to a representation in which the data set is sparse and contains a maximum of  $L$  nonzero samples. To meet the requirements of an overcomplete dictionary,  $\mathbf{H}\bar{\mathbf{S}}$  must be a matrix with full row rank. When the number of actual targets

of interest is small, this can be ensured by augmenting the target frequency response matrix  $\mathbf{H}$  with additional rows chosen to ensure that the overcomplete dictionary is of full row rank. These additional rows may be chosen arbitrarily as long as the rank constraint is met, and how this choice is made is not the focus in this work. However, it is worth noting that any clutter sources of known response could be considered as additional targets within this framework to simultaneously ensure the rank constraint is met while also obtaining additional information about these sources.

**Step 2: Compress received signal** using  $Q \times K$  sampling matrix  $\mathbf{C}$  with  $Q \geq L$ , so that the result has enough data points to describe the targets of interest. It is worth noting here that compressed sensing requires low coherence between  $\mathbf{C}$  and  $\mathbf{H}\bar{\mathbf{S}}$  to ensure the Restricted Isometry Property (RIP) [53] is met. As it is difficult to verify that the RIP is met, an alternative metric will be considered to ensure incoherence which was defined in [54]: the mutual coherence of  $\mathbf{C}\mathbf{H}\bar{\mathbf{S}}$ . Though minimizing the mutual coherence is not directly equivalent to satisfying the RIP, a decrease in mutual coherence corresponds to increased incoherence between  $\mathbf{C}$  and  $\mathbf{H}\bar{\mathbf{S}}$  and has proved effective for compressed sensing. In this work,  $\mathbf{C}$  and  $\mathbf{S}$  are designed specifically toward meeting this requirement.

**Step 3: Reconstruct the reflection coefficient matrix** given the known overcomplete dictionary and sampling matrices. The measurement matrix in the noiseless case is

$$\tilde{\mathbf{Z}} = \sqrt{p}\tilde{\mathbf{H}}\bar{\mathbf{S}}\Lambda, \quad (\text{III.1.1})$$

where  $\tilde{\mathbf{H}} = [\mathbf{H}_1 | \cdots | \mathbf{H}_L | \mathbf{H}_{\text{aug}}]$  and  $\tilde{\Lambda} = \begin{bmatrix} \Lambda \\ \Lambda_{\text{aug}} \end{bmatrix}$  are the augmented matrices of target frequency responses and reflection coefficients, respectively, with  $\mathbf{H}_{\text{aug}}$  of dimension

$K \times K(N_{\text{aug}})$  and  $\Lambda_{\text{aug}}$  of dimension  $TN_{\text{aug}} \times R$  and  $\tilde{\mathbf{S}} = \mathbf{I}_{(L+N_{\text{aug}})} \otimes \mathbf{S}$  where  $N_{\text{aug}}$  is a number chosen to be large enough to ensure the rank constraint on the overcomplete dictionary is met. Thus, the processed signal matrix in the noiseless case becomes

$$\tilde{\mathbf{D}} = \mathbf{C}\tilde{\mathbf{Z}} = \sqrt{p}\mathbf{C}\tilde{\mathbf{H}}\tilde{\mathbf{S}}\tilde{\Lambda}, \quad (\text{III.1.2})$$

and in the scene reconstruction process, the part of  $\tilde{\Lambda}$  corresponding to augmented rows of the target frequency response matrix may be discarded.

From the perspective of radar waveform design, the objective is to obtain the matrices corresponding to the transmitted waveforms and the receiver filters,  $\mathbf{S}$  and  $\mathbf{C}$  respectively, that imply optimal reconstruction of the reflection coefficient matrix  $\Lambda$  given the measurements  $\tilde{\mathbf{Z}}$ , the sampling matrix  $\mathbf{C}$ , and the overcomplete dictionary  $\tilde{\mathbf{H}}\tilde{\mathbf{S}}$ . Processing each received signal vector in parallel, the problem then becomes

$$\min \|\tilde{\lambda}_r\|_1 \text{ subject to } \|\tilde{\mathbf{d}}_r - \Phi\tilde{\lambda}_r\|_2^2 \leq \epsilon, \quad r = 1, \dots, R \quad (\text{III.1.3})$$

where  $\tilde{\lambda}_r$  and  $\tilde{\mathbf{d}}_r$  are the  $r$ -th column of the reflection coefficient matrix and the processed signal matrix, respectively. Note that this method of parallel compressed sensing based reconstruction requires less storage and computational complexity than reconstructing the entire reflection coefficient matrix at once, and a similar approach has been used with favorable results in recent work [55]. Several sparse reconstruction procedures have already been developed [52, 56, 57, 65], any of which could be used to perform the reconstruction. Of these existing methods, the Regularized Orthogonal Matching Pursuit (ROMP) algorithm [52] will be used in this work so that attention can instead be focused on the waveform and receiver filter design problem. If the received signal is processed individually from each receive direction as in (III.1.3),

the mathematical representation of the multiple extended target detection problem appears similar to that of the point target detection problem presented in [44], for which the overcomplete dictionary and sampling matrices are designed simultaneously using the approach of [58]. However, even though the mathematical representations are similar, the framework in which compressed sensing is applied in the current approach is completely different than that in [44], allowing frequency-domain waveform synthesis for detection of extended targets.

Following this approach, the Gram matrix needed to determine the mutual coherence of  $\Phi = \mathbf{C}\tilde{\mathbf{H}}\tilde{\mathbf{S}}$  is defined as

$$\mathbf{G} = \Phi^H \Phi = (\mathbf{C}\tilde{\mathbf{H}}\tilde{\mathbf{S}})^H (\mathbf{C}\tilde{\mathbf{H}}\tilde{\mathbf{S}}) \quad (\text{III.1.4})$$

with corresponding mutual coherence  $\mu(\Phi) = \max_{i \neq j} \left| \frac{g_{i,j}}{\sqrt{g_{i,i}g_{j,j}}} \right|$ , where  $g_{i,j} = \phi_i^H \phi_j$  and  $\phi_i$  is the  $i$ -th column of  $\Phi$ . As the mutual coherence is determined by the maximum magnitude of the off-diagonal elements, the goal is to design  $\mathbf{C}$  and  $\tilde{\mathbf{H}}\tilde{\mathbf{S}}$  so that the off-diagonal elements are small. This can be stated as:

$$\arg \min_{\mathbf{C}, \tilde{\mathbf{S}}} \left\| \mathbf{G} - \tilde{\mathbf{G}} \right\|_F^2 \quad (\text{III.1.5})$$

where  $\tilde{\mathbf{G}} = \text{diag}\{g_{0,0}, \dots, g_{i,i}, \dots, g_{(L+N_{\text{aug}})T, (L+N_{\text{aug}})T}\}$  and  $\|\cdot\|_F$  denotes the Frobenius norm. Expanding the expression for  $\mathbf{G}$  gives:

$$\arg \min_{\mathbf{C}, \tilde{\mathbf{S}}} \left\| \tilde{\mathbf{S}}^H \tilde{\mathbf{H}}^H \mathbf{C}^H \mathbf{C} \tilde{\mathbf{H}} \tilde{\mathbf{S}} - \tilde{\mathbf{G}} \right\|_F^2. \quad (\text{III.1.6})$$

As in [44], a similar, related design criterion can be used:

$$\arg \min_{\mathbf{C}, \tilde{\mathbf{S}}} \left\| \mathbf{C}\tilde{\mathbf{H}}\tilde{\mathbf{S}} - \mathbf{U}\tilde{\mathbf{G}}^{1/2} \right\|_F^2 \text{ such that } \mathbf{U}^H \mathbf{U} = \mathbf{I} \quad (\text{III.1.7})$$

where  $\mathbf{U}$  is an arbitrary semiunitary matrix to be designed.

The problem can then be written as [44]

$$\arg \min_{\mathbf{C}, \mathbf{S}, \mathbf{U}} \left\| \mathbf{C} \tilde{\mathbf{H}} (\mathbf{I}_{(L+N_{\text{aug}})} \otimes \mathbf{S}) \tilde{\mathbf{G}}^{-1/2} - \mathbf{U} \right\|_F^2. \quad (\text{III.1.8})$$

The resulting design algorithms presented in the following sections will fix either  $\mathbf{C}$  or  $\mathbf{S}$ , and then iteratively solve for  $\mathbf{U}$  and either  $\mathbf{S}$  or  $\mathbf{C}$ , respectively. As noted in [44], this method was shown to have good local convergence properties in [59].

### III.1.1 OPTIMAL WAVEFORM DESIGN PROCEDURE

Fixing  $\mathbf{C}$  and  $\mathbf{U}$  in (III.1.8) implies that the optimal waveform matrix  $\mathbf{S}$  is sought to minimize

$$\left\| (\mathbf{I}_{L+N_{\text{aug}}} \otimes \mathbf{S}) - \underbrace{(\mathbf{C} \tilde{\mathbf{H}})^\dagger \mathbf{U} \tilde{\mathbf{G}}^{1/2}}_{\mathbf{\Psi}_s} \right\|_F^2$$

where  $(\cdot)^\dagger$  indicates the Moore-Penrose pseudoinverse. Noting that all off-diagonal blocks of  $\mathbf{I}_{L+N_{\text{aug}}} \otimes \mathbf{S}$  will be zero and as such can not be optimized, one should instead design  $\mathbf{S}$  for an individual target  $\ell$  where  $\ell = 1, \dots, \ell, \dots, (L + N_{\text{aug}})$  using the corresponding block  $\mathbf{\Psi}_s^{(\ell)}$  of dimension  $K \times T$  along the diagonal of  $\mathbf{\Psi}_s$ :

$$\begin{aligned} \min_{\mathbf{S}} \|\mathbf{S} - \mathbf{\Psi}_s^{(\ell)}\|_F^2 &= \min_{\mathbf{S}} \text{Tr} \left[ (\mathbf{S} - \mathbf{\Psi}_s^{(\ell)}) (\mathbf{S} - \mathbf{\Psi}_s^{(\ell)})^H \right] \\ &= \min_{\mathbf{S}} \text{Tr} [\mathbf{S} \mathbf{S}^H - 2\mathbf{S} \mathbf{\Psi}_s^{(\ell)}]. \end{aligned} \quad (\text{III.1.9})$$

To perform joint optimization for all targets, a weighted sum of the diagonal blocks of  $\mathbf{\Psi}_s$  is used with weight values  $\kappa_\ell$  corresponding to the priority of each target:

$$\min_{\mathbf{S}} \sum_{\ell=1}^{(L+N_{\text{aug}})} \kappa_\ell \text{Tr} [\mathbf{S} \mathbf{S}^H - 2\mathbf{S} \mathbf{\Psi}_s^{(\ell)}]. \quad (\text{III.1.10})$$

Therefore, the optimal waveform matrix  $\mathbf{S}$  can be computed as

$$\mathbf{S} = \frac{2}{\sum_{\ell=1}^{(L+N_{\text{aug}})} \kappa_\ell} \sum_{\ell=1}^{(L+N_{\text{aug}})} \kappa_\ell \mathbf{\Psi}_s^{(\ell)} \quad (\text{III.1.11})$$

resulting in **Algorithm 1** for radar waveform design.

---

**Algorithm 1 – Radar Waveform Design**

- 1: **Input:** initial  $\mathbf{C}$  and  $\mathbf{S}$  matrices; tolerance  $\epsilon_1$ .
  - 2: **while**  $\Delta_1 = \max_d \|\mathbf{s}_d^{(m)} - \mathbf{s}_d^{(m-1)}\| < \epsilon_1$  **do**
  - 3:   Compute  $\mathbf{U} = \mathbf{U}_1 \mathbf{U}_2^H$  where  $\mathbf{U}_1 \Sigma \mathbf{U}_2^H$  is the singular value decomposition of  $\mathbf{C} \tilde{\mathbf{H}}(\mathbf{I}_{(L+N_{\text{aug}})} \otimes \mathbf{S}) \tilde{\mathbf{G}}^{-1/2}$
  - 4:   Update  $\mathbf{S}$  using (III.1.11) and normalize columns  
 $\mathbf{s}_d = \mathbf{s}_d / \|\mathbf{s}_d\|, d = 1, \dots, T$ .
  - 5: **end while**
  - 6: **Output:** optimized radar waveform matrix  $\mathbf{S}$ .
- 

Fig. 5: Compressed sensing based radar waveform design algorithm

### III.1.2 OPTIMAL RECEIVER FILTER DESIGN PROCEDURE

Fixing  $\mathbf{S}$  and  $\mathbf{U}$  in equation (III.1.8) implies that the optimal receiver filter  $\mathbf{C}$  satisfies

$$\mathbf{C} \underbrace{\tilde{\mathbf{H}}(\mathbf{I}_{(L+N_{\text{aug}})} \otimes \mathbf{S}) \tilde{\mathbf{G}}^{-1/2}}_{\Psi_c} = \mathbf{U}. \quad (\text{III.1.12})$$

from where the least squares estimate of  $\mathbf{C}$  is computed as

$$\mathbf{C} = ([(\Psi_c^H)^\dagger \mathbf{U}^H])^H = \mathbf{U} \Psi_c^H (\Psi_c \Psi_c^H)^{-1} \quad (\text{III.1.13})$$

This procedure results in **Algorithm 2** for receiver filter design.

### III.1.3 JOINT WAVEFORM-RECEIVER FILTER DESIGN PROCEDURE

Upon application of the radar waveform and receiver filter design procedures the norm  $\|\mathbf{G} - \tilde{\mathbf{G}}\|_F^2$  will be decreased, and since any norm is lower bounded by zero, iterative application of the updates implied by **Algorithms 1** and **2** is guaranteed to reach a fixed point. Numerically, this fixed point is defined with respect to a

---

**Algorithm 2 – Receiver Filter Design**

- 1: **Input:** Initial  $\mathbf{C}$  and optimized  $\mathbf{S}$  (from Algorithm 1); tolerance  $\epsilon_2$ .
  - 2: **while**  $\Delta_2 = \max_k \|\mathbf{c}_k^{(m)} - \mathbf{c}_k^{(m-1)}\| < \epsilon_2$  **do**
  - 3:   Compute  $\mathbf{U} = \mathbf{U}_1 \mathbf{U}_2^H$  where  $\mathbf{U}_1 \Sigma \mathbf{U}_2^H$  is the singular value decomposition of  $\mathbf{C} \tilde{\mathbf{H}}(\mathbf{I}_{(L+N_{\text{aug}})} \otimes \mathbf{S}) \tilde{\mathbf{G}}^{-1/2}$
  - 4:   Update  $\mathbf{C}$  using (III.1.13) and normalize each column of  $\mathbf{C}$ :  
 $\tilde{\mathbf{c}}_k = \mathbf{c}_k / \|\mathbf{c}_k\|, k = 1, \dots, K$ .
  - 5:   Use updated  $\mathbf{C}$  to compute  $\mathbf{U}$
  - 6: **end while**
  - 7: **Output:** optimized receiver filter matrix  $\mathbf{C}$ .
- 

Fig. 6: Compressed sensing based radar receiver filter design algorithm

predefined tolerance value  $\epsilon$ , and the fixed point is reached when  $\|\mathbf{G} - \tilde{\mathbf{G}}\|_F^2 \leq \epsilon$ . Therefore, joint optimization of the radar waveforms and corresponding receiver filters may be accomplished by iteratively applying **Algorithms 1 and 2** as stated formally in **Algorithm 3**.

### III.2 TARGET DETECTION

The target detection problem is posed in terms of a number of  $L \times T \times R$  parallel binary hypothesis testing problems, one for each element of the reflection coefficient matrix:

$$\begin{aligned}
 \mathcal{H}0_{rd}^{(\ell)} : \hat{\lambda}_{rd}^{(\ell)} &= \delta_{rd}^{(\ell)} \\
 \mathcal{H}1_{rd}^{(\ell)} : \hat{\lambda}_{rd}^{(\ell)} &= \lambda_{rd}^{(\ell)} + \delta_{rd}^{(\ell)}, \\
 r &= 1, \dots, R; \quad d = 1, \dots, T; \quad \ell = 1, \dots, L,
 \end{aligned} \tag{III.2.1}$$

where  $\hat{\lambda}_{rd}^{(\ell)}$  is the reconstructed reflection coefficient of target  $\ell$  at location  $(r, d)$  and  $\delta_{rd}^{(\ell)}$  represents a perturbation to the corresponding reconstructed reflected coefficient

---

**Algorithm 3 – Joint Waveform & Receiver Filter Design**
**1: Input:**

- Number of transmitted waveforms/beams  $T$ , receiver beams  $R$ , targets  $L$ , and frequencies of interest  $K$ .
- Target frequency responses, normalized to have unit energy  $\mathbf{H}_\ell$ ,  $\ell = 1, \dots, L$  and associated priorities  $\kappa_\ell$
- Pre-defined fixed tolerances  $\epsilon_1, \epsilon_2, \epsilon_3$

2: Fix  $\mathbf{C}$  using normally distributed random complex numbers and initialize  $\mathbf{S}$  to fixed values

3: **while**  $\Delta_3 = \|\mathbf{G} - \tilde{\mathbf{G}}\|_F^2$ . If  $\Delta_3 > \epsilon_3$  **do**

4:   Optimize  $\mathbf{S}$  using **Algorithm 1**

5:   Optimize  $\mathbf{C}$  using **Algorithm 2**

6: **end while**

7: **Output:** Jointly optimized radar waveform and receiver filter matrices  $\mathbf{S}$  and  $\mathbf{C}$ .

---

Fig. 7: Compressed sensing based joint waveform and receiver filter design algorithm

due to noise.

To decide on the target presence/absence, the detection thresholds  $x = 0$  are set in all of the  $L \times T \times R$  hypothesis testing problems in (III.2.1). This implies that a target is said to be present in each cell where the magnitude of the reconstructed reflection coefficient matrix is greater than zero. This is similar to Detection Architecture 1 that was presented in [60] and is a natural choice for detection in a compressed sensing context. This is different from the traditional thresholding approach taken for detection, in which a threshold may be varied to observe a continuous change in false alarm rates and detection rates for a given SNR. This difference is due to the sparse reconstruction technique used which requires that only a few of the reconstructed

cells be nonzero, resulting in the presence of only sparse impulsive noise in the reconstructed reflection coefficient matrix. Future work could include the analysis of how noise is translated through a chosen sparse reconstruction algorithm as in [60], and development of associated algorithms to vary the detection threshold in order to maintain a constant false alarm rate. However, such analysis is beyond the scope of this work.

The detection rate is defined as the number of instances in which  $\mathcal{H}1_{rd}^{(\ell)}$  is decided to be true when a target is present within the location illuminated by the beam cell pair  $(r, d)$ , divided by the number of actual targets present in the scene. The false alarm rate is defined as the number of instances in which  $\mathcal{H}1_{rd}^{(\ell)}$  is decided to be true when a target is not present within the location illuminated by the beam cell pair  $(r, d)$ , divided by the number cells in the actual reflection coefficient matrix in which a target is not present. As the sparse reconstruction process does not lend itself well to defining a constant false alarm rate for the system, a system in which the maximum allowable false alarm rate is defined is considered instead. The ROMP algorithm requires a sparsity level  $m$  to be defined based on the maximum number of expected targets in the scene, and guarantees that no more than  $2m$  values of each reconstructed column will be nonzero. Using this knowledge, an upper bound on the false alarm rate can be computed:

$$P_{FA} \leq (2 \times m \times T)/(L \times T \times R), \quad (\text{III.2.2})$$

which assumes the worst-case scenario in which all identified nonzero values were at locations where no target was present.

### III.3 SIMULATIONS AND NUMERICAL RESULTS

To illustrate the performance of the proposed procedure a scenario which includes transmitter and receiver array parameter definitions, as well as fluctuating targets and clutter that may be present in the scene was considered. The joint waveform and receiver filter design procedure outlined in **Algorithm 3** was used on a scene with multiple targets with the following numerical parameters similar to those in [44]:  $K = 201$  frequency bands from  $-40$  MHz to  $40$  MHz (implying a  $3.75\text{m}$  range resolution), noise variance  $\sigma_n^2 = 0.01$ . The simulations assume that phased arrays with  $N_T = N_R = 24$  and half wavelength spacing are used at each the transmitter and receiver and that classical beamforming is used for transmission and reception over  $T = R = 25$  beams as depicted in Figure 3 so that all beams cover a combined radial span of  $85^\circ$  centered at a  $45^\circ$  angle measured from the baseline between the transmitter and receiver. A number  $L = 5$  targets are located at Transmit-Receive positions  $(4, 7), (10, 6), (14, 15), (15, 13), (19, 12)$ , resulting in reflection coefficients shown in Figure 8, where the reflection coefficients for all targets have been superimposed to a single  $L \times T$  grid to illustrate the scene. For convenience, the reflection coefficient matrix for each target has been normalized to have a maximum magnitude of 1.

The impulse responses corresponding to each target are set as follows.

- Multiple Point Targets: First, the case in which multiple point targets is considered, in which the target is assumed to act as a point reflector of the transmitted signal. In this case, each target of interest has the same resulting target frequency response matrix which is a  $(K \times K)$  identity matrix:  $\mathbf{H}_\ell = \mathbf{I}_K$ .
- Multiple Known Extended Targets: Next, the case of multiple known extended

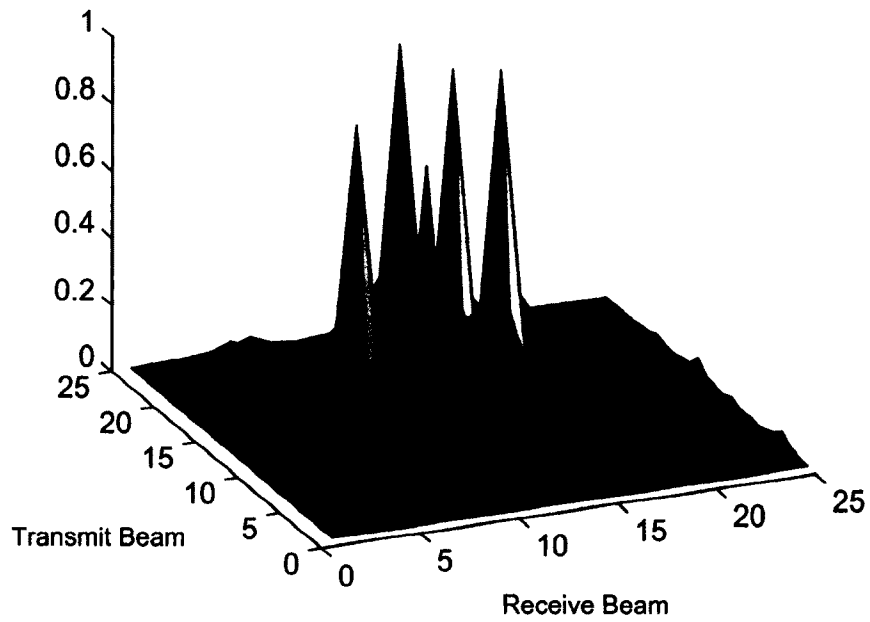


Fig. 8: Reflection coefficients for the simulated example

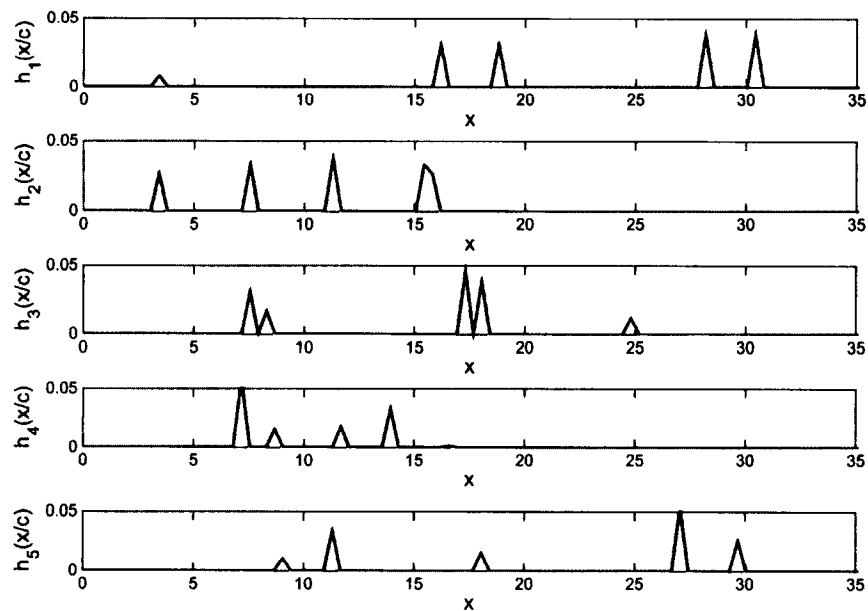


Fig. 9: Target impulse responses where  $x$  is the distance along the target in meters and  $c = 3 \times 10^8$  m/s (assuming free space wave propagation)

targets is considered in which each extended target is comprised of multiple reflection centers as in (II.2.1). This impulse response is then discretized, and the Discrete Fourier Transform (DFT) is computed to obtain the discretized target frequency response. Five such extended targets are considered, each with five reflection centers, similarly to the two targets modeled in [25]. The impulse response for the individual targets used for these simulations are shown in Figure 9.

- Multiple Fluctuating Extended Targets: Finally, the case in which the target frequency response may not be exactly known is considered by assuming that each reflection center can be considered as a Swerling Type I [61] point target so that each of the reflection centers now varies exponentially about the mean, with the mean amplitude given to be the deterministic values of the known targets in the previous scenario.

In the design algorithm, equal priorities were assigned to each target of interest. In all cases, the sampling matrix dimension  $Q = T \times L$  and the algorithm precisions were  $\epsilon_1 = \epsilon_2 = 0.01$ ,  $\epsilon_3 = 0.2$

To validate the results, the optimized waveforms  $\mathbf{S}$  and receiver filter matrix  $\mathbf{C}$  were used to reconstruct the pre-defined target scene. The results were then compared to two benchmark cases: the first using a statically defined random receiver filter matrix  $\mathbf{C}_r$  and random transmitted waveform matrix  $\mathbf{S}_r$  as suggested in [62] and the second using  $\mathbf{C}_r$  with a transmitted waveform matrix  $\mathbf{S}_a$  whose columns are cubic phase Alltop sequences [63] that are often used in compressed sensing applications because they are known to have minimal correlation magnitudes. In each case, the

scene is reconstructed using an input sparsity level of  $\lceil L/R \rceil$ . This implies an upper bound on the system false alarm rate of  $P_{FA} \leq 0.016$ , though the actual false alarm rate remained well below 0.01 for all waveform/receiver filter pairs in all scenarios considered. Both cluttered and uncluttered scenarios are considered. In the cluttered environment, it is assumed that additive white Gaussian Noise (AWGN) with mean  $\mu = 0$ , and variance  $\sigma_c^2 = 10^{-4}$  corrupts the reflection coefficient matrix.

### III.3.1 RECONSTRUCTION RESULTS

In all examples, the reconstruction error is measured to be the average difference between columns of the reconstructed reflection coefficient matrix and the original reflection coefficient matrix. That is,

$$\Delta = \frac{1}{R} \sum_{r=1}^R |\tilde{\lambda}_r - \hat{\lambda}_r| \quad (\text{III.3.1})$$

where  $\hat{\lambda}_r$  is the  $r$ -th received column of the reconstructed reflection coefficient matrix for either known or fluctuating extended targets. To account for variations in  $\tilde{\mathbf{H}}$  in the fluctuating target case, the reconstruction errors were averaged over 1,000 iterations of the simulation. The errors for point targets are shown in Table 2, while the errors for known and fluctuating extended targets are given in Tables 3 and 4, respectively. In the case of point targets, the reconstruction error resulting when using statically defined waveforms is smaller. This is likely because the statically defined waveforms are designed to have minimum coherence with each other in the absence of any specific known target frequency response. Because point targets are represented by an identity matrix,  $\mathbf{C}_r$  and  $\tilde{\mathbf{H}}\mathbf{S}_a$  (or similarly  $\tilde{\mathbf{H}}\mathbf{S}_r$ ) should already be highly incoherent without any special design that takes  $\tilde{\mathbf{H}}$  into account. From the results of Tables 3 and 4, a

comparable or decreased reconstruction error is observed when using the optimized  $\mathbf{C}$  and  $\mathbf{S}$  compared to both  $\mathbf{S}_a, \mathbf{C}_r$ , and  $\mathbf{S}_r, \mathbf{C}_r$  in all extended target cases.

Table 2: Observed error for point targets

Environment	Waveforms, Receiver Filter	$\Delta$
Uncluttered	$\mathbf{S}, \mathbf{C}$	0.1388
	$\mathbf{S}_a, \mathbf{C}_r$	0.1283
	$\mathbf{S}_r, \mathbf{C}_r$	0.1455
Cluttered	$\mathbf{S}, \mathbf{C}$	0.1526
	$\mathbf{S}_a, \mathbf{C}_r$	0.1401
	$\mathbf{S}_r, \mathbf{C}_r$	0.1811

Table 3: Observed error for known extended targets

Environment	Waveforms, Receiver Filter	$\Delta$
Uncluttered	$\mathbf{S}, \mathbf{C}$	0.1056
	$\mathbf{S}_a, \mathbf{C}_r$	0.1110
	$\mathbf{S}_r, \mathbf{C}_r$	0.1126
Cluttered	$\mathbf{S}, \mathbf{C}$	0.1088
	$\mathbf{S}_a, \mathbf{C}_r$	0.1178
	$\mathbf{S}_r, \mathbf{C}_r$	0.1292

Table 4: Observed error for fluctuating extended targets

Environment	Waveforms, Receiver Filter	$\Delta$
Uncluttered	$\mathbf{S}, \mathbf{C}$	0.1466
	$\mathbf{S}_a, \mathbf{C}_r$	0.1583
	$\mathbf{S}_r, \mathbf{C}_r$	0.1601
Cluttered	$\mathbf{S}, \mathbf{C}$	0.1497
	$\mathbf{S}_a, \mathbf{C}_r$	0.1662
	$\mathbf{S}_r, \mathbf{C}_r$	0.1693

### III.3.2 DETECTION RESULTS

One can consider another indicator of the accuracy of the scene reconstruction to be the associated detection rate after performing the thresholding operation on the reconstructed scene. When thresholding, a decision is made about the presence or

absence of each target at each grid location using the threshold  $x = 0$  as discussed in Section IV.B. Resulting detection rates are shown in Tables 5 and 7 with corresponding false alarm rates shown in Tables 6 and 8, respectively. From these results, improved detection is observed using the designed  $\mathbf{C}, \mathbf{S}$  for all noiseless scenarios considered. Additionally, the resulting false alarm rate using each method remains essentially constant and well below the upper bound stated for the considered system.

Table 5: Observed detection rates for point targets in the noiseless scenario

	Environment	Detection Rate		
		$\mathbf{S}, \mathbf{C}$	$\mathbf{S}_a, \mathbf{C}_r$	$\mathbf{S}_r, \mathbf{C}_r$
Known	Uncluttered	0.9312	0.9580	0.9290
	Cluttered	0.9206	0.9584	0.8572

Table 6: Observed false alarm rates for point targets in the noiseless scenario

	Environment	False Alarm Rate		
		$\mathbf{S}, \mathbf{C}$	$\mathbf{S}_a, \mathbf{C}_r$	$\mathbf{S}_r, \mathbf{C}_r$
Known	Uncluttered	0.0042	0.0048	0.0045
	Cluttered	0.0025	0.0031	0.0032

Table 7: Observed detection rates for extended targets in the noiseless scenario

	Environment	Detection Rate		
		$\mathbf{S}, \mathbf{C}$	$\mathbf{S}_a, \mathbf{C}_r$	$\mathbf{S}_r, \mathbf{C}_r$
Known	Uncluttered	0.9998	0.9990	0.9910
	Cluttered	0.9988	0.9986	0.9960
Fluctuating	Uncluttered	0.8690	0.8314	0.8300
	Cluttered	0.8752	0.8264	0.8236

### III.4 CHAPTER SUMMARY

This chapter presented a new procedure for joint waveform and receiver filter design in MIMO radar systems which is based on a compressed sensing approach. By

Table 8: Observed false alarm rates for the noiseless scenario

	Environment	False Alarm Rate		
		$S, C$	$S_a, C_r$	$S_r, C_r$
Known	Uncluttered	0.0053	0.0054	0.0049
	Cluttered	0.0037	0.0036	0.0032
Fluctuating	Uncluttered	0.0051	0.0050	0.0049
	Cluttered	0.0042	0.0041	0.0039

using transmit-receive beamforming to partition the radar scene along with a compact representation of the radar system in terms of a set of discrete frequencies, the presence of multiple extended targets was detected by identifying the corresponding values of their reflection coefficients and corresponds to a sparse scene reconstruction problem. Compressed sensing was used to reconstruct the scene and to design the transmitted radar waveforms, and formal algorithms for joint optimization of the radar waveforms and receiver filters were stated for the noiseless case.

The proposed approach was illustrated with numerical results obtained from simulations which compare the performance of jointly optimized radar waveforms and receiver filters using the proposed approach with that of statically-defined radar waveforms and receiver filters commonly used in a compressed sensing context. Specifically, lower reconstruction errors were obtained and increased target detection rates were observed when transmitted waveform and receiver filter matrices designed using the proposed approach were employed.

Future work could include the consideration of Doppler shift for moving targets, which complicates the problem by adding a third dimension to the reflection coefficient matrix. Additional future work could consider known clutter sources within the target response matrix to further reduce the effect of clutter on target detection.

**CHAPTER IV**

**COMPRESSED SENSING DESIGN OF RADAR**

**WAVEFORMS AND RECEIVER FILTERS FOR TARGET**

**DETECTION IN NOISY ENVIRONMENT**

This chapter considers the actual scenario implied by (II.3.13) in which the noise matrix  $\mathbf{N}$  is present. Compressing the received signal in this case results in

$$\tilde{\mathbf{D}} = \mathbf{C}(\sqrt{p}\tilde{\mathbf{H}}\tilde{\mathbf{S}}\tilde{\mathbf{\Lambda}} + \mathbf{N}) = \Phi_1\tilde{\mathbf{\Lambda}} + \Phi_2\mathbf{N}$$

where  $\Phi_1 = \sqrt{p}\mathbf{C}\tilde{\mathbf{H}}\tilde{\mathbf{S}}$  and  $\Phi_2 = \mathbf{C}$  are the measurement matrices as applied to the reflection coefficient matrix and noise matrix, respectively. Note that under the assumptions regarding the noise matrix  $\mathbf{N}$ , the filtered noise matrix  $\mathbf{C}\mathbf{N}$  will also be Gaussian distributed but will only be white when  $\mathbf{C}$  is chosen to have orthogonal rows.

**IV.1 SCENE RECONSTRUCTION FROM NOISY MEASUREMENTS**

In this case, the  $R$  parallel reconstruction problems become:

$$\min \|\tilde{\lambda}_r\|_1 \text{ subject to } \|\tilde{\mathbf{d}}_r - \Phi_1\tilde{\lambda}_r\|_2^2 \leq \epsilon, \quad r = 1, \dots, R. \quad (\text{IV.1.1})$$

However, in this case  $\tilde{\mathbf{d}}_r$ , which is the  $r$ -th column of  $\tilde{\mathbf{D}}$ , includes the noise term and the sparse reconstruction problem now requires minimum mutual coherence of not only  $\Phi_1$ , but also of  $\Phi_2$ . While minimizing the off-diagonal entries of the Gram

matrix  $\mathbf{G}$  ensured minimum mutual coherence of  $\Phi_1$ , no steps have yet been taken to ensure minimum mutual coherence for  $\Phi_2$  or, equivalently, that  $\mathbf{C}$  has orthogonal rows as required for compressed sensing.

Along these lines, a matrix similar to the optimized  $\mathbf{C}$  can be found which is denoted by  $\hat{\mathbf{C}}$  that meets the minimum mutual coherence requirement for  $\Phi_2$  by taking the singular value decomposition (SVD) of  $\mathbf{C}$

$$\mathbf{C} = \mathbf{U}_C \mathbf{\Sigma}_C \mathbf{V}_C^H \quad (\text{IV.1.2})$$

and setting  $\hat{\mathbf{C}} = \mathbf{U}_C \mathbf{V}_C^H$  to minimize  $\|\mathbf{C} - \hat{\mathbf{C}}\|_F^2$  subject to the constraint  $\hat{\mathbf{C}}\hat{\mathbf{C}}^H = \mathbf{I}$ , similarly to the approach used to compute  $\mathbf{U}$  in **Algorithm 3**. It is expected that  $\hat{\mathbf{C}}\tilde{\mathbf{H}}\tilde{\mathbf{S}}$  will still have small mutual coherence since  $\hat{\mathbf{C}}$  retains the information contained in the left and right eigenvectors of  $\mathbf{C}$ . This leads to **Algorithm 4** for joint radar waveform and receiver filter design for scene reconstruction from noisy measurements. To the author's knowledge, no previous works have designed such a receiver filter with specific intent to minimize the effect of noise present within the scene in the compressed sensing context.

Note that the SVD step of **Algorithm 4** is completed after all other steps of the optimization algorithm, as it can be expected that any modification to  $\mathbf{C}$  would render it somewhat suboptimal in the noiseless case.

## IV.2 SIMULATIONS AND NUMERICAL RESULTS

In studying the noisy scenario, an uncluttered but noisy environment ( $\mathbf{N} \neq 0$ ) is considered in which the transmit energy  $\sqrt{p}$  for all waveforms is adjusted given the noise variance  $\sigma_n = 0.1$  to ensure a consistent SNR  $\gamma$  for each combination of

---

**Algorithm 4 – Joint Waveform & Receiver Filter Design**

1: **Input:**

- Number of transmitted waveforms/beams  $T$ , receiver beams  $R$ , targets  $L$ , and frequencies of interest  $K$ .
- Target frequency responses, normalized to have unit energy  $\mathbf{H}_\ell$ ,  $\ell = 1, \dots, L$  and associated priorities  $\kappa_\ell$
- Pre-defined fixed tolerances  $\epsilon_1, \epsilon_2, \epsilon_3$

2: Initialize  $\mathbf{C}$  using normally distributed random complex numbers and initialize  $\mathbf{S}$  to pre-defined values

3: **while**  $\Delta_3 = \|\mathbf{G} - \tilde{\mathbf{G}}\|_F^2$ . If  $\Delta_3 > \epsilon_3$  **do**

4:   Optimize  $\mathbf{S}$  using **Algorithm 1**

5:   Optimize  $\mathbf{C}$  using **Algorithm 2**

6: **end while**

7: Use the SVD (IV.1.2) to obtain  $\hat{\mathbf{C}} = \mathbf{U}_C \mathbf{V}_C^H$ . and normalize each column of  $\hat{\mathbf{C}}$  to obtain the optimized receiver matrix.

8: **Output:** Jointly optimized radar waveform and receiver filter matrices  $\mathbf{S}$  and  $\hat{\mathbf{C}}$ .

---

Fig. 10: Compressed sensing based joint waveform and receiver filter design algorithm for noisy scenario

transmitted waveform matrix and receiver filter matrix.

To illustrate the performance of the proposed procedure a scenario similar to the one considered in Chapter 3 is considered. The joint waveform and receiver filter design procedures outlined in **Algorithm 3** and **Algorithm 4** were used on a scene with multiple targets in the noisy scenario:  $K = 201$  frequency bands from  $-40$  MHz to  $40$  MHz (implying a  $3.75\text{m}$  range resolution), noise variance  $\sigma_n^2 = 0.01$ . The simulations assume that phased arrays with  $N_T = N_R = 25$  and  $1/2$  wavelength spacing are used at each the transmitter and receiver, and that classical beamforming is used for transmission and reception over  $T = R = 25$  beams as depicted in Figure 3 so that all beams cover a combined radial span of  $85^\circ$  centered at a  $45^\circ$  angle measured

from the baseline between the transmitter and receiver. A number,  $L = 5$ , of targets are located at Transmit-Receive positions  $(4, 7), (10, 6), (14, 15), (15, 13), (19, 12)$ , resulting in reflection coefficients shown in Figure 8, where the reflection coefficients for all targets have been superimposed to a single  $L \times T$  grid to illustrate the scene. For convenience, the reflection coefficient matrix for each target has been normalized to have a maximum magnitude of 1.

The ROMP algorithm was used for reconstruction, with an input sparsity level of  $\lceil L/R \rceil$ . Using equation III.2.2 the upper bound on the system false alarm rate is  $P_{FA} \leq 0.016$ , though the actual false alarm rate remained well below 0.01 for all waveform/receiver filter pairs in all scenarios considered. Both cluttered and uncluttered scenarios are considered. In the cluttered environment, it is assumed that additive white Gaussian Noise (AWGN) with mean  $\mu = 0$ , and variance  $\sigma_c^2 = 10^{-4}$  corrupts the reflection coefficient matrix.

#### IV.2.1 RECONSTRUCTION RESULTS

The reflection coefficient matrix was reconstructed using the designed  $\mathbf{S}, \hat{\mathbf{C}}$  and the statically defined  $\mathbf{S}_a, \mathbf{C}_r$ , and  $\mathbf{S}_r, \mathbf{C}_r$ . To account for variations in  $\mathbf{N}$  (and variations

Table 9: Observed reconstruction error for point targets

Waveforms Receiver Filter	$\Delta, \gamma = 10$ dB	$\Delta, \gamma = 20$ dB	$\Delta, \gamma = 30$ dB
$\mathbf{S}, \hat{\mathbf{C}}$	3.6708	0.5009	0.1489
$\mathbf{S}_a, \mathbf{C}_r$	5.2307	0.7143	0.2104
$\mathbf{S}_r, \mathbf{C}_r$	6.7304	0.9125	0.2586

in  $\tilde{\mathbf{H}}$  in the fluctuating target case), the reconstruction error was computed after reconstruction and averaged over 1,000 iterations of the simulation. The observed

Table 10: Observed reconstruction error for known extended targets

Waveforms Receiver Filter	$\Delta, \gamma = 10$ dB	$\Delta, \gamma = 20$ dB	$\Delta, \gamma = 30$ dB
$\mathbf{S}, \hat{\mathbf{C}}$	2.9723	0.4610	0.1368
$\mathbf{S}_a, \mathbf{C}_r$	5.3648	0.6795	0.1657
$\mathbf{S}_r, \mathbf{C}_r$	6.4290	0.8236	0.1938

Table 11: Observed reconstruction error for fluctuating extended targets

Waveforms Receiver Filter	$\Delta, \gamma = 10$ dB	$\Delta, \gamma = 20$ dB	$\Delta, \gamma = 30$ dB
$\mathbf{S}, \hat{\mathbf{C}}$	1.8472	0.3563	0.1768
$\mathbf{S}_a, \mathbf{C}_r$	3.0832	0.4968	0.1946
$\mathbf{S}_r, \mathbf{C}_r$	4.0737	0.6088	0.2134

error for point targets is shown in Table 9, while the error for known and fluctuating extended targets are shown in Tables 10 and 11, respectively. From these results, improved reconstruction is observed when using the optimized  $\hat{\mathbf{C}}$  and  $\mathbf{S}$  compared to both  $\mathbf{S}_a, \mathbf{C}_r$ , and  $\mathbf{S}_r, \mathbf{C}_r$  in all cases, noting that transmission of Alltop sequences provides improved reconstruction over transmission of randomly generated waveforms as expected.

Table 12: Observed reconstruction error for point targets in cluttered environment

Waveforms Receiver Filter	$\Delta, \gamma = 10$ dB	$\Delta, \gamma = 20$ dB	$\Delta, \gamma = 30$ dB
$\mathbf{S}, \hat{\mathbf{C}}$	3.6738	0.5164	0.1575
$\mathbf{S}_a, \mathbf{C}_r$	5.1109	0.7526	0.2137
$\mathbf{S}_r, \mathbf{C}_r$	6.5153	0.9476	0.2874

Assuming now that the received signal is corrupted by both additive noise and clutter, where it is again assumed that clutter is modeled as additive white Gaussian

Table 13: Observed reconstruction error for known extended targets in cluttered environment

Waveforms Receiver Filter	$\Delta, \gamma = 10$ dB	$\Delta, \gamma = 20$ dB	$\Delta, \gamma = 30$ dB
$\mathbf{S}, \hat{\mathbf{C}}$	3.0335	0.4316	0.1495
$\mathbf{S}_a, \mathbf{C}_r$	5.3692	0.7041	0.1757
$\mathbf{S}_r, \mathbf{C}_r$	6.4301	0.8240	0.1879

Table 14: Observed reconstruction error for fluctuating extended targets in cluttered environment

Waveforms Receiver Filter	$\Delta, \gamma = 10$ dB	$\Delta, \gamma = 20$ dB	$\Delta, \gamma = 30$ dB
$\mathbf{S}, \hat{\mathbf{C}}$	1.8943	0.3641	0.1913
$\mathbf{S}_a, \mathbf{C}_r$	3.0763	0.5113	0.2096
$\mathbf{S}_r, \mathbf{C}_r$	4.0728	0.6307	0.2222

Noise (AWGN) with  $\mu = 0, \sigma_c^2 = 10^{-4}$  which corrupts the reflection coefficient matrix, results in the reconstruction errors shown in Tables 12-14. From these results, a smaller reconstruction error using the optimized  $\hat{\mathbf{C}}$  and  $\mathbf{S}$  is observed when compared to both  $\mathbf{S}_a, \mathbf{C}_r$ , and  $\mathbf{S}_r, \mathbf{C}_r$  in all cases for the noisy, cluttered environment.

#### IV.2.2 DETECTION RESULTS

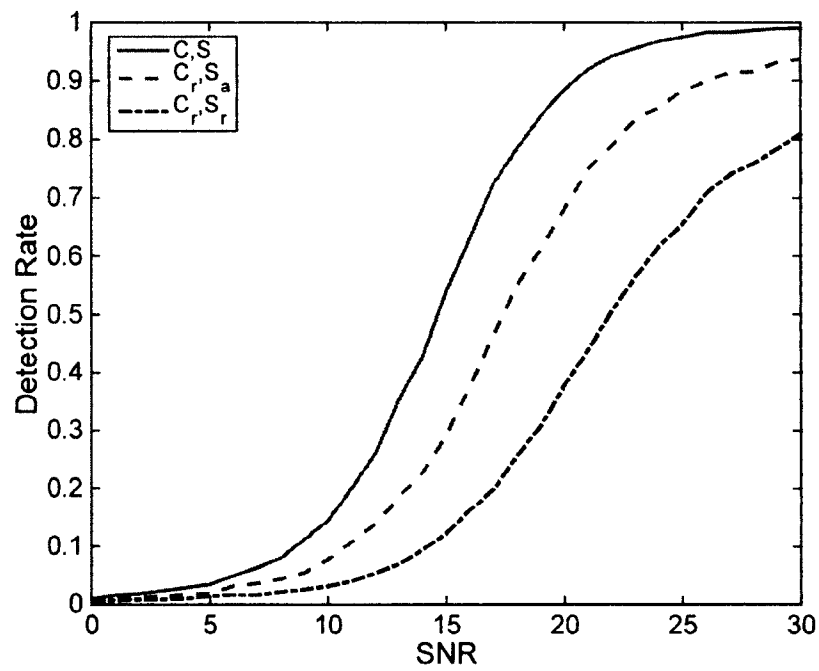
The detection rate for SNRs of  $[0, 1, \dots, 30]$  is computed in the uncluttered environment with the resulting detection rates in the case of point targets and known extended targets shown in Figure 11 and Figure 12, respectively, noting that each data point was again averaged over 1,000 iterations of the simulation. From these results it is observed that in the case of both point targets and known extended targets, the proposed optimized  $\mathbf{S}$  and  $\hat{\mathbf{C}}$  provide improved detection over the statically

defined  $\mathbf{S}_a$ ,  $\mathbf{C}_r$  and  $\mathbf{S}_r$ ,  $\mathbf{C}_r$ .

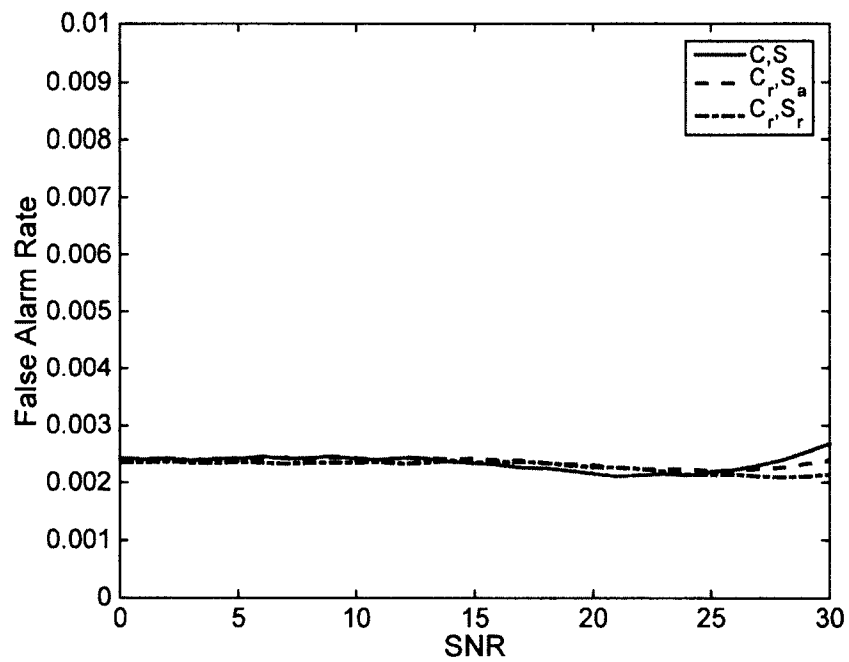
The resulting detection rates in the case of fluctuating extended targets are shown in Figure 13, and each data point was again averaged over 1,000 iterations. From these results it is observed that in the case of fluctuating extended targets, the proposed optimized  $\mathbf{S}$  and  $\hat{\mathbf{C}}$  provide improved detection over the statically defined  $\mathbf{S}_a$ ,  $\mathbf{C}_r$  and  $\mathbf{S}_r$ ,  $\mathbf{C}_r$ . Worth noting is that the improvement in this case is less pronounced which is to be expected since waveforms are designed for specific known target impulse responses, while the actual impulse response (as determined the reflection centers of each target) varies stochastically about the corresponding expected values. For all considered target types, the detection performance is improved when transmitting  $\mathbf{S}_a$  over the randomly generated  $\mathbf{S}_r$ . This is again consistent with the reconstruction results, which indicated reduced reconstruction error for  $\mathbf{S}_a$  over  $\mathbf{S}_r$ . The corresponding false alarm rates for point targets, known extended targets, and fluctuating extended targets are depicted in Figure 11, Figure 12 and Figure 13, respectively, and are below the stated upper bound for the system and remain essentially constant for all cases.

Again, the case in which the received signal is corrupted by both additive noise and clutter is considered as in the previous section on reconstruction, and the corresponding detection rates are obtained as shown in Figure 14 for point targets, Figure 15 for known targets, and Figure 16 for fluctuating targets.

From these results, improved detection rates are observed when using the designed waveforms and receiver filters in the case where both noise and clutter are present for all target types, with a more pronounced improvement when the target frequency responses are known and a less pronounced improvement for fluctuating targets. The

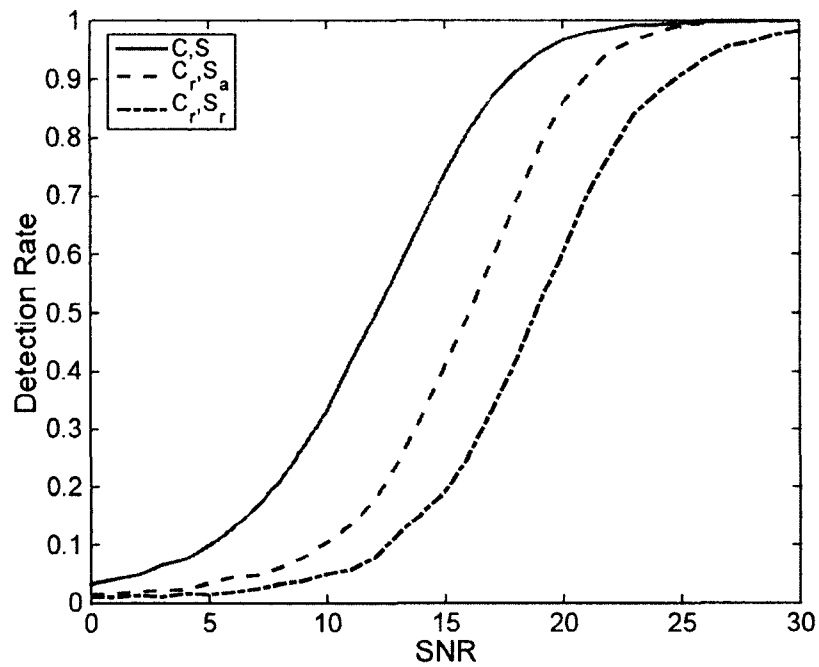


(a)

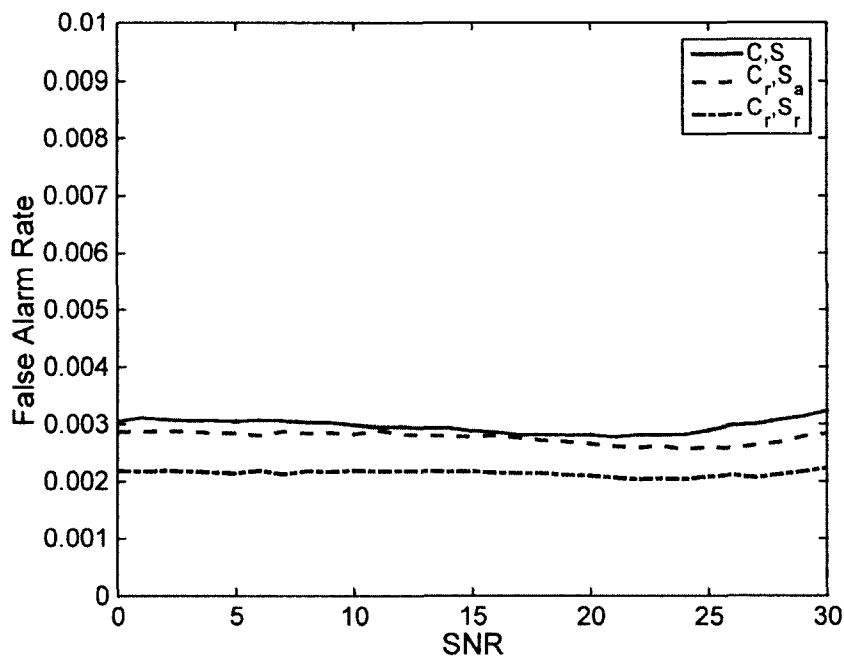


(b)

Fig. 11: Detection and false alarm rates for point targets in noisy environment

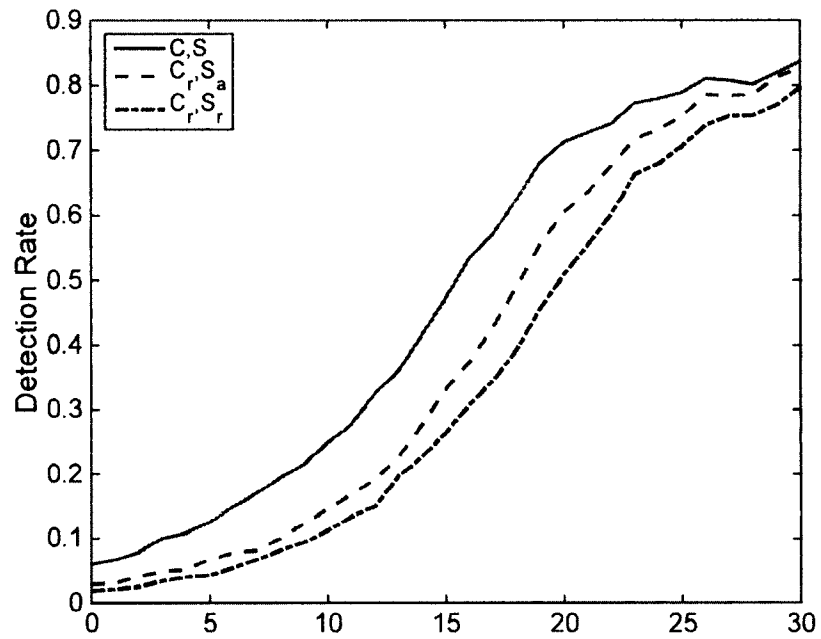


(a)

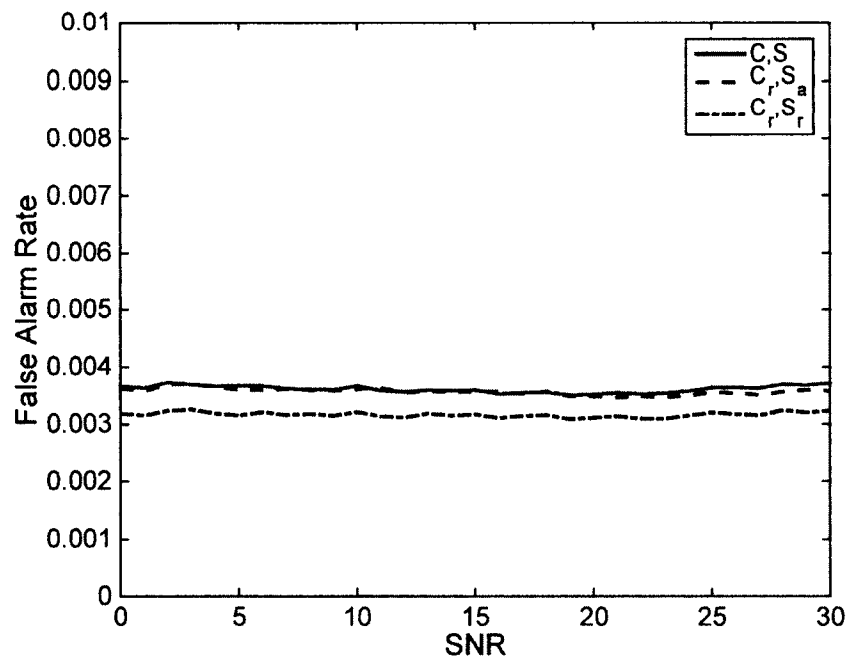


(b)

Fig. 12: Detection and false alarm rates for known extended targets in noisy environment

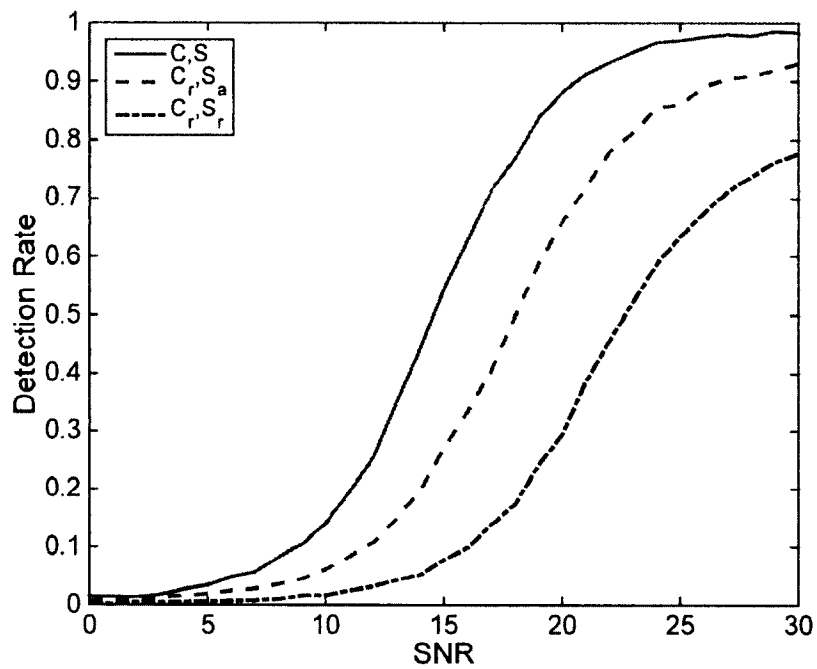


(a)

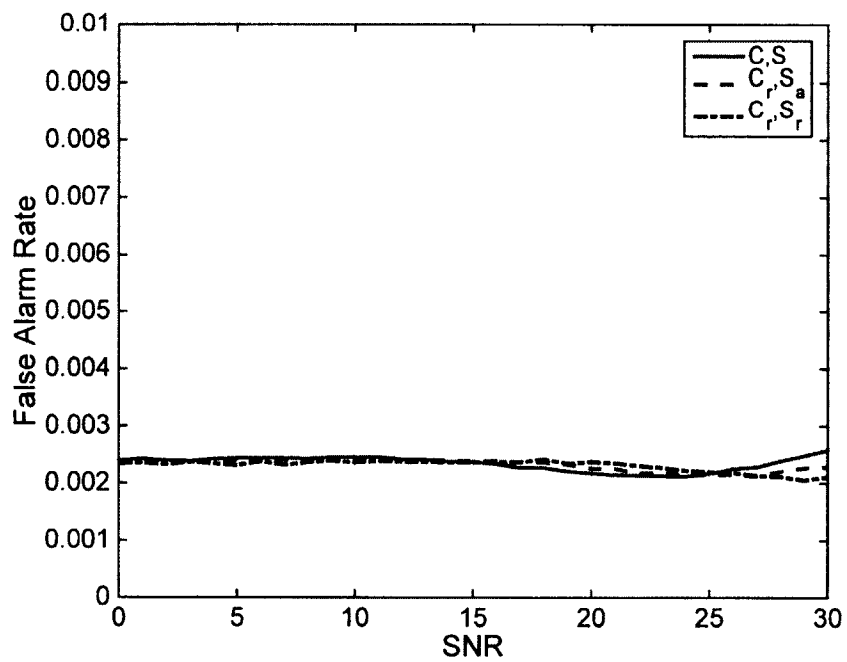


(b)

Fig. 13: Detection and false alarm rates for fluctuating extended targets in noisy environment

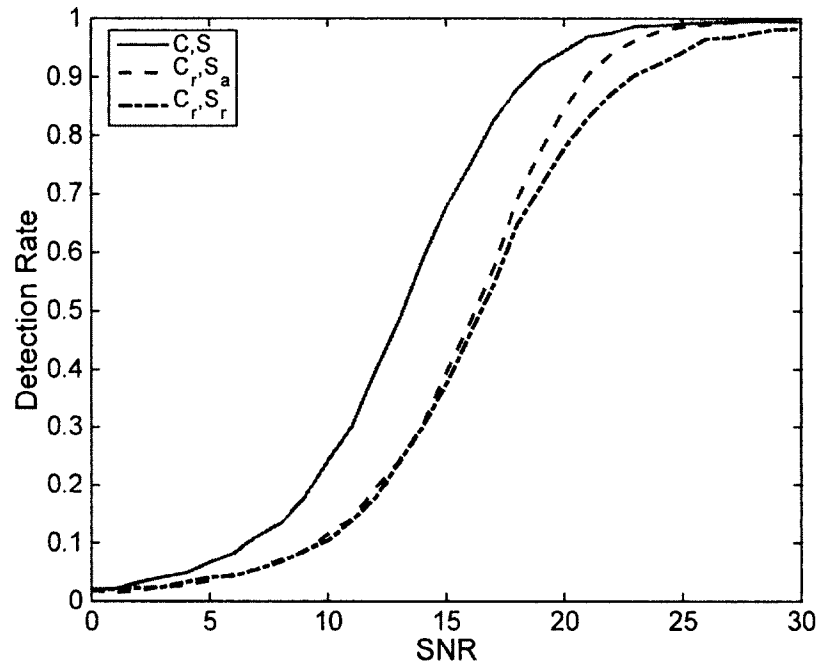


(a)

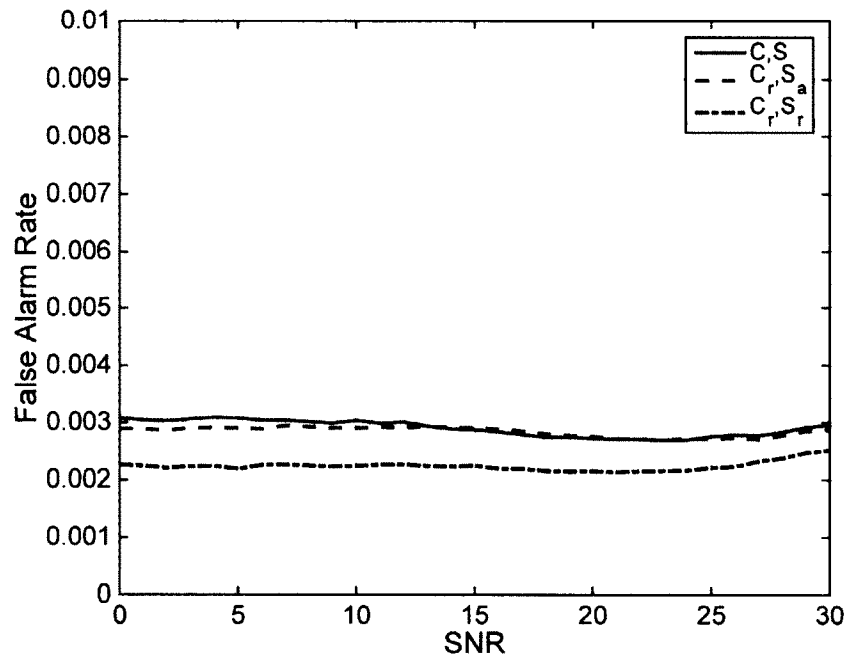


(b)

Fig. 14: Detection and false alarm rates for point targets in noisy environment with clutter

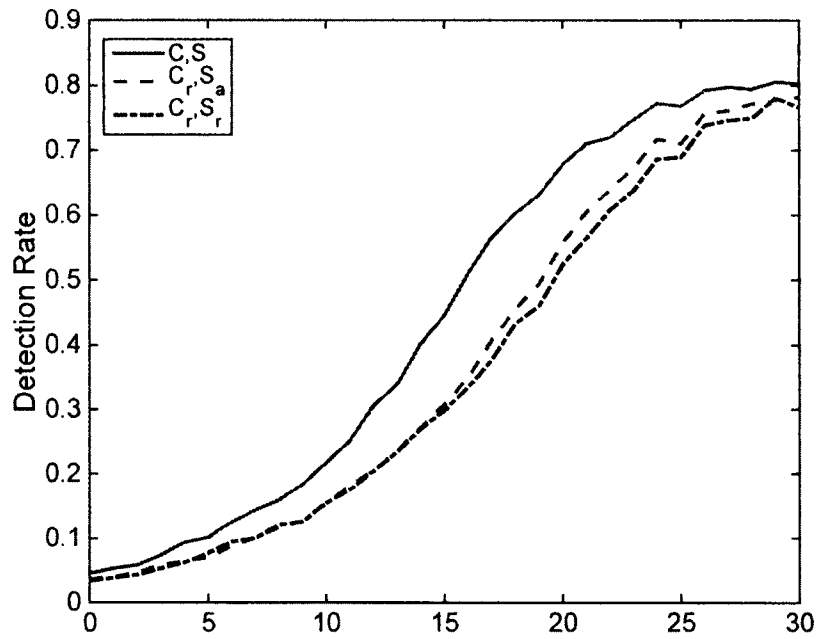


(a)

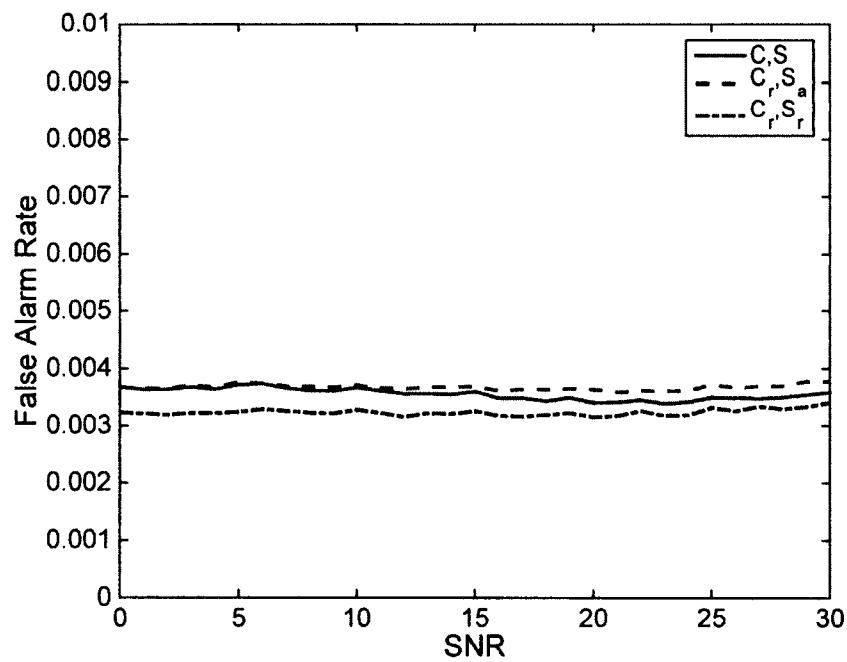


(b)

Fig. 15: Detection and false alarm rates for known extended targets in noisy environment with clutter



(a)



(b)

Fig. 16: Detection and false alarm rates for fluctuating extended targets in noisy environment with clutter

corresponding false alarm rates for point targets, known extended targets, and fluctuating extended targets are depicted in Figure 14, Figure 15 and Figure 16, respectively, and are again below the stated upper bound for the system and remain essentially constant for all cases.

### IV.3 CHAPTER SUMMARY

This chapter extended the compressed sensing based procedure for joint waveform and receiver filter design in MIMO radar systems of Chapter 3 for the noisy scenario, and a formal algorithm for joint optimization of the radar waveforms and receiver filters in the noisy case was presented.

The proposed approach was illustrated with numerical results obtained from simulations which compare the performance of jointly optimized radar waveforms and receiver filters using the proposed approach with that of statically-defined radar waveforms and receiver filters commonly used in a compressed sensing context. Specifically, lower reconstruction errors were obtained and increased target detection rates were observed when transmitted waveform and receiver filter matrices designed using the proposed approach were employed.

## CHAPTER V

### GREEDY SINR MAXIMIZATION BASED DESIGN OF RADAR WAVEFORMS FOR TARGET ESTIMATION

Though modern radar systems are able to simultaneously detect and track multiple targets, most of the recent work in information theoretic waveform design for radar systems has considered single target scenarios. Few works have considered estimating the frequency responses of multiple extended targets simultaneously. Of note is the work in [25], in which a monostatic MIMO radar system was considered for the estimation of multiple target frequency responses using information theoretic techniques. The performance metric used in their study was the mutual information between the received signal and the frequency response of the target similarly to the single target mutual information measure defined in [6].

This chapter presents a new perspective on the similar problem of estimating multiple extended targets using a bistatic MIMO radar system with beamforming within the proposed vector channel framework. Using this framework, it is possible to draw a parallel between the considered radar system and a related information transmission system, allowing waveform and receiver filter design using a similar technique and also allowing the definition of the multiple target radar channel sum capacity (or equivalent spectral efficiency) performance metric which is related to the mutual information measure used in [25].

In the considered scenario, the goal is to design waveforms that maximize the mutual information between the reflected and received signal for targets present at

known locations with unknown impulse response. While the actual impulse response of each target is unknown, it is assumed that some information regarding its statistics may be known a-priori as in [25].

## V.1 WAVEFORM DESIGN FOR MULTIPLE TARGET ESTIMATION

Consider the system model of (II.3.4), with a set of waveforms transmitted toward the known location of each target:

$$\mathbf{s}_\ell = \sum_{w=1}^{N_{\text{wfms}}} \mathbf{s}_\ell^{(w)}, \quad (\text{V.1.1})$$

where  $N_{\text{wfms}}$  is the total number of waveforms in the set. Transmitting a greater number of waveforms for each target will result in an increase in signal diversity, which has been shown to improve radar target estimation performance [67]. We consider that these waveforms are jointly designed to optimally estimate the frequency responses of multiple targets over the frequency band of interest. Joint estimation in this scenario will look in each individual target direction to estimate the target frequency response using auxiliary knowledge of waveforms transmitted for other targets as well as any known statistics of frequency responses corresponding to other targets. The problem in this case is similar to that of designing codewords for optimal interference avoidance in the multibase wireless communication channel scenario of [68] which uses a collaborative approach. Additionally, joint waveform design in the case of the considered radar system may be more feasible in practice than in the multibase communication system scenario since in the radar system there is a single array of antennas at each the transmitter and receiver which may easily share information regarding all targets and all transmitted waveforms simultaneously. This is different

from the communication scenario in [68] in which information was assumed to be shared among multiple base stations, which may be more difficult to implement in practice.

Starting with the vector channel model, let  $T = R = L$  so that the system looks only in the known target directions from both the transmitter and receiver. It is assumed that beamforming at the transmitter is defined such that the transmitted waveform set for each target is only reflected by its intended target as in [25] which implies  $\lambda_{rd}^{(\ell)} = 0, \forall d \neq \ell$ . However, reflections from each target may scatter so that they are observed from many directions at the receiver as determined by the reflection coefficients  $\lambda_{r\ell}^{(\ell)}$  which, though typically small, will in general be nonzero for arbitrary  $r \neq \ell$ . In this particular case, (II.3.4) can be rewritten as

$$\mathbf{z}_r = \sum_{\ell=1}^L \lambda_{r\ell}^{(\ell)} \mathbf{H}_\ell s_\ell \sqrt{p_\ell} + \mathbf{n}_r, \quad r = 1, \dots, L, \quad (\text{V.1.2})$$

where again  $\mathbf{n}_r = \mathbf{W} \mathbf{v}_p^*$ .

To facilitate joint processing of the reflected signals, the total signal received over all directions can be written as a single vector:

$$\mathbf{z} = \sum_{\ell=1}^L \underbrace{\bar{\mathbf{H}}_\ell s_\ell \sqrt{p_\ell}}_{\mathbf{y}_\ell} + \mathbf{n} \quad (\text{V.1.3})$$

where

$$\mathbf{z} = \begin{bmatrix} \mathbf{z}_1 \\ \vdots \\ \mathbf{z}_r \\ \vdots \\ \mathbf{z}_L \end{bmatrix}, \quad \bar{\mathbf{H}}_\ell = \begin{bmatrix} \lambda_{1\ell}^{(\ell)} \mathbf{H}_\ell \\ \vdots \\ \lambda_{r\ell}^{(\ell)} \mathbf{H}_\ell \\ \vdots \\ \lambda_{L\ell}^{(\ell)} \mathbf{H}_\ell \end{bmatrix}, \quad \mathbf{n} = \begin{bmatrix} \mathbf{n}_1 \\ \vdots \\ \mathbf{n}_r \\ \vdots \\ \mathbf{n}_L \end{bmatrix}. \quad (\text{V.1.4})$$

Note that this model appears similar to the one presented in [68]. Subsequently, the autocorrelation of the received signal vector can be computed as

$$\mathbf{R} = E[\mathbf{z}\mathbf{z}^H] = E \left[ \left( \sum_{\ell=1}^L \bar{\mathbf{H}}_{\ell} \mathbf{s}_{\ell} \sqrt{p_{\ell}} + \mathbf{n} \right) \left( \sum_{m=1}^L \bar{\mathbf{H}}_m \mathbf{s}_m \sqrt{p_m} + \mathbf{n} \right)^H \right]. \quad (\text{V.1.5})$$

Assuming that each target's frequency response is uncorrelated with the additive noise that corrupts the reflected signal at the receiver, this expression can be rewritten as

$$\mathbf{R} = \sum_{\ell=1}^L \sum_{m=1}^L \sqrt{p_{\ell}} \sqrt{p_m} E[\bar{\mathbf{H}}_{\ell} \mathbf{s}_{\ell} \mathbf{s}_m^H \bar{\mathbf{H}}_m^H] + \mathbf{N}, \quad (\text{V.1.6})$$

where  $\mathbf{N} = E[\mathbf{n}\mathbf{n}^H]$ . Additionally, it is assumed that the frequency response of target  $\ell$  is assumed uncorrelated with target  $m$  for all  $\ell \neq m$  so that  $E[H_{\ell}(f_k)S_{\ell}(f_k)S_m^*(f_k)H_m^*(f_k)] = 0$  and that the reflected signal at each frequency is uncorrelated with the reflected signal at all other frequencies so that  $E[H_{\ell}(f_j)S_{\ell}(f_j)S_{\ell}^*(f_k)H_{\ell}^*(f_k)] = 0$  for all  $j \neq k$ . With these assumptions, the expression for the autocorrelation matrix of the received signal vector can be further simplified as

$$\mathbf{R} = \sum_{\ell=1}^L p_{\ell} E \left[ \underbrace{\bar{\mathbf{H}}_{\ell} \mathbf{s}_{\ell} \mathbf{s}_{\ell}^H \bar{\mathbf{H}}_{\ell}^H}_{\mathbf{R}_{\ell}} \right] + \mathbf{N}. \quad (\text{V.1.7})$$

To optimally estimate each target, the goal is to maximize the mutual information between the reflected and received signal vectors given the known (designed) transmitted waveforms [6], defined as

$$I(\mathbf{y}_{\ell}, \mathbf{z} | \mathbf{s}_1, \dots, \mathbf{s}_L) = \frac{1}{2} \sum_{k=1}^K \sum_{r=1}^R \log_2 \left[ 1 + \frac{|\lambda_{rd}^{(\ell)}|^2 \sigma_{h_{\ell}}^2(f_k) p_{\ell} |s_{\ell}(f_k)|^2}{\sigma_n^2} \right] \text{ [bits/transmission]}, \quad (\text{V.1.8})$$

where  $\sigma_{h_{\ell}}^2(f_k)$  is the PSD of target  $\ell$  at frequency  $f_k$ ,  $\sigma_n^2$  is the variance of the noise.

This is equivalent to maximizing the individual capacity for each radar target channel

[69]. That is:

$$C_\ell = \max_{\mathbf{s}_\ell^{(q)}} I(\mathbf{y}_\ell, \mathbf{z} | \mathbf{s}_1, \dots, \mathbf{s}_L), \quad \ell = 1, \dots, L. \quad (\text{V.1.9})$$

Combining these mutual information measures over all channels, one can consider a joint optimization constraint to be the sum capacity over all channels represented by the multiple radar targets.

$$C_{\text{sum}} = \sum_{\ell=1}^L \max_{\{\mathbf{s}_1, \dots, \mathbf{s}_L\}} I(\mathbf{y}_\ell, \mathbf{z}, \{\mathbf{s}_1, \dots, \mathbf{s}_L\}) \quad [\text{bits/transmission}]. \quad (\text{V.1.10})$$

The sum capacity can also be rewritten in terms of the autocorrelation matrix in (V.1.7):

$$C_{\text{sum}} = \frac{1}{2} \log_2 |\mathbf{R}| - \frac{1}{2} \log_2 |\mathbf{R}_i + \mathbf{N}| \quad [\text{bits/transmission}], \quad (\text{V.1.11})$$

where  $|\cdot|$  indicates the matrix determinant operation and  $\mathbf{R}_i$  represents the autocorrelation of the total interference seen at the receiver. That is,

$$\mathbf{R}_i = \sum_{\ell=1}^L \sum_{q=1}^{N_{\text{wfms}}} p_\ell \left( \sum_{r=1, r \neq \ell}^L |\lambda_{r\ell}^{(\ell)}|^2 \right) E[\mathbf{H}_\ell \mathbf{s}_\ell^{(q)} (\mathbf{s}_\ell^{(q)})^H \mathbf{H}_\ell^H]. \quad (\text{V.1.12})$$

Converting units to bits/s/Hz, and considering that waveforms are transmitted with duration  $T$  over (double-sided) bandwidth  $2B$ , the sum capacity can also be expressed as the spectral efficiency of the combined channel:

$$C_{\text{sum}} = \frac{1}{TB} \left( \frac{1}{2} \log_2 |\mathbf{R}| - \frac{1}{2} \log_2 |\mathbf{R}_i + \mathbf{N}| \right) \quad [\text{bits/s/Hz}]. \quad (\text{V.1.13})$$

The joint optimization goal in this framework is to maximize the sum capacity of the combined radar target channel, which will in turn maximize the sum of the individual mutual information measures for each target. Following a similar approach to [68], the sum capacity can be maximized using a Greedy SINR maximization approach in which the individual SINR for each waveform designed for each target is maximized when reflections received due to all other waveforms are regarded as interference.

## V.2 GREEDY SINR MAXIMIZATION FOR MULTIPLE TARGET ESTIMATION

Suppose that the received signal is processed using a  $(KR \times 1)$  linear receiver filter  $\tilde{\mathbf{c}}_\ell$  for estimating target  $\ell$  which is located in direction  $\rho_\ell$ . Assuming the radar system looks only in the direction of target  $\ell$  to estimate the frequency response of target  $\ell$ ,  $\tilde{\mathbf{c}}_\ell$  will be composed of zeros except for the  $\ell$ -th block of dimension  $K \times 1$ . That is:

$$\tilde{\mathbf{c}}_\ell = \begin{bmatrix} 0 \\ \vdots \\ 0 \\ \mathbf{c}_\ell \\ 0 \\ \vdots \\ 0 \end{bmatrix} \leftarrow \ell\text{-th } K \times 1 \text{ block.} \quad (\text{V.2.1})$$

The SINR can be defined for the  $q$ -th waveform designed for target  $\ell$  along with the associated matched receiver filter  $\mathbf{c}_\ell^{(q)}$

$$\gamma_\ell^{(q)} = \frac{(\mathbf{c}_\ell^{(q)})^H \mathbf{Y}_\ell^{(q)} \mathbf{c}_\ell^{(q)}}{(\mathbf{c}_\ell^{(q)})^H \mathbf{R}_i^{(q)} \mathbf{c}_\ell^{(q)}} \quad (\text{V.2.2})$$

where the reflected signal power due to the  $q$ -th transmitted waveform in the direction of target  $\ell$  is:

$$\mathbf{Y}_\ell^{(q)} = |\lambda_{\ell\ell}^{(q)}|^2 p_\ell E \left[ \mathbf{H}_\ell \mathbf{s}_\ell^{(q)} (\mathbf{s}_\ell^{(q)})^H \mathbf{H}_\ell^H \right], \quad (\text{V.2.3})$$

and the combined noise and interference as seen from the perspective of the  $q$ -th waveform in the direction of target  $\ell$  is

$$\mathbf{R}_i^{(q)} = \underbrace{\sum_{\kappa=1, \kappa \neq q}^{N_{\text{wfms}}} |\lambda_{\ell\ell}^{(\kappa)}|^2 p_\ell E \left[ \mathbf{H}_\ell \mathbf{s}_\ell^{(\kappa)} (\mathbf{s}_\ell^{(\kappa)})^H \mathbf{H}_\ell^H \right]}_{\text{self-interference}} + \underbrace{\sum_{\eta=1}^{N_{\text{wfms}}} \sum_{m=1, m \neq \ell}^L |\lambda_{\ell m}^{(\eta)}|^2 p_m E \left[ \mathbf{H}_m \mathbf{s}_m^{(\eta)} (\mathbf{s}_m^{(\eta)})^H \mathbf{H}_m^H \right]}_{\text{interference}} + \underbrace{\sigma_n^2 \mathbf{I}_K}_{\text{noise}}, \quad (\text{V.2.4})$$

where reflections from all other waveforms are viewed as interference. Note that  $\mathbf{R}_i$ ,  $\mathbf{R}_i^{(q)}$  and  $\mathbf{Y}_\ell^{(q)}$  will each be diagonal as long as  $E[H_\ell(f_j)H_\ell(f_k)] = 0 \quad \forall j \neq k$ , and  $\mathbf{N} = \sigma_n^2 \mathbf{I}_K$  as in (A.17) under the previously stated assumptions regarding the noise corrupting the received signal.

The SINR  $\gamma_\ell^{(q)}$  as perceived for the  $q$ -th waveform generated for target  $\ell$  will be maximized when  $\mathbf{c}_\ell^{(q)}$ , and consequently  $\mathbf{s}_\ell^{(q)}$ , is the eigenvector corresponding to the maximum generalized eigenvalue of the matrix pair  $(\mathbf{Y}_\ell^{(q)}, \mathbf{R}_i)$  [70, p. 50], that is:

$$\mathbf{Y}_\ell^{(q)} \mathbf{c}_\ell^{(q)} = \zeta \mathbf{R}_i \mathbf{c}_\ell^{(q)} \quad \ell = 1, \dots, L, \quad q = 1, \dots, N_{\text{wfms}} \quad (\text{V.2.5})$$

This procedure is repeated for each waveform in the ensemble for  $\ell = 1, \dots, L, \quad q = 1, \dots, N_{\text{wfms}}$ , with each waveform normalized to have equal energy and under a joint power constraint until the designed waveforms have all converged to within a fixed point tolerance  $\epsilon$ . That is until  $\max_{\ell, q} |\mathbf{s}_\ell^q - \tilde{\mathbf{s}}_\ell^q| < \epsilon$ , where  $\mathbf{s}_\ell^q$  is the value of the designed waveform at iteration  $i$  and  $\tilde{\mathbf{s}}_\ell^q$  is the value of the designed waveform at iteration  $(i-1)$ . This algorithm is ensured to converge to a fixed point since it monotonically increases the sum capacity which is upper bounded. Additionally, the algorithm should achieve the maximum sum capacity for arbitrary waveform initializations using random values

as in [68]. This procedure for waveform design is formally stated in Algorithm V.2.

---

**Algorithm 5 – Waveform & Receiver Filter Design Via Greedy SINR Maximization**

**1: Input:**

- Number of targets  $L$  to be estimated, number of frequencies of interest  $K$ .
- Target frequency responses, normalized to have unit energy  $\mathbf{H}_\ell$ ,  $\ell = 1, \dots, L$
- Target reflection coefficients  $\lambda_{rd}^\ell, \forall d = \ell = 1, \dots, L, r = 1, \dots, L$
- Pre-defined fixed tolerance  $\epsilon$

2: Initialize waveforms  $\mathbf{s}_\ell^{(q)}, \ell = 1, \dots, L, q = 1, \dots, N_{\text{wfms}}$  using normally distributed random numbers

3: **while**  $\max_{\ell, q} |\mathbf{s}_\ell^{(q)} - \tilde{\mathbf{s}}_\ell^{(q)}| > \epsilon$  **do**

4:   **for**  $\ell = 1, \dots, L$  **do**

5:     **for**  $q = 1, \dots, N_{\text{wfms}}$  **do**

6:       Set  $\mathbf{s}_\ell^{(q)} = \mathbf{c}_\ell^{(q)}$  where  $\mathbf{c}_\ell^{(q)}$  is computed to be the eigenvector corresponding to the maximum generalized eigenvalue defined by (V.2.5)

7:       Normalize  $\mathbf{s}_\ell^{(q)} = \frac{p_\ell}{\sqrt{N_{\text{wfms}}}} \frac{\mathbf{s}_\ell^{(q)}}{|\mathbf{s}_\ell^{(q)}|}$

8:     **end for**

9:   **end for**

10: **end while**

11: **Output:** Optimized radar waveforms  $\mathbf{s}_\ell^{(q)}$  and associated receiver filters  $\mathbf{c}_\ell^{(q)}$  for  $\ell = 1, \dots, L, q = 1, \dots, N_{\text{wfms}}$ .

---

Fig. 17: Greedy SINR-maximization based joint waveform and receiver filter design algorithm

Each waveform designed in this context can be viewed as an incremental addition to the total sum waveform set generated for target  $\ell$ , and designing waveforms using this strategy will result in the same allocation of power over the frequencies of interest for each target as if a simultaneous water filling [36] approach was used as determined in [68]. This is intuitive since each individual waveform designed for each target can be thought of as an incremental allocation of the total power available for that target.

Worth noting is that the maximum eigenvalue  $\zeta_{\max}$  is often unique, in which case the designed waveform vector  $\mathbf{s}_\ell^{(q)}$  will be a canonical eigenvector such that power is allocated to a single frequency. As such, designing more waveforms for each target results in greater frequency diversity of the designed total waveform  $\mathbf{s}_\ell$  which can be expected to result in an improved ability to estimate the frequency response of each target.

### V.3 SIMULATIONS AND NUMERICAL RESULTS

To illustrate the performance of the presented approach, a system setup similar to those presented in Chapter 3 and Chapter 4 was considered. A total power constraint was enforced such that the total power transmitted for all waveforms was  $P_{T_x}$ , and the total expected SNR at the receiver was defined as

$$\gamma_{R_x} = \frac{P_{T_x}}{K\sigma_n^2} \sum_{\ell=1}^L \sum_{r=1}^L |\lambda_{r\ell}^{(\ell)}|^2. \quad (\text{V.3.1})$$

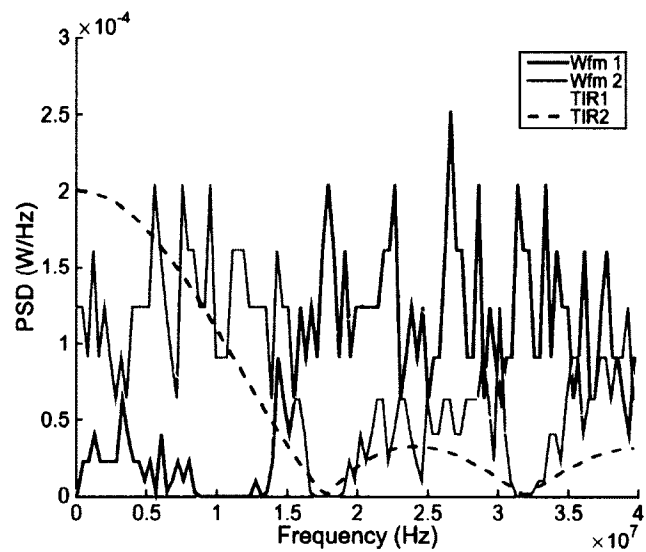
This expression was achieved using V.1.7 and considering the ideal target response of  $\mathbf{H}_\ell = \mathbf{I}_K$  (equivalent to assuming a point target).  $K = 201$  frequency bands were considered over an 80MHz bandwidth centered at a carrier frequency of 8GHz (implying a 3.75m range resolution), with waveforms designed at baseband from 0 to 40 MHz over 101 frequency bins. The simulations assume that phased arrays with  $N_T = N_R = 25$  elements and  $1/2$  wavelength spacing were used at the transmitter and receiver, that classical beamforming was used for transmission and reception over  $T = R = L$  beams, and that the transmitter and receiver were separated by 12km.

As in [25] the target frequency responses are assumed to be random, with known

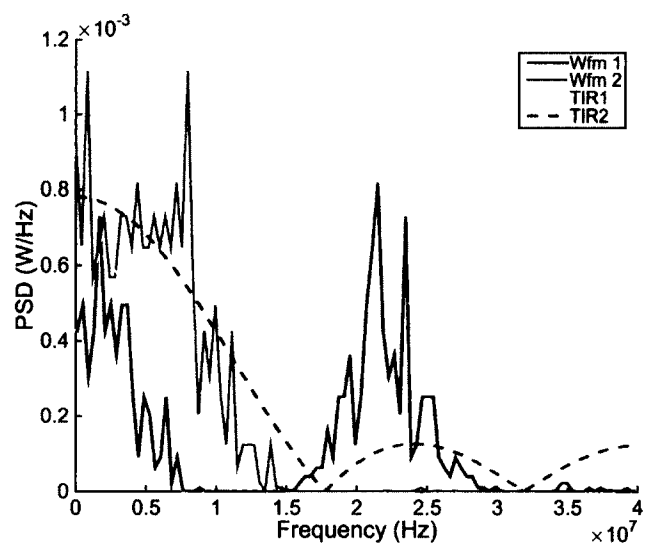
power spectral density (PSD) and are defined as implied by taking the Fourier transform of the discrete-time impulse responses depicted in Figure 9, scaled to have unit norm.

### V.3.1 Weak Interference

In the case of weak interference, targets which are separated by 3 degrees from the perspective of the receiver are considered, similarly to [25]. To analyze the generated waveforms in the case of weak interference, the simulation considered the case in which  $N_{\text{wfms}} = 500$  waveforms were generated for each of  $L = 2$  targets, using the first two target impulse responses of Figure 9 for  $\ell = 1$  and  $\ell = 2$ , respectively. The targets were located at  $(\tau_\ell, \rho_\ell) = [(75, 70), (48, 73)]$  degrees relative to the baseline between the transmitter and receiver in the case of weak interference in both high and low SNR cases. In the case of high SNR, a transmit power of 1kW is assumed to achieve a similar SNR to the one in [25] on the order of  $\sim 35$ dB in the presence of AWGN with variance  $\sigma_n^2 = -164$ dBm/Hz as in [25]. In the case of low SNR, a noise variance of  $-141$ dBm/Hz is assumed corresponding to a total received SNR on the order of  $\sim 18$  dB. The waveforms designed for each target are illustrated in Figure 18 for both the high and low SNR scenarios. In each plot, the target frequency response has been normalized and scaled by the norm of the sum of all waveforms directed toward the corresponding target. From these results, it can be observed in the high SNR scenario that when the targets are widely separated from the perspective of the receiver (so that interference between targets is weak), a significant portion of the total energy directed toward each target is allocated to frequencies occupied by waveforms designed for the other target. This agrees with the observations made



(a)

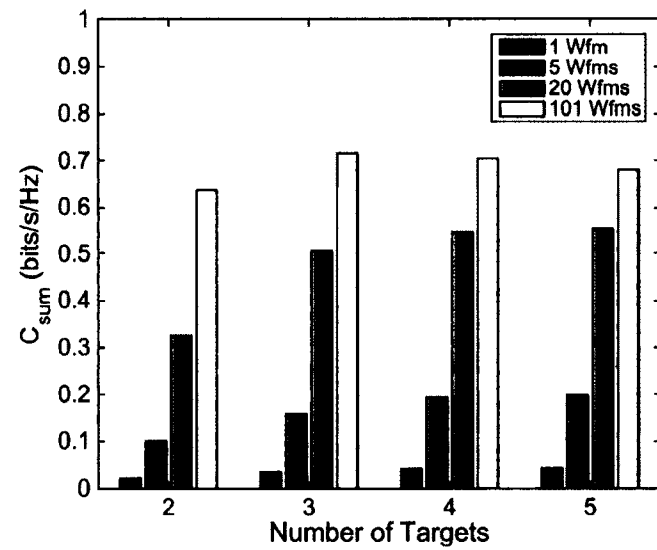


(b)

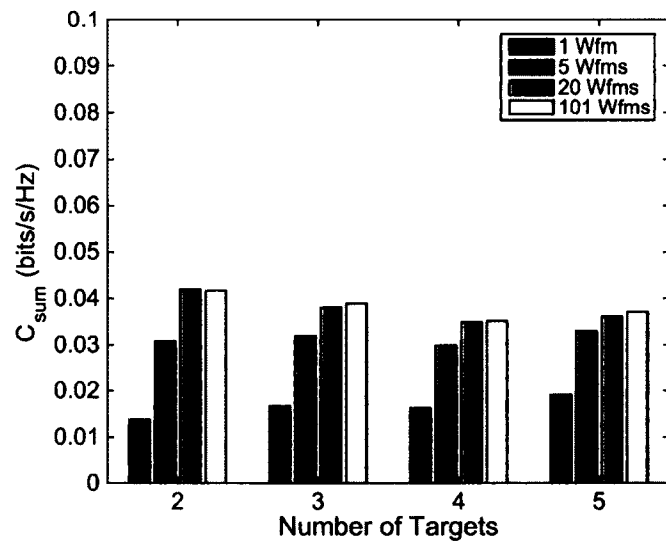
Fig. 18: Waveforms designed for two weakly-interfering targets (a) High SNR (b) Low SNR

in [25] using a different waveform design method for a similar two-target estimation problem. Additionally, it can be observed in the high SNR case that the shapes of the transmitted waveforms do not tend to closely follow the shapes of the target frequency responses. In the low SNR scenario, the designed waveforms overlap in frequencies which is expected since interference is not the driving parameter when the SINR is noise-dominated. However, waveforms in the low SNR case tend to follow the shape of the target responses more closely than in the high SNR scenario. This makes sense intuitively since the shape of the target should help distinguish the target from the flat frequency response of the additive white Gaussian noise.

To observe how the achievable sum capacity varies with the number of waveforms generated, scenarios were considered in which  $N_{\text{wfms}} = \{1, 5, 20, 101\}$  waveforms were generated for the estimation of  $L = \{1, 2, 3, 4, 5\}$  targets. The targets were located at  $[(75, 70), (48, 73), (59, 77), (71, 67), (44, 80)]$  degrees relative to the baseline between the transmitter and receiver for the case of weak interference. The resulting sum capacity achieved in each case is illustrated in Figure 19. From the results, it can be observed that sum capacity increases with the number of waveforms generated. Additionally, in the high SNR scenario, this improvement in sum capacity is diminished when more interfering users are present. Regarding each target similarly to a single user in the multibase wireless communication system studied in [68] allows comparison with the similar result regarding an increase in capacity with the number of codewords generated for each user in their system. Additionally, in the low SNR case the improvement in sum capacity appears to be independent of the number of targets present. This result is intuitive since increasing the number of waveforms



(a)



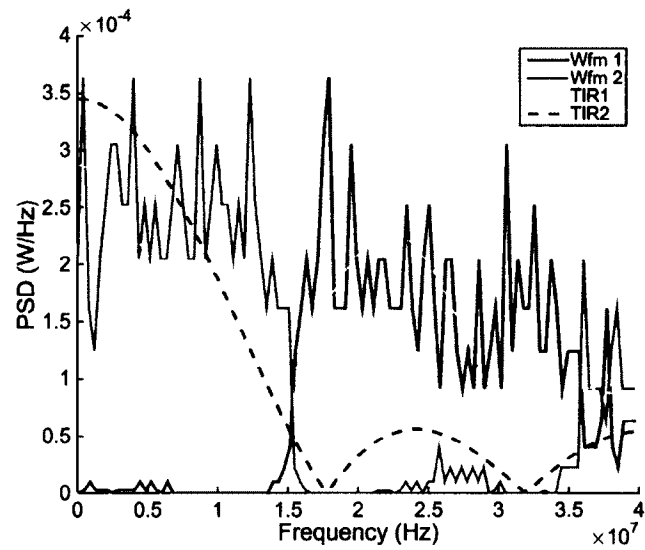
(b)

Fig. 19: Sum Capacity for weakly-interfering targets (a) High SNR (b) Low SNR

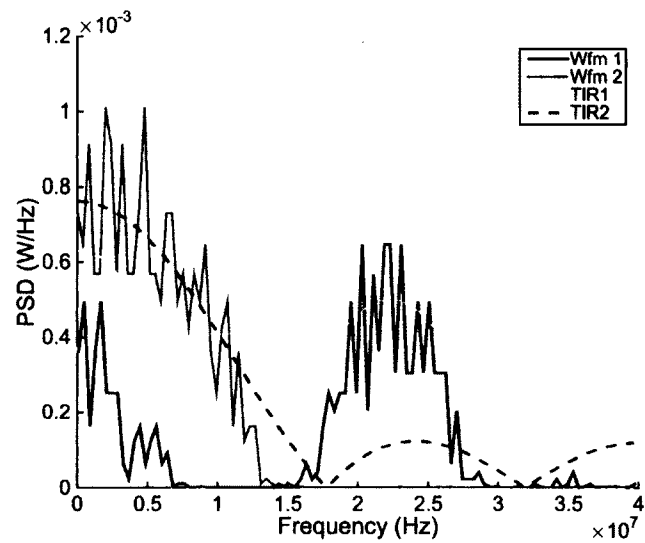
increases the degrees of freedom in the waveform design process, allowing the total waveform set for each target to more closely approximate the response of each target so that it can be more easily distinguished from the white noise. As the SINR is noise-dominated in the low SNR case, the sum capacity also appears to be limited to significantly lower values than in the high SNR case.

### V.3.2 Moderate Interference

Define the moderate interference case in which targets are separated by 1 degree from the perspective of the receiver. To analyze the generated waveforms in the case of moderate interference, the simulation considered the case in which  $N_{\text{wfms}} = 500$  waveforms were generated for the same two targets considered in the weak interference case but now located at  $[(75, 70), (55, 71)]$  degrees relative to the baseline between the transmitter and receiver in both high and low SNR cases with transmit power and noise again defined as in the case of weak interference. The waveforms designed for each target are illustrated in Figure 20 for both the high and low SNR scenarios. In each plot, the each target frequency response has been normalized and scaled by the norm of the sum of all waveforms directed toward the corresponding target. From these results, it can be observed in the high SNR scenario that when the targets are moderately close together from the perspective of the receiver, less of the total energy directed toward each target is allocated to frequencies occupied by waveforms designed for the other target. Additionally, it can be observed in the high SNR case that the shapes of the transmitted waveforms do not tend to closely follow the shapes of the target frequency responses. In the low SNR scenario, the designed waveforms again overlap in frequencies, and waveforms in the low SNR case tend to follow the

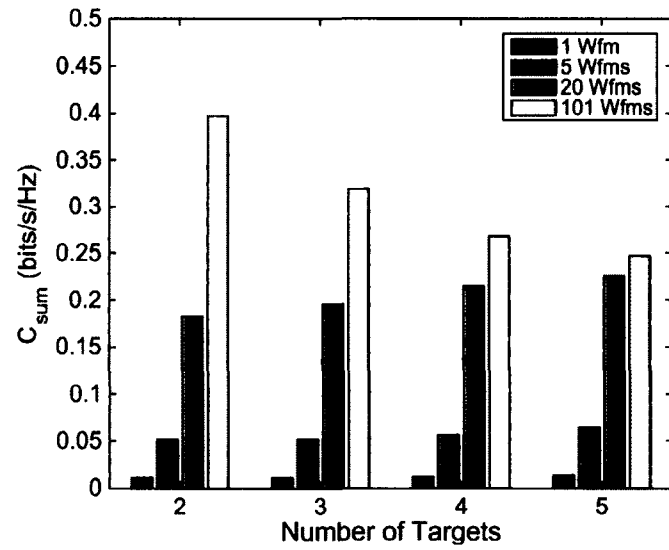


(a)

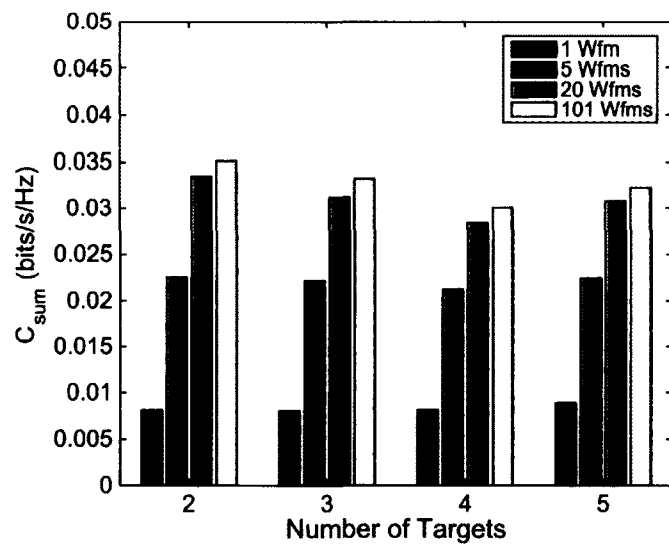


(b)

Fig. 20: Waveforms designed for two moderately-interfering targets (a) High SNR (b) Low SNR



(a)



(b)

Fig. 21: Sum Capacity for moderately-interfering targets (a) High SNR (b) Low SNR

shape of the target responses more closely than in the high SNR scenario.

To observe how the achievable sum capacity varies with the number of waveforms generated, scenarios were considered in which  $N_{\text{wfms}} = \{1, 5, 20, 101\}$  waveforms were generated for the estimation of  $L = \{1, 2, 3, 4, 5\}$  targets. The targets were located at  $[(75, 70), (55, 71), (65, 69), (70, 68), (47, 72)]$  degrees relative to the baseline between the transmitter and receiver for the case of moderate interference. The resulting sum capacity achieved in each case is illustrated in Figure 21. From the results, it can be observed that sum capacity increases with the number of waveforms generated similar to the weak interference case and to the related communication channel scenario in [68]. However, it is worth noting that in the case of [68] the sum capacity increased with the number of transmitting users while in the case of the radar system, the sum capacity tends to decrease with the number of targets of interest when the scene is interference-dominated. This is intuitive since each transmitter in the communication system has its own independent power budget, while in the case of the radar system the waveform set designed for each target draws from a total combined system power constraint. The improvement in sum capacity in the low SNR case is again similar regardless of the number of targets present, which suggests that the scene is dominated by noise rather than interference between targets in the defined low SNR scenario for 1 degree target separation.

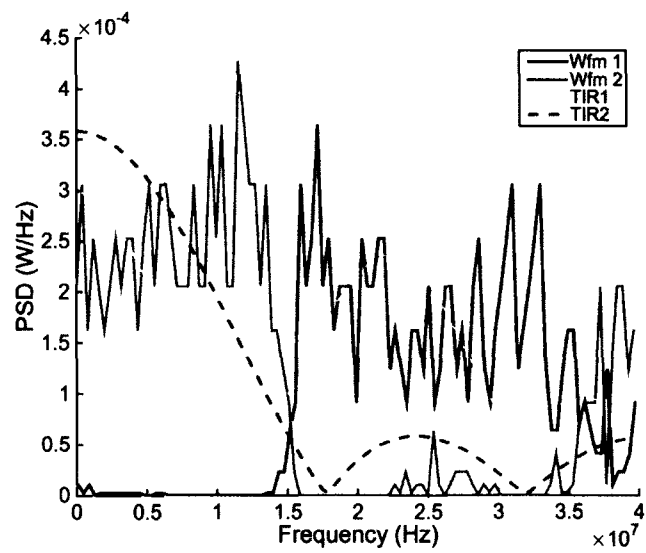
### V.3.3 Strong Interference

Define the strong interference case in which targets are separated by 0.5 degree from the perspective of the receiver. To analyze the generated waveforms in the case of moderate interference, the simulation considered the case in which  $N_{\text{wfms}} =$

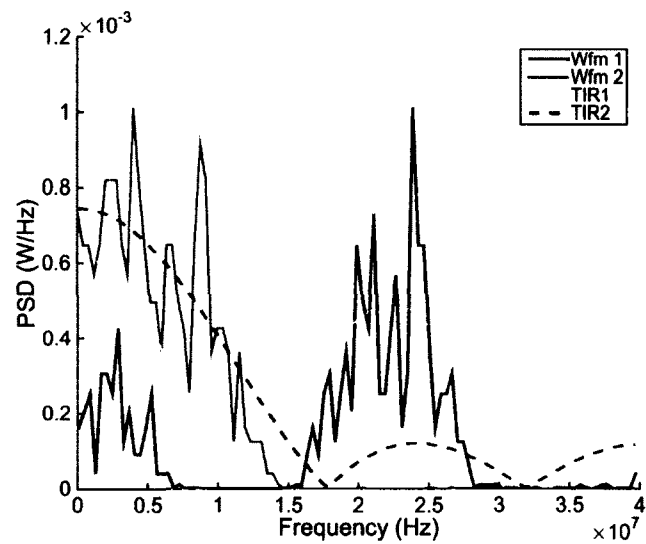
500 waveforms were generated for the same two targets considered in the weak and moderate interference cases but now located at  $[(75, 70), (55, 70.5)]$  degrees relative to the baseline between the transmitter and receiver in both high and low SNR cases with transmit power and noise again defined as in the previous scenarios.

The waveforms designed for each target are illustrated in Figure 22 for both the high and low SNR scenarios. In each plot, each target frequency response has been normalized and scaled by the norm of the sum of all waveforms directed toward the corresponding target. From these results, it can be observed in the high SNR scenario that when the targets are close together from the perspective of the receiver (so that interference between targets is stronger), very little of the total energy directed toward each target is allocated to frequencies occupied by waveforms designed for the other target. This again agrees with the observations made in [25] using a different waveform design method for a similar two-target estimation problem. Additionally, it can be observed in the high SNR case the shapes of the transmitted waveforms do not tend to closely follow the shapes of the target frequency responses. In the low SNR scenario, the designed waveforms again overlap in frequencies, and waveforms in the low SNR case tend to follow the shape of the target responses more closely than in the high SNR

To observe how the achievable sum capacity varies with the number of waveforms generated, scenarios were considered in which  $N_{\text{wfms}} = \{1, 5, 20, 101\}$  waveforms were generated for the estimation of  $L = \{1, 2, 3, 4, 5\}$  targets. The targets were located at  $[(75, 70), (55, 70.5), (65, 69), (68, 71), (48, 69.5)]$  degrees relative to the baseline between the transmitter and receiver for the case of strong interference. The resulting

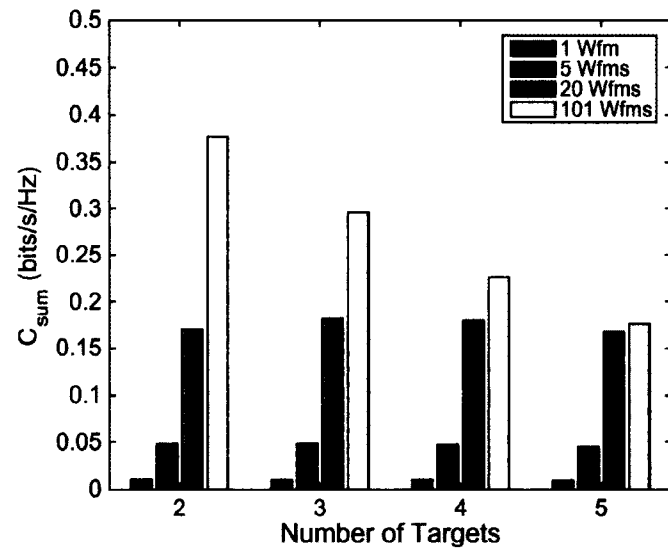


(a)

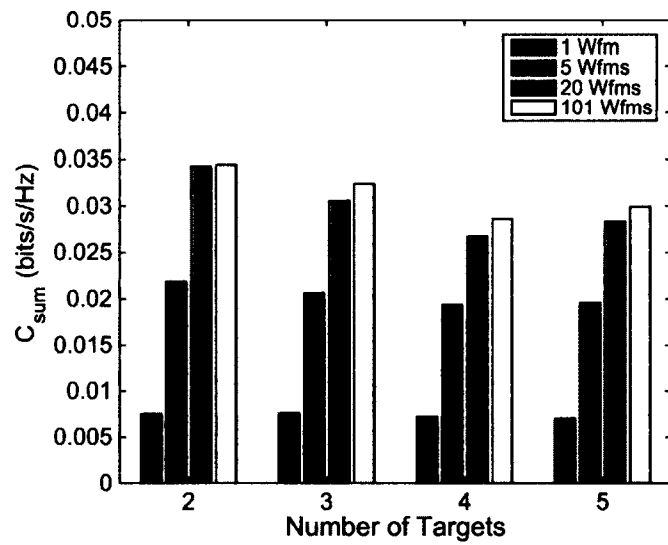


(b)

Fig. 22: Waveforms designed for two strongly-interfering targets (a) High SNR (b) Low SNR



(a)



(b)

Fig. 23: Sum Capacity for strongly-interfering targets (a) High SNR (b) Low SNR

sum capacity achieved in each case is illustrated in Figure 23. From the results, it can be observed that sum capacity increases with the number of waveforms generated similar to the moderate interference case. The improvement in sum capacity in the low SNR case is again similar regardless of the number of targets present, which suggests that the scene is still dominated by noise rather than interference between targets in the defined low SNR scenario for 0.5 degree target separation.

#### V.4 CHAPTER SUMMARY

In this chapter, the multiple extended target estimation problem was introduced and related to the similar information theoretic problem of estimating the information transmitted by multiple interfering users in a multibase wireless communication system. Using this relationship, a similar waveform design procedure for the multiple radar target estimation problem was presented using a greedy SINR maximization based approach. Results from two numerical simulations were presented. The first illustrated the spectral allocation of power for waveforms designed in the two target case, while the second analyzed the sum capacity achievable using the proposed approach for 1 – 5 targets. Results from the first simulation indicate that when targets are received from well separated arrival angles more of the waveform power is allocated to overlapping frequency bands from one target to another. When the separation is smaller, less power is allocated to overlapping frequency bins. Results from the second simulation indicate that sum capacity increases with the number of waveforms designed for each target. Additionally, when the scene is interference-dominated, the improvement in sum capacity is more significant between the single waveform and 20

waveform case than between the 20 waveform case and the 101 waveform case. This agrees with a similar result reached for a collaborative multibase wireless communication system and suggests that an acceptable sum capacity may be achieved with only a few waveforms in the interference-dominated scenario.

Future work includes consideration of the scenario in which the priority for estimating some targets may be higher than others. This is of particular interest in the case where the total radar cross section of some targets are significantly smaller than others so that estimation of that target may be more difficult.

## CHAPTER VI

### CONCLUSIONS AND FUTURE RESEARCH

In this chapter, the contributions of this dissertation are summarized and some useful directions for future research are discussed.

#### VI.1 CONCLUSIONS

Recently, there has been growing interest in adaptive waveform design for software-defined and cognitive radar systems. Preliminary works have leveraged information-theoretic concepts used in communication systems in the context of radar waveform design. Illustrating a clear parallel between radar systems and information transmission systems can allow radar waveform design methods to draw from the broad existing knowledge base of waveform/codeword design techniques for communication systems. This dissertation has contributed a framework for modeling the radar system that describes these similarities and has considered the multiple extended target detection and estimation problems within the proposed model. These contributions can be summarized as follows.

First, a novel vector channel model was presented illustrating the parallel composition of the multiple target MIMO radar system and the multiple user vector communication channel model. The MIMO radar system modeled can easily be particularized for different scenarios and the framework allows consideration of both detection and estimation problems. As such, this description facilitates comparison of similar communication system scenarios and provides a basis for realizing similarities

among optimal waveform adaptation schemes developed for each system.

Next, a new procedure was presented for joint waveform and receiver filter design for detection of multiple extended targets in MIMO radar systems using a compressed sensing approach. Using transmit-receive beamforming to partition the radar scene allowed a spatially sparse representation of the radar scene when few targets of interest are present. Compressed sensing was then used to reconstruct the sparse scene and to design the transmitted radar waveforms with formal algorithms for joint optimization of the radar waveforms and receiver filters stated for the noiseless case. Results indicated that lower reconstruction errors were obtained and increased target detection rates were observed when transmitted waveform and receiver filter matrices designed using the proposed procedure compared to statically defined waveforms typically used in compressed sensing.

Next, this procedure was modified for detection of multiple extended targets in the noisy case, specifically designing waveforms for compressed-sensing based reconstruction when additive white Gaussian noise corrupts the signal at the receiver. Results in this scenario also indicated that lower reconstruction errors were obtained and increased target detection rates were observed when transmitted waveform and receiver filter matrices designed using the proposed procedure compared to statically defined waveforms typically used in compressed sensing.

Finally, the multiple extended target estimation problem was studied in the proposed framework and related to the similar information theoretic problem of estimating the information transmitted by multiple interfering users in a multibase wireless communication system. Using this relationship, a joint waveform design procedure

was presented for the estimation of multiple extended targets using a greedy SINR maximization based approach. Results indicated that when target interference is high less waveform power is allocated to overlapping frequency bins and that sum capacity increases with the number of waveforms designed for each target.

## VI.2 FUTURE RESEARCH

Throughout this work, several areas were identified as interesting directions for future research. In the short term, it would be interesting to compare the waveforms designed for target detection in Chapter 3 and Chapter 4 to those designed for target estimation in Chapter 5. Preliminary observations indicate that there are similarities among waveforms designed using the two methods, though more work needs to be done to fully analyze and understand the connection between the results of the two design procedures and its implications. Additionally, including varied target priorities in each design algorithm in Chapters 3-5 could provide meaningful insight, particularly in the case where the total radar cross section of some targets are significantly smaller than others so that detection estimation of that target may be more difficult when compared to other targets. In the long term, Doppler shift parameters could be included for each target, and known clutter sources could be considered. Additionally, while Chapters 3-5 considered waveform design in frequency domain, additional work could include consideration of time domain design of radar waveforms and receiver filters using the time domain model of Chapter 2.

## BIBLIOGRAPHY

- [1] T. Williamson and N. Spencer, "Development and operation of the traffic alert and collision avoidance system (TCAS)," *Proceedings of the IEEE*, vol. 77, no. 11, pp. 1735–1744, 1989.
- [2] W.-M. Boerner, "Recent advances in extra-wide-band polarimetry, interferometry and polarimetric interferometry in synthetic aperture remote sensing and its applications," *IEE Proceedings - Radar, Sonar and Navigation*, vol. 150, no. 3, pp. 113–124, 2003.
- [3] H. Wang and L. Cai, "On adaptive spatial-temporal processing for airborne surveillance radar systems," *IEEE Transactions on Aerospace and Electronic Systems*, vol. 30, no. 3, pp. 660–670, 1994.
- [4] S. P. Sira, A. Papandreou-Suppappola, D. Morrell, D. Cochran, and M. Rangaswamy, "Waveform-agile sensing for tracking," *IEEE Signal Processing Magazine*, vol. 26, no. 1, pp. 53–64, January 2009.
- [5] H. L. Van Trees, *Detection, Estimation, and Modulation Theory, Part 1*. New York: Wiley, 1968.
- [6] M. Bell, "Information theory and radar waveform design," *IEEE Transactions on Information Theory*, vol. 39, no. 5, pp. 1578–1597, September 1993.
- [7] Y. Bar-Shalom and T. E. Fortman, *Tracking and Data Association*. New York: Academic Press, 1988.

- [8] F. M. Henderson and e. A. J. Lewis, *Manual of Remote Sensing, Volume 2: Principles and Applications of Imaging Radar*. New York, 3rd edition: John Wiley and Sons, 1998.
- [9] C. A. Balanis, *Antenna Theory: Analysis and Design*, 2nd ed. New York: John Wiley and Sons, Inc., 1997.
- [10] D. Garmatyuk, J. Schuerger, and K. Kauffman, "Multifunctional software-defined radar sensor and data communication system," *IEEE Sensors Journal*, vol. 11, no. 1, pp. 99–106, 2011.
- [11] S. Haykin, Y. Xue, and P. Setoodeh, "Cognitive radar: Step toward bridging the gap between neuroscience and engineering," *Proceedings of the IEEE*, vol. 100, no. 11, pp. 3102–3130, 2012.
- [12] D. Kershaw and R. Evans, "Optimal waveform selection for tracking systems," *IEEE Transactions on Information Theory*, vol. 40, no. 5, pp. 1536–1550, 1994.
- [13] S. Haykin, A. Zia, Y. Xue, and I. Arasaratnam, "Control theoretic approach to tracking radar: first step towards cognition," *Digital Signal Processing*, vol. 21, no. 5, pp. 576–585, 2011.
- [14] S. Sira, A. Papandreou-Suppappola, and D. Morrell, "Dynamic configuration of time-varying waveforms for agile sensing and tracking in clutter," *IEEE Transactions on Signal Processing*, vol. 55, no. 7, pp. 3207–3217, July 2007.
- [15] S. Haykin, "Cognitive radar: a way of the future," *Signal Processing Magazine, IEEE*, vol. 23, no. 1, pp. 30–40, 2006.

- [16] P. Chavali and A. Nehorai, "Scheduling and power allocation in a cognitive radar network for multiple-target tracking," *IEEE Transactions on Signal Processing*, vol. 60, no. 2, pp. 715–729, 2012.
- [17] X. Zhang and C. Cui, "Signal detection for cognitive radar," *Electronics Letters*, vol. 49, no. 8, 2013.
- [18] R. Romero and N. Goodman, "Cognitive radar network: Cooperative adaptive beamsteering for integrated search-and-track application," *Aerospace and Electronic Systems, IEEE Transactions on*, vol. 49, no. 2, pp. 915–931, 2013.
- [19] N. Goodman, P. Venkata, and M. Neifeld, "Adaptive waveform design and sequential hypothesis testing for target recognition with active sensors," *Selected Topics in Signal Processing, IEEE Journal of*, vol. 1, no. 1, pp. 105–113, 2007.
- [20] M. R. Bell, "Information theory and radar: mutual information and the design and analysis of radar waveforms and systems," Ph.D. dissertation, California Institute of Technology, Pasadena, March 1988.
- [21] M. H. M. Costa, "Writing on dirty paper," *IEEE Transactions on Information Theory*, vol. IT-29, no. 13, pp. 439–441, May 1983.
- [22] P. M. Woodward, *Probability and Information Theory with Applications to Radar*. London: Pergamon, 1953.
- [23] P. M. Woodward, "Information theory and the design of radar receivers," *IRE Proceedings*, vol. 39, pp. 1521–1524, Dec. 1951.

- [24] V. Frost and K. Shanmugan, "The information content of synthetic aperture radar images of terrain," *IEEE Transactions on Aerospace and Electronic Systems*, vol. AES-19, no. 5, pp. 768–774, sept. 1983.
- [25] A. Leshem, O. Naparstek, and A. Nehorai, "Information theoretic adaptive radar waveform Design for multiple extended targets," *IEEE Journal of Selected Topics in Signal Processing*, vol. 1, no. 1, pp. 42–55, June 2007.
- [26] Y. Yang and R. Blum, "MIMO radar waveform design based on mutual information and minimum mean-square error estimation," *IEEE Transactions on Aerospace and Electronic Systems*, vol. 43, no. 1, pp. 330–343, January 2007.
- [27] T. Naghibi and F. Behnia, "MIMO radar waveform design in the presence of clutter," *IEEE Transactions on Aerospace and Electronic Systems*, vol. 47, no. 2, pp. 770–781, 2011.
- [28] S. Kay, "Waveform design for multistatic radar detection," *IEEE Transactions on Aerospace and Electronic Systems*, vol. 45, no. 3, pp. 1153–1166, july 2009.
- [29] S. Sen, "Ofdm radar space-time adaptive processing by exploiting spatio-temporal sparsity," *IEEE Transactions on Signal Processing*, vol. 61, no. 1, pp. 118–130, 2013.
- [30] S. Sen and A. Nehorai, "Adaptive design of ofdm radar signal with improved wideband ambiguity function," *IEEE Transactions on Signal Processing*, vol. 58, no. 2, pp. 928–933, 2010.

- [31] S. Sen and A. Nehorai, "Target detection in clutter using adaptive ofdm radar," *Signal Processing Letters, IEEE*, vol. 16, no. 7, pp. 592–595, 2009.
- [32] H. Wang, J. Wang, and H. Li, "Target detection using cdma based passive bistatic radar," *Systems Engineering and Electronics, Journal of*, vol. 23, no. 6, pp. 858–865, 2012.
- [33] C. Sturm and W. Wiesbeck, "Waveform design and signal processing aspects for fusion of wireless communications and radar sensing," *Proceedings of the IEEE*, vol. 99, no. 7, pp. 1236–1259, 2011.
- [34] J. Xu, X.-Z. Dai, X.-G. Xia, L.-B. Wang, J. Yu, and Y.-N. Peng, "Optimizations of multisite radar system with MIMO radars for target detection," *IEEE Transactions on Aerospace and Electronic Systems*, vol. 47, no. 4, pp. 2329–2343, Oct 2011.
- [35] J. W. Brewer, "Kronecker products and matrix calculus in system theory," *IEEE Transactions on Circuits and Systems*, vol. CAS-25, no. 9, pp. 772–781, Sept 1978.
- [36] W. Yu, W. Rhee, S. Boyd, and J. M. Cioffi, "Iterative water-filling for gaussian vector multiple-access channels," *IEEE Transactions on Information Theory*, vol. 50, no. 1, pp. 145–152, January 2004.
- [37] A. Goldsmith, *Wireless Communications*. New York: Cambridge University Press, 2005.

- [38] E. Candes, J. Romberg, and T. Tao, "Robust uncertainty principles: exact signal reconstruction from highly incomplete frequency information," *IEEE Transactions on Information Theory*, vol. 52, no. 2, pp. 489–509, 2006.
- [39] D. Donoho, "Compressed sensing," *IEEE Transactions on Information Theory*, vol. 52, no. 4, pp. 1289–1306, 2006.
- [40] S. Sarvotham, D. Baron, and R. G. Baraniuk, "Measurements vs. bits: Compressed sensing meets information theory," in *Allerton Conference on Communication, Control and Computing*, Allerton, IL, Sep. 2006.
- [41] W. Bajwa, J. Haupt, A. Sayeed, and R. Nowak, "Compressed channel sensing: A new approach to estimating sparse multipath channels," *Proceedings of the IEEE*, vol. 98, no. 6, pp. 1058–1076, June 2010.
- [42] J. Paredes, G. Arce, and Z. Wang, "Ultra-wideband compressed sensing: Channel estimation," *IEEE Journal of Selected Topics in Signal Processing*, vol. 1, no. 3, pp. 383–395, Oct 2007.
- [43] C. Berger, Z. Wang, J. Huang, and S. Zhou, "Application of compressive sensing to sparse channel estimation," *IEEE Communications Magazine*, vol. 48, no. 11, pp. 164–174, November 2010.
- [44] J. Zhang, D. Zhu, and G. Zhang, "Adaptive compressed sensing radar oriented toward cognitive detection in dynamic sparse target scene," *IEEE Transactions on Signal Processing*, vol. 60, no. 4, pp. 1718–1729, 2012.

- [45] M. Herman and T. Strohmer, "High-resolution radar via compressed sensing," *IEEE Transactions on Signal Processing*, vol. 57, no. 6, pp. 2275–2284, June 2009.
- [46] R. Baraniuk and P. Steeghs, "Compressive radar imaging," in *2007 IEEE Radar Conference*, April 2007, pp. 128–133.
- [47] M. Hyder and K. Mahata, "Maximum a posteriori based approach for target detection in mti radar," *IEEE Journal on Emerging and Selected Topics in Circuits and Systems*, vol. 2, no. 3, pp. 392–401, 2012.
- [48] C.-Y. Chen and P. Vaidyanathan, "Compressed sensing in MIMO radar," in *42nd Asilomar Conference on Signals, Systems and Computers*, October 2008, pp. 41–44.
- [49] Y. Yu, A. Petropulu, and H. Poor, "Measurement matrix design for compressive sensing-based MIMO radar," *IEEE Transactions on Signal Processing*, vol. 59, no. 11, pp. 5338–5352, Nov 2011.
- [50] Y. Yu, S. Sun, R. Madan, and A. Petropulu, "Power allocation and waveform design for the compressive sensing based MIMO radar," *IEEE Transactions on Aerospace and Electronic Systems*, vol. 50, no. 2, pp. 898–909, April 2014.
- [51] C.-Y. Chen and P. Vaidyanathan, "MIMO radar waveform optimization with prior information of the extended target and clutter," *IEEE Transactions on Signal Processing*, vol. 57, no. 9, pp. 3533–3544, Sept 2009.

- [52] D. Needell and R. Vershynin, "Uniform uncertainty principle and signal recovery via regularized orthogonal matching pursuit," *Foundations of Computational Mathematics*, vol. 9, pp. 317–334, 2008.
- [53] E. J. Candes, "The restricted isometry property and its implications for compressed sensing," *Compte Rendus de l'Academie des Sciences*, vol. 346, no. 9, pp. 589–592, 2008.
- [54] M. Elad, "Optimized projections for compressed sensing," *IEEE Transactions on Signal Processing*, vol. 55, no. 12, pp. 5695–5702, Dec 2007.
- [55] H. Fang, S. A. Vorobyov, H. Jiang, and O. Taheri, "Permutation meets parallel compressed sensing: How to relax restricted isometry property for 2d sparse signals," *Signal Processing, IEEE Transactions on*, vol. 62, no. 1, pp. 196–210, Jan 2014.
- [56] S. Chen, D. Donoho, and M. Saunders, "Atomic decomposition by basis pursuit," *SIAM Journal on Scientific Computing*, vol. 20, no. 1, pp. 33–61, 1998.
- [57] J. A. Tropp and A. C. Gilbert, "Signal recovery from partial information by orthogonal matching pursuit," *IEEE Transactions on Information Theory*, vol. 53, pp. 4655–4666, 2008.
- [58] J. Duarte-Carvajalino and G. Sapiro, "Learning to sense sparse signals: Simultaneous sensing matrix and sparsifying dictionary optimization," *IEEE Transactions on Image Processing*, vol. 18, no. 7, pp. 1395–1408, 2009.

- [59] J. Li, P. Stoica, and X. Zheng, "Signal synthesis and receiver design for mimo radar imaging," *IEEE Transactions on Signal Processing*, vol. 56, no. 8, pp. 3959–3968, Aug 2008.
- [60] L. Anitori, A. Maleki, M. Otten, R. Baraniuk, and P. Hoogeboom, "Design and analysis of compressed sensing radar detectors," *IEEE Transactions on Signal Processing*, vol. 61, no. 4, pp. 813–827, Feb 2013.
- [61] P. Swerling, "Probability of detection for fluctuating targets," *IRE Transactions on Information Theory*, vol. 6, no. 2, pp. 269–308, April 1960.
- [62] M. Shastry, R. Narayanan, and M. Rangaswamy, "Compressive radar imaging using white stochastic waveforms," in *2010 International Waveform Diversity and Design Conference*, August 2010, pp. 000 090–000 094.
- [63] W. Alltop, "Complex sequences with low periodic correlations (corresp.)," *IEEE Transactions on Information Theory*, vol. 26, no. 3, pp. 350–354, May 1980.
- [64] E. Candes and M. Wakin, "An introduction to compressive sampling," *IEEE Signal Processing Magazine*, vol. 25, no. 2, pp. 21–30, March 2008.
- [65] D. Needell and J. A. Tropp, "CoSaMP: Iterative Signal Recovery from Incomplete and Inaccurate Samples," *Applied and Computational Harmonic Analysis*, vol. 26, no. 3, pp. 301–321, 2009.
- [66] E. Candes and T. Tao, "Decoding by linear programming," *IEEE Transactions on Information Theory*, vol. 51, no. 12, pp. 4203–4215, Dec 2005.

- [67] J. Li and P. Stoica, *MIMO Radar Signal Processing*. Hoboken, NJ: John Wiley and Sons, Inc, 2008.
- [68] O. Popescu and C. Rose, "Greedy SINR maximization in collaborative multi-base wireless systems," *EURASIP Journal on Wireless Communications and Networking*, vol. 2, pp. 201–209, December 2004.
- [69] A. Daniel and D. C. Popescu, "A vector channel approach to waveform optimization in radar systems," in *Proceedings 46<sup>th</sup> Conference on Information Sciences and Systems - CISS 2012*, Princeton, NJ, March 2012.
- [70] F. P. Gantmacher and M. G. Krein, *Oscillation Matrices and Kernels and Small Vibrations of Mechanical Systems*. Providence, RI: American Mathematical Society: Chelsea Publishing, 2002.

## Appendix A

### PROOF THAT $\mathbf{R}_{\mathbf{n}_R}$ IS DIAGONAL

Starting with the noise vector as seen after beamforming,  $\mathbf{n}_r = \mathbf{W}\mathbf{v}_r^*$ , its correlation matrix can be written as

$$E\{\mathbf{n}_r\mathbf{n}_r^H\} = E\{\mathbf{W}\mathbf{v}_r^*\mathbf{v}_r^T\mathbf{W}^H\}. \quad (\text{A.1})$$

Since the random quantities are in the matrix  $\mathbf{W}$ , it is not straightforward to propagate the expected value operator within this expression, so instead consider individual elements of  $\mathbf{n}_r$ :

$$\mathbf{n}_r = \begin{bmatrix} n_{r1} \\ \vdots \\ n_{rk} \\ \vdots \\ n_{rK} \end{bmatrix}. \quad (\text{A.2})$$

subsequently giving the elements of the noise cross-correlation matrix of the  $p$ -th beamformed signal  $N_r(i, j) = E\{n_{ri}n_{rj}^*\}$ :

$$\begin{aligned} N_r(i, j) &= E\left\{\left(\sum_{\epsilon=1}^{N_R} W_\epsilon(f_i)v_{r\epsilon}^*\right)\left(\sum_{\epsilon=1}^{N_R} W_\epsilon(f_j)v_{r\epsilon}^*\right)^*\right\} \\ &= \sum_{\epsilon=1}^{N_R} \sum_{\epsilon=1}^{N_R} v_{r\epsilon}^*v_{r\epsilon} E\{W_\epsilon(f_i)W_\epsilon(f_j)^*\}. \end{aligned} \quad (\text{A.3})$$

Under the stated assumptions,

$$\begin{aligned} E\{W_\epsilon(f_i)W_\epsilon(f_j)^*\} &= \delta_{\epsilon\epsilon} \\ E\{W_\epsilon(f_i)W_\epsilon(f_j)^*\} &= \delta_{ij} \end{aligned} \quad (\text{A.4})$$

where  $\delta_{\epsilon\epsilon}$  and  $\delta_{ij}$  correspond to Kronecker  $\delta$  operators defined with respect to  $\epsilon, \epsilon$  and  $i, j$  respectively gives

$$\begin{aligned} N_r(i, j) &= \sum_{\epsilon=1}^{N_R} \sum_{\epsilon=1}^{N_R} v_{r\epsilon}^* v_{r\epsilon} E\{W_\epsilon(f_i)W_\epsilon(f_j)^*\} \delta_{\epsilon\epsilon} \delta_{ij} \\ &= \begin{cases} \sum_{\epsilon=1}^{N_R} |v_{r\epsilon}|^2 E\{|W_\epsilon(f_i)|^2\}, & i = j \\ 0, & i \neq j \end{cases}, \end{aligned} \quad (\text{A.5})$$

which implies that the noise correlation matrix  $\mathbf{R}_{n_r}$  from direction  $r$  is diagonal.

Letting  $\mathcal{R}_\epsilon = E[w_\epsilon(t)w_\epsilon^*(t+\tau)]$  be the autocorrelation matrix of the noise  $w_\epsilon$  at receive antenna  $\epsilon$  and taking the Fourier transform gives the PSD  $Q_\epsilon(f) = \mathcal{F}\{\mathcal{R}_\epsilon(\tau)\}$ , which can be computed at frequency  $f_i$  as:

$$E[|W_\epsilon(f_i)|^2] = E[W_\epsilon(f_i)W_\epsilon^*(f_i)] \quad (\text{A.6})$$

$$= E\left[\left(\int_{-\infty}^{\infty} w_\epsilon(t)e^{-j2\pi f_i t} dt\right)\left(\int_{-\infty}^{\infty} w_\epsilon(\tau)e^{-j2\pi f_i \tau} d\tau\right)^*\right] \quad (\text{A.7})$$

$$= E\left[\int_{-\infty}^{\infty} \int_{-\infty}^{\infty} w_\epsilon(t)w_\epsilon^*(\tau)e^{-j2\pi f_i(t-\tau)} dt d\tau\right] \quad (\text{A.8})$$

$$= \int_{-\infty}^{\infty} \int_{-\infty}^{\infty} \underbrace{E[w_\epsilon(t)w_\epsilon^*(\tau)]}_{\mathcal{R}_\epsilon(t,\tau)\delta(t-\tau)} e^{-j2\pi f_i(t-\tau)} dt d\tau \quad (\text{A.9})$$

$$= \int_{-\infty}^{\infty} \mathcal{R}_\epsilon(\tau)e^{-j2\pi f_i \tau} d\tau = Q_\epsilon(f_i) \quad (\text{A.10})$$

$$\text{Thus, } E[|n_{r_i}|^2] = \sum_{\epsilon=1}^{N_R} |v_{r\epsilon}|^2 Q_\epsilon(f_i) \text{ and}$$

$$\mathbf{R}_{n_r} = \text{diag}\{E[|n_{r1}|^2], \dots, E[|n_{rK}|^2]\}. \quad (\text{A.11})$$

Further simplification can be obtained by assuming that the noise at each receive

antenna is white with the same autocorrelation function

$$\mathcal{R}_\epsilon(\tau) = \sigma^2 \delta(\tau) \quad \forall \epsilon = 1, \dots, N_R \quad (\text{A.12})$$

$$Q_\epsilon(f_i) = \sigma^2 \quad \forall \epsilon = 1, \dots, N_R, f_i = 1, \dots, K \quad (\text{A.13})$$

$$E[|n_{ri}|^2] = \sum_{\epsilon=1}^{N_R} |v_{r\epsilon}|^2 Q_\epsilon(f_i) = \sigma^2 \sum_{\epsilon=1}^{N_R} |v_{r\epsilon}|^2 = \sigma^2 \|\mathbf{v}_r\|^2. \quad (\text{A.14})$$

Assuming that both Transmit and Receive beamforming vectors are normalized to have unit norm,

$$\|\mathbf{u}_d\|^2 = 1, \forall d = 1, \dots, T \quad (\text{A.15})$$

$$\|\mathbf{v}_r\|^2 = 1, \forall r = 1, \dots, R \quad (\text{A.16})$$

results in  $E[|n_{ri}|^2] = \sigma^2, \quad \forall i = 1, \dots, K$ , which implies that the noise correlation matrix from direction  $r$  is a scaled identity matrix and proves the desired result:

$$\mathbf{R}_{\mathbf{n}_r} = \sigma^2 \mathbf{I}_K, \quad r = 1, \dots, R. \quad (\text{A.17})$$

## Appendix B

### COMPRESSED SENSING BACKGROUND

There are many scenarios in which a large amount of data is collected and processed when a relatively small amount of this information is useful to the end user. Compressed sensing is a technique used to construct a dense representation of data that is sparse in some domain, such that the original sparse data can be reconstructed from the dense (compressed) representation. Compressed sensing draws upon the idea that a signal vector that is sparse in one domain has a dense representation in another domain [64]. The main steps of a compressed sensing algorithm are as follows.

- Compose a sparse representation of the  $N$ -sample input data by multiplying by an  $N \times N$  transformation matrix  $\mathbf{T}$  to convert the input signal to a basis in which the data set is  $M$ -sparse (so that  $M \ll N$  samples contain nonzero values). It is worth noting that  $\mathbf{T}$  must be of full row rank to completely cover the signal space. While typically a square transformation matrix is used, an overcomplete dictionary which has more columns than rows may also be used as long as the rank constraint is met.
- Multiply by a  $M \times N$  sampling matrix  $\mathbf{A}$  which is also of full row rank. Typically a random matrix is used to insure independence of each row.
- Reconstruct the original data vector  $\mathbf{x}$ , given the measurements  $\mathbf{y}$ , the sampling matrix  $\mathbf{A}$ , and the transformation matrix,  $\mathbf{T}$ .

The setup for this process is illustrated in Figure 24.

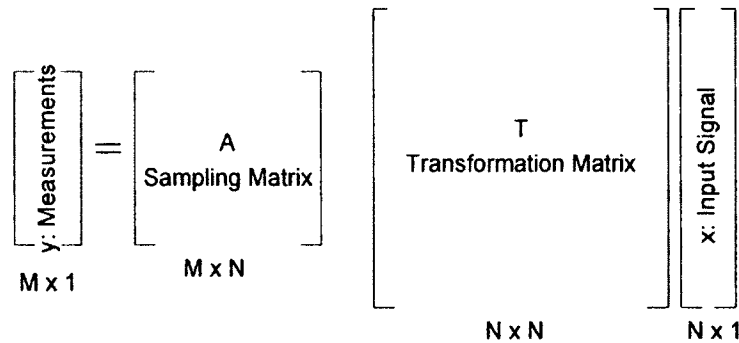


Fig. 24: Conceptual diagram of compressed sensing problem

The reconstruction problem can then be written as a standard underdetermined linear reconstruction problem of reconstructing each column of  $\mathbf{x}$  given  $\mathbf{y} = \mathbf{A}\mathbf{T}\mathbf{x}$ . Because the system is underdetermined, there are infinite possible solutions to this problem, and it has been shown that the ideal solution minimizes the number of nonzero elements in the reconstructed vector. Though the measure of nonzero elements in a vector is not strictly speaking a vector norm, it is often referred to as the “ $\ell_0$ -norm” in compressed sensing literature. Finding the solution that minimizes the  $\ell_0$ -norm is known to be an NP-hard problem. However, it was shown in [38] and [39], that finding the solution which instead minimizes the  $\ell_1$ -norm can reconstruct the desired sparse signal under certain reasonable conditions. Reconstruction minimizing the  $\ell_1$ -norm is a convex optimization problem, written as:

$$\min \|\hat{\mathbf{x}}\|_1, \text{ subject to } \|\mathbf{A}\mathbf{T}\hat{\mathbf{x}} - \mathbf{A}\mathbf{T}\mathbf{x}\|_2 < \epsilon \quad (\text{B.1})$$

where  $\hat{\mathbf{x}}$  is the reconstructed sparse signal vector. Solving this optimization problem is referred to as Basis Pursuit (BP) [56] and can be accomplished using linear programming techniques, making the solution much more straightforward than minimizing

the  $\ell_0$ -norm. Alternatively, efficient greedy algorithms, which typically allow a pre-determined maximum number of elements of the reconstructed vector to be nonzero, have been shown to provide good signal reconstruction. Some such greedy algorithms are Orthogonal Matching Pursuit (OMP) [57], Regularized Orthogonal Matching Pursuit (ROMP) [52], and Compressed Sampling Matching Pursuit (CoSaMP) [65].

The combination of conditions ensuring good signal reconstruction are as follows:

1. The signal  $\mathbf{x}$  must be sufficiently sparse when represented in the basis given by  $\mathbf{T}$ .
2. The sampling and transformation matrices ( $\mathbf{A}$  and  $\mathbf{T}$ , respectively) must be sufficiently incoherent.

To meet the requirement on the incoherence of  $\mathbf{A}$  and  $\mathbf{T}$ , two main approaches have been considered. The first approach considers that  $\mathbf{A}$  and  $\mathbf{T}$  must meet the restricted isometry property (RIP), introduced by Candes and Tao in [66]. The RIP is said to be satisfied if there exists some small  $\delta_M$  such that  $\mathbf{A}$  satisfies:

$$(1 - \delta_M)\|\mathbf{T}\mathbf{x}\|^2 \leq \|\mathbf{A}\mathbf{T}\mathbf{x}\|^2 \leq (1 + \delta_M)\|\mathbf{T}\mathbf{x}\|^2 \quad (\text{B.2})$$

for all possible  $M$ -sparse vectors  $\mathbf{T}\mathbf{x}$ . However, it is often mathematically difficult to ensure that the RIP is met. A second, alternate framework was proposed in [54], which showed that minimizing the mutual coherence of  $\mathbf{A}\mathbf{T}$  also ensures that exact reconstruction of the sparse signal can be achieved with with very high probability. The mutual coherence of  $\mathbf{B} = \mathbf{A}\mathbf{T}$  can be defined as:

$$\mu(\mathbf{B}) = \max_{i,j,i \neq j} \frac{|\mathbf{b}_i^T \mathbf{b}_j|}{\|\mathbf{b}_i\| \cdot \|\mathbf{b}_j\|} \quad (\text{B.3})$$

where  $\mathbf{b}_i$  is the  $i$ -th column of  $\mathbf{B}$ . This measure of mutual coherence is equivalent to the maximum off-diagonal element of the Gram matrix  $\mathbf{G}_\mathbf{B} = \mathbf{B}^H \mathbf{B}$ .

Because numerous sparse reconstruction procedures have already been developed (e.g., [52, 56, 57, 65]), it is beyond the scope of this work to consider the details of actually performing the reconstruction. Instead, the focus will remain on the design of  $\mathbf{A}$  and  $\mathbf{T}$  to ensure that the requirement on the mutual coherence of  $\mathbf{B}$  is satisfied such that it is indeed possible to reconstruct the desired signal using existing reconstruction methods.

## VITA

Amanda Joan Angell Daniel  
Department of Electrical and Computer Engineering  
Old Dominion University  
Norfolk, VA 23529

### EDUCATION

- M.S. Electrical Engineering, 2009, Stanford University, Stanford, CA
- B.S. Electrical Engineering, 2007, Northeastern University, Boston, MA

### PUBLICATIONS

- Amanda Daniel and Dimitrie C. Popescu. "MIMO Radar Waveform Design for Multiple Extended Targets using Compressed Sensing," in *2014 IEEE Radar Conference*, pp.0567-0572, 19-23 May 2014
- Amanda Daniel, and Dimitrie C. Popescu. "Multiple Extended Target Detection Using MIMO Radar and Compressed Sensing," in *2014 IEEE Military Communications Conference (MILCOM)*, pp.777-782, 6-8 Oct. 2014
- Amanda Daniel and Dimitrie C. Popescu, "A Vector Channel Approach to Waveform Design for Radar Systems," in *46th Annual Conference on Information Sciences and Systems (CISS), 2011*, pp.1-5, 21-23 Mar. 2012.
- Amanda Daniel, Dimitrie C. Popescu, and Stephan Olariu, "A Study of Beaconing Mechanism for Vehicle-to-Infrastructure Communications," in *2012 IEEE International Conference on Communications (ICC)*, pp.7146-7150, 10-15 Jun. 2012.
- Amanda Angell and Carey Rappaport, "Computational Modeling Analysis of Radar Scattering by Metallic Body-Worn Explosive Devices Covered with Wrinkled Clothing," in *2007 IEEE/MTT-S International Microwave Symposium*, pp.1943-1946, 3-8 Jun. 2007.